

***Mycobacterium tuberculosis* kinases as potential drug targets:  
Production of recombinant kinases in *E. coli* for functional characterization and  
enzyme inhibition screening against the medicinal plant *Pelargonium sidoides***

by

VISHANI LUKMAN

submitted in accordance with the requirements for the degree of

MASTER OF SCIENCE

in the subject

LIFE SCIENCES

at the

UNIVERSITY OF SOUTH AFRICA

Supervisor: Prof. J. Dewar

January 2015

*Dedicated with profound gratitude  
to my four pillars of strength, my grandparents,  
Mr Vallabh Lukman, Mrs Kalavati Lukman, Mr Dalpat Vanmalli & Mrs Jaya Vanmalli*

# Declaration

---



I \_\_\_\_\_ hereby declare that the dissertation/thesis, which I hereby submit for the degree of \_\_\_\_\_ at the University of South Africa, is my own work and has not previously been submitted by me for a degree at this or any other institution.

I declare that the dissertation /thesis does not contain any written work presented by other persons whether written, pictures, graphs or data or any other information without acknowledging the source.

I declare that where words from a written source have been used the words have been paraphrased and referenced and where exact words from a source have been used the words have been placed inside quotation marks and referenced.

I declare that I have not copied and pasted any information from the Internet, without specifically acknowledging the source and have inserted appropriate references to these sources in the reference section of the dissertation or thesis.

I declare that during my study I adhered to the Research Ethics Policy of the University of South Africa, received ethics approval for the duration of my study prior to the commencement of data gathering, and have not acted outside the approval conditions.

I declare that the content of my dissertation/thesis has been submitted through an electronic plagiarism detection program before the final submission for examination.

Student signature: \_\_\_\_\_

Date: \_\_\_\_\_

# Summary

---

***Mycobacterium tuberculosis* kinases as potential drug targets:  
Production of recombinant kinases in *E. coli* for functional characterization and enzyme  
inhibition screening against the medicinal plant *Pelargonium sidoides***

By

Vishani Lukman

Supervisor: Prof. J. Dewar  
Department of Life and Consumer Sciences  
College of Agriculture and Environmental Sciences  
University of South Africa

Co-supervisors: Dr. R.L. Roth  
Prof C.P. Kenyon  
Biosciences  
CSIR

for the degree MSc in Life Sciences

Tuberculosis (TB) is an infectious and fatal disease that ranks as the second leading killer worldwide. It is caused by *Mycobacterium tuberculosis* (Mtb) which is an obligate intracellular parasite that colonizes the alveolar macrophages of the immune system. The major health concern associated with TB is its co-infection with HIV and the development of strains with multi-drug resistance. The elimination of TB has been hindered due to the lack of understanding of the survival strategies used by this pathogen.

Thus, research towards discovering new effective antibacterial drugs is necessary and a group of Mtb kinase enzymes were targeted in this study because these enzymes are crucial for metabolism, pathogenesis and, hence, the survival of Mtb. Kinases are a group of structurally distinct and diverse proteins that catalyze the transfer of the phosphate group from high energy donor molecules such as ATP (or GTP) to a substrate. The phosphorylation of proteins modifies the activity of specific proteins which is subsequently used to control complex cellular processes within Mtb.

The starting point of this research targeted eight specific Mtb kinases namely; Nucleoside diphosphokinase, Homoserine kinase, Acetate kinase, Glycerol kinase, Thiamine monophosphate kinase, Ribokinase, Aspartokinase and Shikimate kinase. The aim of this project was to subclone the gene sequences for these eight recombinant Mtb kinases and express them in *Escherichia coli*, to purify the proteins and determine their activity. In the effort to find new lead compounds, the final stage of this study focused on the basic screening of the TB kinases against an extract prepared from *Pelargonium sidoides*, a medicinal plant, to identify any inhibitory effects. Although this traditional medicinal plant has been broadly researched and extensively used to treat TB, there is still a lack of understanding of this plant's scientific curative effect.

Various molecular and biochemical methods were used to achieve the aims of this project. The putative gene sequence was obtained from the annotated genome of H37Rv, deposited at NCBI as NC\_000962.2. The genes encoding the kinases were successfully PCR-amplified from genomic DNA, cloned into an expression vector in-frame with a C- or N-terminal 6-histidine-tag and expressed in *E. coli* BL21 (DE3). The purification of the protein was complex, but various different methods and techniques were explored to obtain sufficient amounts of protein. The functional characterization of the kinases involved an HPLC enzyme assay that showed that the recombinant kinases were active. These enzymes were then screened against the potential

inhibitory compounds in *P. sidoides* using enzyme assays to generate dose-response curves. This allowed an effective comparison not only of the Mtb kinases' activity under normal conditions but also the kinases' activity in the presence of a potential inhibitor. Overall, the inhibition of the enzymes required the presence of higher concentrations of the *P. sidoides* extract. However, the SK enzyme results presented a significantly higher inhibition and the lowest IC<sub>50</sub> value, in comparison to the other kinases, which makes this kinase an attractive potential drug target against TB.

In summation, cloning and purification of SK was successful, resulting in a concentration of 2030 µg/ml of purified enzyme and its activity analysis demonstrated enzyme functionality. This activity was reduced to zero in the presence of 1 x 10<sup>2</sup> mg/ml dilution of *P. sidoides* plant extract.

This research conducted has extended the quality of information available in this field of study. These interesting results, proposing and identifying SK as a suitable potential target can be a starting point to significantly contribute and progress in this field of research, with the eventual goal of developing a drug to combat this fatal disease.

#### Key Terms:

Tuberculosis, *Mycobacterium tuberculosis*, Kinases, Nucleoside diphosphokinase, Homoserine kinase, Acetate kinase, Glycerol kinase, Thiamine monophosphate kinase, Ribokinase, Aspartokinase, Shikimate kinase, *Pelargonium sidoides*, Cloning, *E. coli* expression, Protein purification, Functional characterization, Inhibitory screens.

# Acknowledgments

---

This dissertation would not have been possible without the guidance and inspiration of my mentor, Dr Robyn Roth. Through her unwavering supervision, she has been pivotal to me successfully developing my skills and techniques in this field of study. I could not have imagined having a better advisor and mentor.

I would like to sincerely thank Professor Colin Kenyon, who presented me with the opportunity to pursue this phenomenal research project. His leadership and immense knowledge has contributed immeasurably to my growth and development as a research scientist.

A special thanks to Professor John Dewar for his continuous support, enthusiasm, motivation and invaluable advice which he had provided throughout this process. I wish to express my appreciation to him, for assisting me, to advance my academic career. I would also like to thank him for his kind words, patience and wisdom.

I would like to thank all my colleagues and the staff at CSIR-Biosciences for their assistance and for providing me access to the facilities required to complete my work.

I would like to acknowledge and thank the National Research Foundation for awarding me with the Innovation Masters Scholarship.

I owe my deepest gratitude to my Dad, Shane Lukman; Mum, Prishiela Lukman; and sister, Karishma Lukman for their affection, blessings and faith in me. I would like to thank Keshan Pillay for his unequivocal support, encouragement and love throughout this journey. Lastly, I would like to thank God, my Bhagwan, my Hanuman, for giving me the ability and strength to achieve this goal.

# Index

---

Declaration.....	iii
Summary .....	iv
Acknowledgments.....	vii
Index .....	viii
List of figures .....	xii
List of tables.....	xv
List of abbreviations .....	xvi
Chapter 1: Introduction.....	1
1.1 Tuberculosis (TB): A fatal disease .....	2
1.2 The infectious agent: <i>Mycobacterium tuberculosis</i> (Mtb).....	3
1.3 Kinases: potential Mtb drug targets.....	5
1.3.1 Nucleoside diphosphokinase (NDK).....	5
1.3.2 Homoserine kinase (HSK).....	6
1.3.3 Acetate kinase (AK) .....	8
1.3.4 Glycerol kinase (GK) .....	9
1.3.5 Thiamine monophosphate kinase (ThiL) .....	10
1.3.6 Ribokinase (RBKS) .....	11
1.3.7 Aspartokinase (ASK) .....	12
1.3.8 Shikimate kinase (SK).....	14
1.4 <i>Pelargonium sidoides</i> : a medicinal plant .....	16
1.5 Research Formulation.....	17
Chapter 2: Gene Identification, Amplification and Cloning.....	19
2.1 Introduction.....	19
2.1.1 Overview of objectives .....	19



2.1.2 Mtb genes .....	20
2.2 Materials and Methods.....	21
2.2.1 Gene identification .....	21
2.2.2 DNA amplification.....	24
2.2.3 Cloning into pGEM®-T Easy vector (Promega. USA).....	25
2.2.4 Identification of successful cloned products.....	27
2.2.5 Cloning into selected pET vector .....	29
2.2.6 Nucleotide sequencing .....	32
2.3 Results and Discussion.....	33
2.3.1 Template authentication .....	33
2.3.2 DNA amplification.....	33
2.3.3 Plasmid construction .....	36
2.3.4 <i>E. coli</i> Transformations.....	39
2.3.5 Restriction enzyme digests gels .....	39
2.3.6 Nucleotide sequencing .....	42
2.4 Chapter conclusion .....	42
Chapter 3: <i>E. coli</i> expression and Protein Purification .....	43
3.1 Introduction.....	43
3.2 Materials and Methods.....	45
3.2.1 <i>E. coli</i> expression and cultivation by induction.....	45
3.2.2 Lysis of cells by sonication .....	45
3.2.3 Sodium Dodecyl Sulfate Polyacrylamide Gel Electrophoresis (SDS-PAGE) analysis	46
3.2.4 Protein Purification .....	46
3.2.5 Dialysis .....	49
3.2.6 Protein Quantitation .....	50
3.3 Results and Discussion.....	51
3.3.1 <i>E. coli</i> expression .....	51

3.3.2 Protein production evaluation .....	51
3.3.3 SDS-PAGE analysis of purified protein .....	52
3.3.4 Determination of Protein Quantitation.....	55
3.4 Chapter conclusion .....	56
Chapter 4: Functional characterization of enzymes.....	57
4.1 Introduction.....	57
4.2 Materials and Methods.....	59
4.2.1 Enzyme activity analysis by High Performance Liquid Chromatography (HPLC) .....	59
4.2.2 ATP concentration gradient assays .....	60
4.3 Results and Discussion.....	62
4.3.1 Determination of enzyme activity.....	62
4.3.2 ATP concentration gradient assay outcome .....	63
4.4 Chapter conclusion .....	69
Chapter 5: Screening of the effect of extracts of <i>Pelargonium sidoides</i> on Mtb kinase activity ..	70
5.1 Introduction.....	70
5.2 Materials and Methods.....	72
5.2.1 Plant Harvesting and Extraction .....	72
5.2.2 Plant inhibitory screens .....	72
5.3 Results and Discussion.....	75
5.3.1 Plant material .....	75
5.3.2 <i>Pelargonium sidoides</i> concentration gradient assay outcome .....	75
5.3.3 Plant inhibitory screens evaluation .....	80
5.4 Chapter conclusion .....	86
Chapter 6: Concluding discussion and future recommendations .....	87
6.1 Concluding discussion .....	87
6.1.1 Insights into combating TB.....	87
6.1.2 Using kinases as potential drug targets.....	87

6.1.3 The gap between traditional <i>P. sidoides</i> usage and modern pharmaceuticals.....	89
6.2 Future recommendations .....	91
Appendices .....	92
References .....	107

# List of figures

---

## Chapter 1

Figure 1-1: Estimated Worlds TB incidence rates, 2012 (World Health Organisation. 2013) .....	2
Figure 1-2: Transmission and growth of Mycobacterium tuberculosis (Davis. 2007) .....	3
Figure 1-3: Structure of Mycobacterium tuberculosis (Microbiology In Pictures. 2013) .....	4
Figure 1-4: 3D Structure of NDK from <i>Dictyostelium discoideum</i> .....	6
Figure 1-5: 3D Structure of HSK from <i>Methanocaldococcus jannaschii</i> .....	7
Figure 1-6: 3D Structure of AK <i>Methanosarcina thermophile</i> .....	9
Figure 1-7: 3D Structure of GK from <i>Escherichia coli</i> .....	10
Figure 1-8: 3D Structure of ThiL from <i>Aquifex aeolicus</i> .....	11
Figure 1-9: 3D Structure of RBKS from <i>Escherichia coli</i> .....	12
Figure 1-10: 3D Structure of AsK from <i>Corynebacterium glutamicum</i> .....	14
Figure 1-11: 3D Structure of SK from <i>Mycobacterium tuberculosis</i> .....	15
Figure 1-12: Image of Pelargonium sidoides plant (Research On Medical. 2013) .....	16

## Chapter 2

Figure 2-1: Agarose gel electrophoresis of the H37Rv genomic DNA template .....	33
Figure 2-2: Agarose gel electrophoresis of the kinase amplicons obtained by PCR amplification using H37Rv genomic DNA as the template .....	34
Figure 2-3: Agarose gel electrophoresis of the kinase amplicons obtained by PCR amplification using H37Rv genomic DNA as the template .....	35
Figure 2-4: Complete plasmid maps.....	37
Figure 2-5: Complete plasmids maps.....	38
Figure 2-6: Agarose gel electrophoresis of the recombinant vector-kinase inserts eluted from agarose gels following restriction enzyme digestions .....	40
Figure 2-7: Agarose gel electrophoresis of the recombinant vector-kinase inserts following restriction enzyme digestions .....	41

## Chapter 3

Figure 3-1: SDS-PAGE gels of the Mtb his-tagged kinases purified from <i>E. coli</i> BL21 (DE3) ....	53
Figure 3-2: SDS-PAGE gels of the Mtb his-tagged kinases purified from <i>E. coli</i> BL21 (DE3) ....	54

## Chapter 4

Figure 4-1: ADP production by His-NDK as a measure of TDP phosphorylating activity .....	64
------------------------------------------------------------------------------------------	----

Figure 4-2: ADP production by His-HSK as a measure of homoserine phosphorylating activity .....64

Figure 4-3: ADP production by His-AK as a measure of Na-acetate phosphorylating activity ....65

Figure 4-4: ADP production by His-GK as a measure of glycerol phosphorylating activity.....65

Figure 4-5: ADP production by His-ThiL as a measure of TMP phosphorylating activity.....66

Figure 4-6: ADP production by His-RBKS as a measure of D-ribose phosphorylating activity ...66

Figure 4-7: ADP production by His-AsK as a measure of aspartate phosphorylating activity .....67

Figure 4-8: ADP production by His-SK as a measure of shikimic acid phosphorylating activity .67

Chapter 5

Figure 5-1: ADP production by His-NDK as a measure against a LOG concentration gradient of *P. sidoides* extract.....76

Figure 5-2: ADP production by His-HSK as a measure against a LOG concentration gradient of *P. sidoides* extract.....76

Figure 5-3: AK - ADP production by His-AK as a measure against a LOG concentration gradient of *P. sidoides* extract.....77

Figure 5-4: GK - ADP production by His-GK as a measure against a LOG concentration gradient of *P. sidoides* extract.....77

Figure 5-5: ADP production by His-ThiL as a measure against a LOG concentration gradient of *P. sidoides* extract.....78

Figure 5-6: ADP production by His-RBKS as a measure against a LOG concentration gradient of *P. sidoides* extract.....78

Figure 5-7: ADP production by His-AsK as a measure against a LOG concentration gradient of *P. sidoides* extract.....79

Figure 5-8: ADP production by His-SK as a measure against a LOG concentration gradient of *P. sidoides* extract.....79

Figure 5-9: Bar graph of ADP production by His-NDK as measured against a concentration gradient of *P. sidoides* plant extract .....81

Figure 5-10: Bar graph of ADP production by His-HSK as measured against a concentration gradient of *P. sidoides* plant extract .....81

Figure 5-11: Bar graph of ADP production by His-AK as measured against a concentration gradient of *P. sidoides* plant extract .....82

Figure 5-12: Bar graph of ADP production by His-GK as measured against a concentration gradient of *P. sidoides* plant extract .....82

Figure 5-13: Bar graph of ADP production by His-ThiL as measured against a concentration gradient of *P. sidoides* plant extract .....83

Figure 5-14: Bar graph of ADP production by His-RBKS as measured against a concentration gradient of *P. sidoides* plant extract .....83

Figure 5-15: Bar graph of ADP production by His-AsK as measured against a concentration gradient of *P. sidoides* plant extract .....84

Figure 5-16: Bar graph of ADP production by His-SK as measured against a concentration gradient of *P. sidoides* plant extract .....84

# List of tables

---

## Chapter 2

Table 2-1: Particular forward and reverse primers used to amplify specific kinase genes. Note also preferred Novagen vector for each construct. ....	22
Table 2-2: Kinase genes and their relevant information.....	23
Table 2-3: Kinase genes and their specific annealing temperatures for the PCR reactions .....	24
Table 2-4: Kinase genes and their respective restriction enzymes and buffers used to confirm insert size.....	28
Table 2-5: Kinase genes with their vectors and respective restriction enzymes and buffers used for digests .....	30
Table 2-6: A list of kinase genes and their respective restriction enzymes and buffer used to confirm final digestion .....	32

## Chapter 3

Table 3-1: Recommended purification method according to kinase solubility .....	47
Table 3-2: Dialysis buffers used to solubilise NDK, HSK, AK, GK, ThiL, RBKS, AsK and SK kinase proteins.....	50
Table 3-3: Concentration of purified kinase proteins (presented in µg/ml) .....	55

## Chapter 4

Table 4-1: Kinase enzymes with their respective enzyme activity assay conditions .....	61
Table 4-2: Reactions of kinases .....	63

## Chapter 5

Table 5-1: Details of kinase reactions in the presence of various dilutions of plant root extract .	74
Table 5-2: Kinases and their respective IC <sub>50</sub> values derived from the dose-response curves ....	80

# List of abbreviations

---

A/T	Adenine Thymine
ACT	Aspartate kinase, chorismate mutase and tyrosine A
ADP	Adenosine diphosphate
AIDS	Acquired Immune Deficiency Syndrome
AK	Acetate kinase
Amp	Ampicillin
AMP	Adenosine MonoPhosphate
AsK	Aspartokinase
ATP	Adenosine triphosphate
Bp	Base pair
Cm	Centimetre
CSIR	Council for Scientific and Industrial Research
dATP	Deoxyadenosine Triphosphate
dATP	ATP deuterated at the C8 position of the adenyl moiety
DNA	Deoxyribonucleic acid
dNTP	Deoxynucleoside-5 <sup>l</sup> -triphosphate
<i>E. coli</i>	<i>Escherichia coli</i>
EC	Enzyme Commission
ECD	Enterprise Creation for Development
EDTA	Ethylenediaminetetraacetic acid
fwd	Forward
g	Gram
<i>g</i>	Relative centrifuge force
gDNA	Genomic DNA
GHMP	Galactokinase, Homoserine, Mevalonate and Phosphomevalonate kinase
GK	Glycerol kinase
GYT	Glycerol, yeast extract, tryptone
HiFi	High fidelity
His	Histidine
HIV	Human Immunodeficiency Virus
HPLC	High Performance Liquid Chromatography



HSK	Homoserine kinase
IDT	Integrated DNA Technologies
IMAC	metal ion affinity chromatography
IPTG	Isopropyl- $\beta$ -D-Thiogalactoside
Kan	Kanamycin
kb	Kilobase pairs
kDa	Kilodalton
kV	Kilovolts
<i>lac</i>	Lactose
<i>lack</i>	$\beta$ -galactosidase
LB	Luria Bertani broth
LOG	Logarithm
M	Molar
Mbp	Mega base pairs
MDR-TB	Multidrug-resistant Tuberculosis
mg	Milligram
ml	Millilitre
mM	Millimolar
Mtb	<i>Mycobacterium tuberculosis</i>
m/v	Mass per volume
MWCO	Molecular weight cut-off
NaOAc	Sodium acetate
NCBI	National Centre for Biotechnology Information
NDK	Nucleoside diphosphokinase
ng	Nanogram
Ni-IDA	Nickel-iminodiacetic acid
Ni-TED	Nickel-tris carboxymethyl ethylene diamine
nm	Nanometers
NMP	Nucleoside monophosphate
NPA	Natural Products and Agroprocessing
NTA	Nitrilotriacetic acid
OD	Optical density
PAGE	Polyacrylamide gel electrophoresis
PCR	Polymerase Chain Reaction

PDB	Protein Data Bank
pET	Plasmid expression vector T7 promoter
pGem	Prostaglandin E2 metabolite
pI	Isoelectric point
<i>P. sidoides</i>	<i>Pelargonium sidoides</i>
RBKS	Ribokinase
RCSB	Research Collaboratory for Structural Bioinformatics
rev	Reverse
RNA	Ribonucleic acid
rpm	Revolutions per minute
Rv	Virulent
SDS	Sodium dodecyl sulfate
SK	Shikimate kinase
Strep	Streptomycin
TAE	Tris base, acetic acid and EDTA
TB	Tuberculosis
TDP	Thymidine diphosphate
TGS	Tris-HCl, glycine, SDS
ThiL	Thiamine monophosphate kinase
TMP	Thiamine monophosphate
Tris	Tris-hydroxymethyl-aminomethane
U	Units
UV	Ultra Violet
V	Volts
v/v	Volume per volume
w/v	Weight per volume
WHO	World Health Organisation
XDR-TB	Extensively drug-resistant Tuberculosis
X-gal	5-bromo-4-chloro-3-indolyl-b-D galactopyranoside
°C	Degree Celsius
μF	Microfarad
μg	Microgram
μl	Microlitre
μm	Micrometre

$\mu\text{M}$

Micromolar

$\mu\text{Moles}$

Micromoles

# Chapter 1: Introduction

---

The 24<sup>th</sup> of March 2014, marked World TB Day, served as a day to raise awareness about the worldwide predicament of Tuberculosis (TB). This occasion provided a platform to discuss and put forward corrective actions in order to prevent the suffering that TB has brought to mankind. It is highly significant to address this public health crisis as TB ranks as the second leading killer worldwide. The objectives set out by the World Health Organisation (WHO) and Stop TB partnership was to find, treat and cure TB and progress towards a TB-free world (World Health Organisation. 2014). These goals and strategies set out can be achieved through the development of novel health systems and on-going TB research.

“In the first papers concerning the aetiology of tuberculosis I have already indicated the dangers arising from the spread of the bacilli-containing excretions of consumptives, and have urged moreover that prophylactic measures should be taken against the contagious disease.”

***Dr Robert Koch, Nobel lecturer in Physiology/Medicine, on the struggle against tuberculosis (1905)***

“The world has made defeating AIDS a top priority. This is a blessing. But TB remains ignored. Today we are calling on the world to recognize that we can't fight AIDS unless we do much more to fight TB as well.”

***Nelson Mandela, Former President, on confronting the joint HIV/TB epidemics at the XV International Aids Conference (2004)***

“We're just silently watching this epidemic unfold and spread over our eyes. TB is very clever because it kills you very slowly and while it's killing you very slowly you're walking around spreading it.”

***Dr Ruth McNerny, Seniou lecturer at the London School of Tropical Medicine, Director of TB Alert, on the global resistance to TB drugs (2013)***

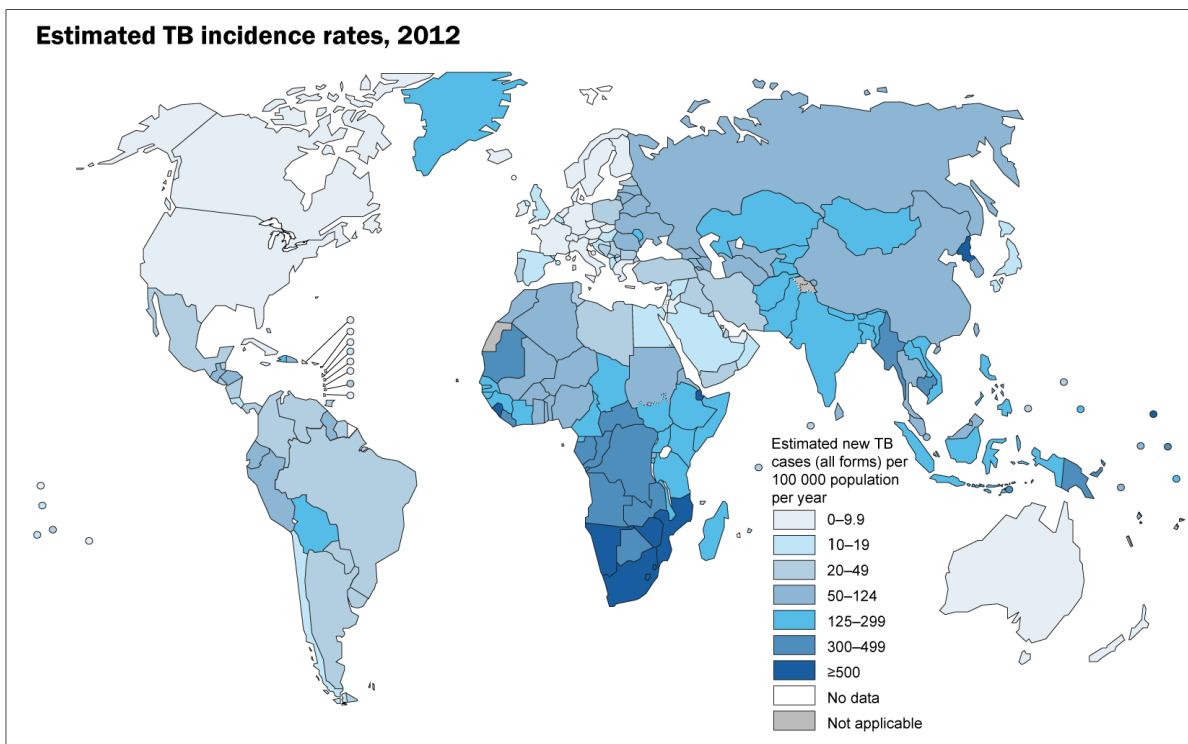
“Too many falsely believe TB is a disease of the past, but to truly relegate this disease to the pages of our history books, we must identify better ways to detect and treat TB and we must stop the emergence of further drug resistance. TB can happen anywhere, in any community. Exposures can happen at school, at work, at home, while traveling, or anywhere that people are in close contact with one another. This is why TB prevention is a public health priority for the nation.”

***Dr. Jonathan Mermin, Director, National Center for HIV/AIDS, Viral Hepatitis, STD, and TB Prevention on the importance of TB prevention (2014)***

## 1.1 Tuberculosis (TB): A fatal disease

Tuberculosis (TB) is a prevalent, and in numerous cases, fatal infectious disease that poses a global threat to human health (Cole et al. 1998). Infection associated with TB is second to HIV/AIDS as the greatest killer globally due to a single initiating infectious agent (World Health Organisation. 2014).

Of the 9 million people a year infected with TB, 3 million are left untreated and are able to spread this disease even further. Many of these 3 million untreated cases are due to poverty and disregarded populations. Over 95% of TB cases and deaths shown in Figure 1-1 are in developing countries, such as South Africa, often where the percentage of AIDS is high and the immune systems of their populations are weak (World Health Organisation. 2014).



The boundaries and names shown and the designations used on this map do not imply the expression of any opinion whatsoever on the part of the World Health Organization concerning the legal status of any country, territory, city or area or of its authorities, or concerning the delimitation of its frontiers or boundaries. Dotted and dashed lines on maps represent approximate border lines for which there may not yet be full agreement.

Data Source: *Global Tuberculosis Report 2013*. WHO, 2013.

© WHO 2013. All rights reserved.



Figure 1-1: Estimated Worlds TB incidence rates, 2012 (World Health Organisation. 2013)

## 1.2 The infectious agent: *Mycobacterium tuberculosis* (Mtb)

Tuberculosis is caused by various strains of mycobacteria, usually *Mycobacterium tuberculosis*, and most commonly affects the lungs. It is easily transferrable from person to person through the air and the recipient just needs to inhale a few of these active microorganisms to become infected, as portrayed in Figure 1-2 (World Health Organisation. 2014). It is an obligate intracellular parasite that colonizes the lungs alveolar macrophages of the host's immune system (Flynn & Chaney. 2003).

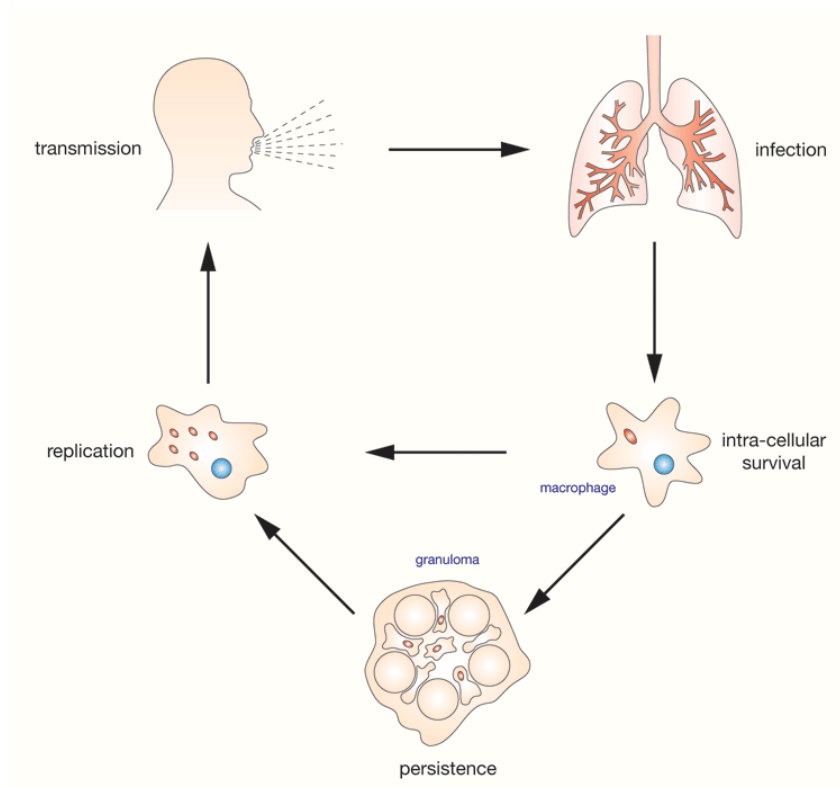


Figure 1-2: Transmission and growth of *Mycobacterium tuberculosis* (Davis. 2007)

The Mtb microorganism is an aerobic, acid-fast, bacillus, shown in Figure 1-3, with a cell wall which has a high lipid content (Kassim & Ray. 2004). This organism is slow-growing with a generation time of 24 hours in synthetic media and infected animals (Murray et al. 2005).

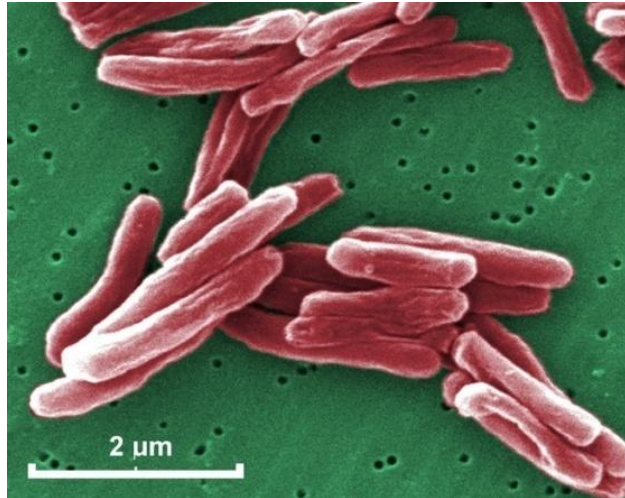


Figure 1-3: Structure of *Mycobacterium tuberculosis* (Microbiology In Pictures. 2013)

The main feature of the organism is its intracellular pathogenesis and its ability to enter a dormant state. The host's macrophages are prevented from breaking down the bacterium because the complex bacterial cell wall prevents the fusion of the macrophagal lysosome with the Mtb by blocking the bridging molecule involved in this process (Flynn & Chaney. 2003). Macrophage acidification and the production of reactive nitrogen intermediates are normally mechanisms that are employed by these specialized immune cells to kill the invading pathogen, but Mtb also has genes that code for the prevention of acidification of the macrophage, as well as the ability to neutralize reactive nitrogen intermediates (Flynn & Chaney. 2003).

The host's immune responses to this organism results in the organism converting to a dormant stage which imitates Mtb's metabolic shutdown, yet does not eliminate the infection. Thus, should the host's immunity diminish over time, the dormant organism can be reactivated resulting in a lethal disease. This phenomenon of conversion from dormancy to reactivation is assumed to be genetically programmed and to involve intracellular signalling pathways (Cole et al. 1998).

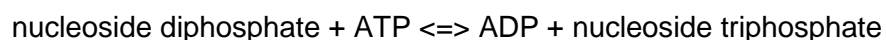
### 1.3 Kinases: potential Mtb drug targets

The secreted and exported Mtb proteins, in particular protein kinases, are important for pathogenesis and are involved in the growth of these bacteria (Tomioka. 2008). Protein kinases are a group of structurally distinct proteins that participate in various metabolic and signalling pathways (Johnson et al. 1993 and Kenyon et al. 2011). These enzymes catalyze the transfer of the phosphate group from high energy donor molecules such as ATP (or GTP) to a substrate. The substrates may be small molecules, protein or lipids which contain an alcohol, amino, carboxyl, or phosphate group as the phosphoryl acceptor (Kenyon et al. 2011, Cheek et al. 2002 and Cheek et al. 2005). The phosphorylation of proteins modifies the activity of specific proteins which is subsequently used to control complex cellular processes. These enzymes are crucial for the metabolism and, hence, the survival of Mtb (Tomioka. 2008). Kinases are categorised into different classes, based on their mechanism of phosphoryl transfer (Kenyon et al. 2012). The diversity and significance of Mtb kinases makes them an ideal object of biochemical research.

The powerful tools of genomics, bioinformatics and genome sequencing have provided information about Mtb in order to facilitate the development of new therapies. The genome of the Mtb strain, H37Rv has been sequenced and annotated, and is deposited at NCBI as NC\_000962.2. This is the source of all the putative gene sequences amplified here.

#### 1.3.1 Nucleoside diphosphokinase (NDK)

Nucleoside diphosphokinase (NDK, EC 2.7.4.6), belongs in the family of transferases and is an enzyme involved in the transfer of the  $\gamma$ -phosphate from ATP to a nucleoside diphosphate to form a nucleoside triphosphate (Xu et al. 1997).



This reaction maintains the nucleotide pool and provides precursors for DNA and RNA synthesis (Sikarwar et al. 2013).

The NDK enzyme is encoded by the *ndkA* gene and is present in almost all organisms, with differing oligomeric structures due to its varied functions (Sikarwar et al. 2013). This enzyme



has been found to play an important role in bacterial growth, signal transduction and pathogenicity, and mycobacterial NDK has been found to prevent phagosome maturation and assist in bacterial survival in the macrophage (Sikarwar et al. 2013).

*Dictyostelium discoideum* Mtb, illustrated as a 3D structure in Figure 1-4, has been previously cloned through the *E. coli* expression system (Xu et al. 1997). The Mtb NDK has also been previously cloned and expressed in *E. coli* (Chen et al. 2002, Kumar et al. 2004) through the use of the H37Rv NDK gene (Rv2445c) and was identified from the annotated Mtb genome.

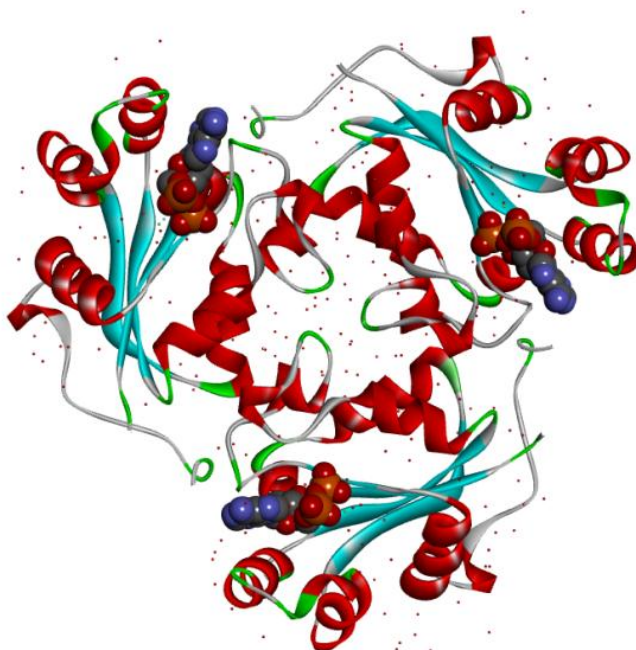


Figure 1-4: 3D Structure of NDK from *Dictyostelium discoideum*. Drawn using Accelrys Discovery Studio 3.5 (Accelrys Inc. San Diego. USA), RCSB accession number 2BEF (Xu et al.1997).

### 1.3.2 Homoserine kinase (HSK)

Homoserine kinase (HSK, EC 2.7.1.39), belongs in a large, unique class of small metabolite kinases, the GHMP kinase family (Zhou et al. 2000). Members in the GHMP kinase superfamily participate in several essential metabolic pathways, such as amino acid biosynthesis, galactose metabolism and the mevalonate pathway. The HSK enzyme is a catalyst for the phosphorylation of L-homoserine to L-homoserine phosphate, which is an intermediate in the production of L-isoleucine and L-threonine (Krishna et al. 2001).



This enzyme plays a vital role in threonine biosynthesis (Krishna et al. 2001). HSK is encoded by the *thrB* gene.

Inactivation of the HSK activity results in threonine auxotrophy in various bacterial species and yeasts (Zhou et al. 2000). This means that the organism loses its ability to synthesize the threonine, which is essential to its growth and survival. These enzyme reactions occur exclusively in prokaryotes and lower eukaryotes (Rees et al. 1992). Therefore, a drug targeting this enzymes activity would have no effect on the host (human), making this kinase a good potential drug target for Mtb.

*Brevibacterium lactofermentum* (Mateos et al. 1987) and *Methanocaldococcus jannaschii* (Zhou et al. 2000) HSK, illustrated as a 3D structure in Figure 1-5, has been previously cloned and expressed in *E. coli*. A putative H37Rv HSK gene (Rv1296) was identified in the annotated genome of Mtb and an amino acid sequence comparison between the two proteins indicates a 48% identity (DNAMAN Version 5.2.10. Lynnon BioSoft).



Figure 1-5: 3D Structure of HSK from *Methanocaldococcus jannaschii*. Drawn using Accelrys Discovery Studio 3.5 (Accelrys Inc. San Diego. USA), RCSB accession number 1FWK (Zhou et al. 2000).

### 1.3.3 Acetate kinase (AK)

Acetate kinase (AK, EC 2.7.2.1), a member of the acetokinase family, plays an important role in carbon cycling and energy metabolism (Boynton et al. 1996). The AK enzyme phosphorylates acetate to acetyl phosphate, which is subsequently converted to acetyl-CoA by phosphotransacetylase (Gorrell et al. 2005).



This enzyme is encoded by the *ackA* gene. Prokaryotic and eukaryotic physiology both depend on the metabolism of acetate, which is the production or consumption of acetyl coenzyme A (Latimer & Ferry. 1993). AK is a vital enzyme in bacteria as it is known to be a potential regulator of signal transduction pathways (Buss et al. 2001).

*Methanosarcina thermophile* AK, illustrated as a 3D structure in Figure 1-6, has been previously cloned and expressed in *E. coli* (Gorrell et al. 2005). The putative Mtb AK gene (Rv0409) was identified and amino acid sequence comparison between the two proteins indicates a 41.34% identity (DNAMAN Version 5.2.10. Lynnon BioSoft). Other mycobacterial AKs have been deposited in the Protein Data Bank ([www.pdb.org](http://www.pdb.org)), with high levels of similarity to the putative Mtb AK (*M. avum*, pdb 3P4I at 74.4% and *M. marinum* pdb 4DQ8 at 75.1%).

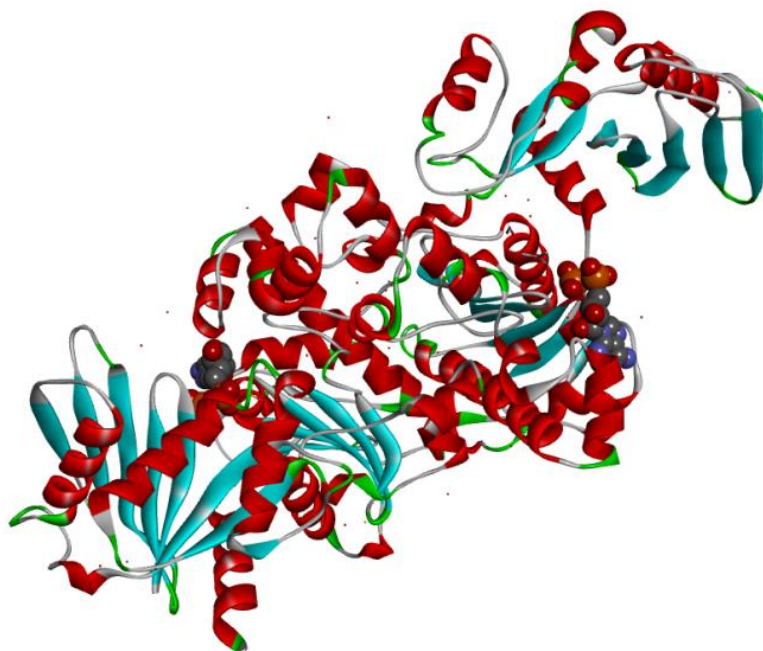


Figure 1-6: 3D Structure of AK *Methanosarcina thermophila*. Drawn using Accelrys Discovery Studio 3.5 (Accelrys Inc. San Diego. USA), RCSB accession number 1TUY (Gorrell et al. 2005).

#### 1.3.4 Glycerol kinase (GK)

Glycerol kinase (GK, EC 2.7.1.30), belongs in the carbohydrate kinase family and catalyses the transfer of the  $\gamma$ -phosphoryl of ATP to glycerol to form glycerol phosphate (Zhang et al. 2011).



The GK enzyme is obligatory for glycerol-related metabolism pathways and the production of glycerol-3-phosphate which is essential for carbohydrate and fatty acid metabolism (Dipple et al. 2001). It is encoded by the *glpK* gene. The enzyme activity is present widely in organisms from bacteria to human.

*Escherichia coli* GK enzyme, illustrated as a 3D structure in Figure 1-7, has been previously overexpressed and purified in *E. coli* (Bystrom et al. 1999). The GK enzyme from *Bacillus subtilis* was also successfully expressed in *E. coli* (Darbon et al. 2002). A putative Mtb GK gene (Rv3696c) was identified and amino acid sequence comparison indicated identity of 49.8% and

46.6% between Mtb GK and *E. coli* and *B. subtilis* GKs, respectively (DNAMAN Version 5.2.10. Lynnnon BioSoft).

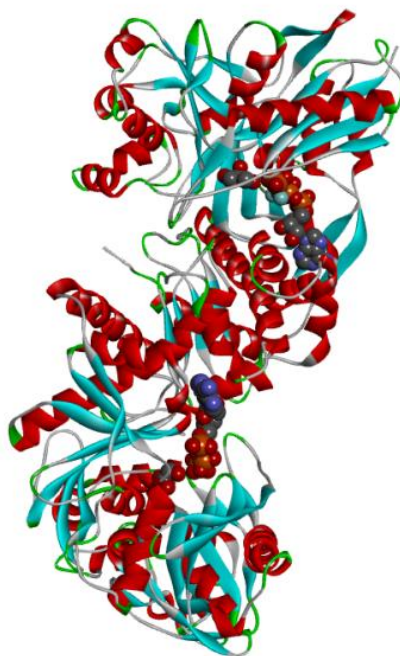
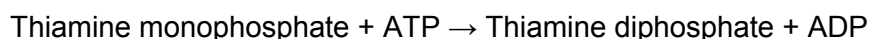


Figure 1-7: 3D Structure of GK from *Escherichia coli*. Drawn using Accelrys Discovery Studio 3.5 (Accelrys Inc. San Diego, USA), RCSB accession number 1BWF (Bystrom et al. 1999).

### 1.3.5 Thiamine monophosphate kinase (ThiL)

Thiamine monophosphate kinase (ThiL, EC 2.7.4.1), part of the transferase family, catalyzes the ATP-dependent phosphorylation of thiamine monophosphate to form thiamine diphosphate (McCulloch et al. 2008).



The ThiL enzyme is encoded by the *thiL* gene. Thiamine metabolism is important as thiamine is an essential vitamin in living organisms as the active form partakes in carbohydrate metabolism and in the pentose phosphate pathway, where ThiL is the final enzyme in the biosynthetic pathway to form thiamine pyrophosphate which is the biologically active form of vitamin B. These enzyme reactions occur exclusively in prokaryotes, therefore a drug targeting this enzymes activity would have no effect on the host (human) and therefore this enzyme is a good

potential drug target for Mtb. The biosynthesis of the thiamine enzyme has been studied in prokaryotic systems both structurally and mechanistically (McCulloch et al. 2008).

*Aquifex aeolicus* ThiL, illustrated as a 3D structure in Figure 1-8, has been previously cloned and expressed in *E. coli* (McCulloch et al. 2008). A putative H37Rv ThiL gene (Rv2977c) was identified and an amino acid sequence comparison between the two proteins indicates only a 25.1% identity (DNAMAN Version 5.2.10. Lynnon BioSoft). ThiL from *Methylobacillus flagellatus* has been deposited in the Protein Data Bank (pdb 3MCQ), also with a low level of 25.4% similarity to the putative Mtb ThiL.



Figure 1-8: 3D Structure of ThiL from *Aquifex aeolicus*. Drawn using Accelrys Discovery Studio 3.5 (Accelrys Inc. San Diego, USA), RCSB accession number 3C9T (McCulloch et al. 2008).

### 1.3.6 Ribokinase (RBKS)

Ribokinase (RBKS, EC 2.7.1.15), belongs in the pfkB family of carbohydrate kinases, also known as the RK family. RBKS catalyzes the phosphorylation of ribose to ribose 5-phosphate, in the presence of ATP and magnesium (Yang et al. 2011).





This reaction occurs during ribose metabolism. D-ribose is an important part of multiple biological molecules but must first be phosphorylated by RBKS to enter metabolic pathways. RBKS is encoded by the *rbks* gene.

The structure of the RBKS enzyme is conserved in several mycobacterial species which suggests its importance for bacterial survival. However, little is known about the function and regulation of this kinase. Various RBKS genes have been found in both prokaryotes and eukaryotes (Yang et al. 2011). The crystal structure of *E. coli* RBKS, illustrated as a 3D structure in Figure 1-9, has been previously determined (Sigrell et al. 1998). Mtb RBKS has been previously expressed, purified and examined for activity (Yang et al. 2011) using the H37Rv RBKS gene, Rv2436.

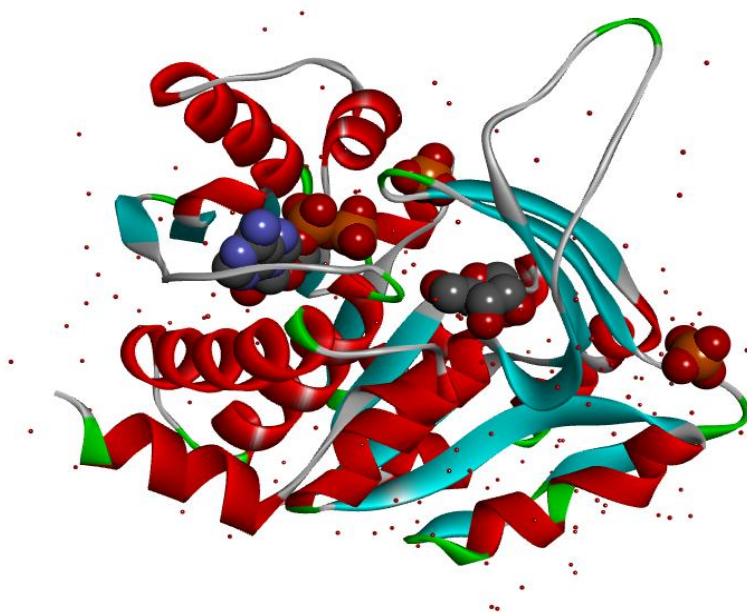


Figure 1-9: 3D Structure of RBKS from *Escherichia coli*. Drawn using Accelrys Discovery Studio 3.5 (Accelrys Inc. San Diego. USA), RCSB accession number 1RKD (Sigrell et al. 1998).

### 1.3.7 Aspartokinase (AsK)

Aspartokinase (AsK, EC 2.7.2.4), belongs in the amino acid kinase family, catalyzes the phosphorylation of the amino acid, aspartate (Kotaka et al. 2006).



The AsK enzyme is encoded by the *ask* gene. This enzyme catalyzes an initial commitment step that is dependent on a feedback system that regulates the aspartate pathway, to synthesis certain amino acids such as lysine, threonine, methionine and isoleucine (Kotaka et al. 2006). Three classes of AsK's exist based on their structure and architecture (Robin et al. 2010). Homo-oligomeric AsK's are divided into either Class I or Class III, with 2 or 4 ACT domains respectively, and has identical subunits (Schuldt et al. 2011). Heterotetrameric AsK's are Class II in which each chain contains 2 ACT domains resulting in  $\alpha_2\beta_2$ -type AsK arranged as a dimer (Yoshida et al. 2010, Schuldt et al. 2011).

This enzyme is present in plants and microorganisms only (Kotaka. 2006). Due to the absence of the aspartate pathway in higher organisms such as humans, inhibition of this kinase is a prospective target for a novel antibacterial drug.

The AsK gene (Rv3709c) was identified in the annotated genome of Mtb and found to be most similar to the  $\alpha_2\beta_2$  heterotetrameric AsK from *Corynebacterium glutamicum*, illustrated as a 3D structure in Figure 1-10 (Yoshida et al. 2010, Crillo et al. 1994). The alpha and beta subunits of *C. glutamicum* AsK have been expressed in *E. coli* (Yoshida et al. 2010), but only the beta subunit of Mtb AsK has been successfully cloned and expressed in *E. coli* (Schuldt et al. 2011). Amino acid sequence alignment of the full-length proteins (alpha subunit) of *C. glutamicum* and Mtb indicate a 71.2% identity.





Figure 1-10: 3D Structure of AsK from *Corynebacterium glutamicum*. Drawn using Accelrys Discovery Studio 3.5 (Accelrys Inc. San Diego. USA), RCSB number 3AAW (Yoshida et al. 2010). This figure illustrates half of the enzyme structure with the alpha domain shown in green and the beta domain shown in purple.

### 1.3.8 Shikimate kinase (SK)

Shikimate kinase (SK, EC 2.7.1.71) is a monomeric enzyme that belongs to the nucleoside monophosphate (NMP) kinase structural family, where a characteristic feature of the NMP kinases is that they undergo large conformational changes during catalysis (Pereira et al. 2004). This enzyme catalyzes the phosphorylation of shikimate to shikimate 3-phosphate.



The SK enzyme is encoded by the *aroK* gene and catalyzes the fifth reaction in the shikimate pathway, in order to generate the aromatic amino acids phenylalanine (Phe), tyrosine (Tyr), and tryptophan (Trp) (Pereira et al. 2004). This enzyme is present in plants and microorganisms only (Pereira et al. 2004) and due to the absence of this enzyme in higher organisms and the potential shikimate pathway targets, inhibition of this kinase is a prospective target for a novel antibacterial drug.

The Mtb SK, illustrated as a 3D structure in Figure 1-11, has been previously cloned and the enzyme overexpressed in soluble form in *E. coli* using the H37Rv gene Rv2539c (Gu et al. 2002). The SK enzyme has been isolated, purified and functionally expressed by Kenyon et al. (2011), and the consequential information has been utilized, and included, in this research project for further tests and examination.



Figure 1-11: 3D Structure of SK from *Mycobacterium tuberculosis*. Drawn using Accelrys Discovery Studio 3.5 (Accelrys Inc. San Diego. USA), RCSB accession number 1L4U (Gu et al. 2002).

#### 1.4 *Pelargonium sidoides*: a medicinal plant

*Pelargonium sidoides*, native to South Africa, is a herbaceous perennial plant with branched stems arising from fleshy tuberous rhizomes (Van der Walt & Vorster. 1988). The leaves are borne on long petioles and the flowers have green sepals with dark maroon-red to black petals (Van der Walt & Vorster. 1988). This plant is widely distributed in the eastern parts of South Africa and in Lesotho (Dreyer & Marais. 2000). Its common names include Umckaloabo and South African Geranium.



Figure 1-12: Image of *Pelargonium sidoides* plant (Research On Medical. 2013)

Medicinal plants are a significant facet of the daily lives of many people and *P. sidoides* has been used as traditional medication and has a rich ethnobotanical history. Studies conducted on *P. sidoides* suggest that its roots contain compounds with antimicrobial and immunomodulating activity, as well as clinically proven effects on the mucociliary system and malaise (Brendler & Van Wyk. 2008). The tubers of this plant contain tannins, coumarins, phenolic acids and phenylpropanoid derivatives. The activity of the medicine prepared from this plant is partly due to the presence of Umckalin, as well as coumarin glycosides and sulphates (Kolodziej. 2007).

Although *P. sidoides* has been cost effectively used to cure various disorders, there is still a lack of good scientific evidence available on the mode of these plants activities. Despite the considerable amount of clinical studies and research conducted (Kolodziej. 2011), to transform this traditional medicinal plant into a successful phytomedicine, there are still many unknowns in this field of study. Hence, it is very important to examine and further access the efficacy and action of this plant.

## **1.5 Research Formulation**

### **1.5.1 The Research Problem**

The treatment of TB is not an easy process as it involves the administration of various antibiotics, such as isoniazid, rifampicin, pyrazinamid, streptomycin and ethambutol, over a long period of time during which patients often misuse the drugs (World Health Organisation. 2014).

Other challenges to effective TB treatment are its co-infection with HIV and the development of strains with multi-drug resistance (Yang et al. 2011). The main cause of multidrug-resistant TB (MDR-TB) is due to the incorrect use of anti-TB drugs or the use of low quality medication (World Health Organisation. 2014). Consequently, the first-line treatment has no effect on these resistant bacteria. This is a disadvantage, as the second line treatment is expensive, limited and the required chemotherapy causes critical drug reactions in patients (World Health Organisation. 2014). In certain exceptional cases, extensively drug-resistant TB (XDR-TB) develops which is usually unaffected by most treatment, including second-line medication. Resistant Mtb strains are present in almost all countries and this is rapidly becoming a major health concern (World Health Organisation. 2014). Thus, the need for new antibacterial drugs is evident.

### **1.5.2 Rationale for study**

The identification of potential drug targets against Mtb is a crucial and on-going field of research. TB is curable and preventable and the vast majority of fatal cases can be eliminated when high-quality medication and treatment is cost effective and readily available. Hence, the research and discovery of novel drug targets to treat TB is highly imperative.

The elimination of TB has been hindered due to the lack of understanding of the survival strategies used by this pathogen when in stressed environments (Yang et al. 2011). There are still gaps missing in this research area and there is a need to build on previous research.

A group of enzymes called kinases are targeted in this study because these enzymes are crucial for the metabolism and, hence, the survival of Mtb. The starting point of this research was to target eight specific Mtb kinases. These enzymes are representatives of different classes

of kinases based on their mechanism of phosphoryl transfer (Kenyon et al. 2012). Due to the properties of the kinases as well as the nature of Mtb physiology, it was highly beneficial, at a preliminary phase, to isolate, purify and functionally express these kinases. This however, has previously been conducted for the SK enzyme, by Kenyon et al. (2011), and the resulting information has been used, and included, in this research project to further investigate this enzyme. The eukaryotic enzymes were included in this study to set a benchmark of comparison, to enable future work to be done. Identifying suitable enzymes within Mtb and being able to use them to screen against potential inhibitory compounds in *P. sidoides*, with the eventual goal of developing a drug, will contribute significantly to progress in this field of research.

### 1.5.3 Research aims

The aim of this project was to produce eight recombinant TB kinases, express them in *Escherichia coli* and purify the proteins in order to determine appropriate expression. Thereafter, each kinase was screened against an extract prepared from *P. sidoides* to identify any inhibitory effect in this plant extract.

### 1.5.4 Research objectives

Chapter 2: Gene Identification, Amplification and Cloning of kinases

- To identify the putative gene sequences of the kinases using information from the annotated genome of Mtb and reported sequences of similar enzymes
- To amplify such kinase genes using polymerase chain reaction (PCR)
- To clone the PCR amplicons into vectors for expression in *E. coli*

Chapter 3: *E. coli* Expression and Protein Purification

- To express these genes in *E. coli* and develop optimal purification methods for each kinase

Chapter 4: Functionality of enzymes

- To develop and optimise validated assays to determine functionality for each kinase

Chapter 5: Screening against *Pelargonium sidoides*

- To screen each kinase against an extract prepared from *P. sidoides* to determine whether enzyme activity is inhibited by the plant extract

# Chapter 2: Gene Identification, Amplification and Cloning

---

## 2.1 Introduction

### 2.1.1 Overview of objectives

This chapter describes the preliminary stages of the study. The aim was to construct recombinant kinase expression vectors and in order to accomplish this, the use of recombinant DNA technology concepts, techniques and methods were applied.

Firstly, the basic principles of genetic manipulation were used to identify and amplify specific DNA fragments from the annotated Mtb H37Rv genome. Selective amplification of the DNA fragments was carried out by Polymerase Chain Reactions (PCR) with the aid of polymerase and specific primers. The successful amplification of DNA fragments and the size of the PCR amplicons were determined following the analysis of electrophoresed agarose gels.

Secondly, the joining of the DNA fragments into a vector, an extra chromosomal element carrier, was carried out. The amplified DNA fragments were cloned into Novagen vectors, via the pGEM®-T Easy vector, through the process of ligation. Screening and selection protocols were used to detect the successful cloned products.

Thirdly, the recombinant DNA was transferred into a living system, a host cell, with the eventual goal of producing useful proteins. This was achieved by the procedures of transformation by electroporation.

Lastly, the sequence of the insert in the expression vector was analysed and verified by nucleotide sequencing.

### **2.1.2 Mtb genes**

The complete genome sequence of the Mtb H37Rv strain has been determined and examined extensively to increase our understanding of this pathogen, with the intention of designing new therapeutic treatments. Using this annotated genome along with reported sequences for similar enzymes, the putative gene sequences were identified for the selected kinases (refer to Section 1.3).

## 2.2 Materials and Methods

### 2.2.1 Gene identification

#### 2.2.1.1 Primer design

The putative kinase genes were identified in the annotated genome of H37Rv Mtb, deposited at NCBI as NC\_000962.2. To amplify these genes, forward and reverse primers were designed (refer to Table 2-1). This was not done for SK, as the Mtb *aroK* gene was received from the laboratory of Chris Abell, University of Cambridge. The construct was originally obtained by them from AZ India. The SK work carried out has been repeated from previous work conducted by Kenyon et al. (2011) to be further investigated in this research study.

These recombinant kinase genes were flanked by restriction endonuclease recognition sequences at the 5' and 3' ends. The PCR primers were designed such that the amplified genes could be cloned into a selected vector, in-frame and with a His-tag at the C- or N-terminal (refer to Table 2-1 and 2-2). All protein structures were checked on the Protein Data bank (PDB) for steric effects, to determine if the His-tag would impact on functionality. On the basis of this, the His-tag was either added at the C- or N-terminal. Refer to Appendix A for the His-tagged Mtb kinase protein sequences.

The forward and reverse primers designed were analysed for specificity, internal stability and potential mis-priming using the software programme DNAMAN (Lynnon Biosoft). This programme also predicts the molecular weight and the pI of the encoded kinases (refer to Table 2-2). The forward and reverse primers were synthesized by Integrated DNA Technologies (IDT). The primers were dissolved in distilled water to a final concentration of 100  $\mu$ M, incubated at 37°C to ensure a complete solution and subsequently stored at -20°C according to the manufacturer's instructions. Working stocks were made to a final concentration of 2.5  $\mu$ M and also stored at -20°C.



Table 2-1: Particular forward and reverse primers used to amplify specific kinase genes. Note also preferred Novagen vector for each construct.

Kinase	Kinase gene	Forward and Reverse primers	pET vector
<b>NDK</b>	<i>ndkA</i> Rv2445c	<i>ndkA</i> -Fwd (5'-GGCATATGACCGAACGGACTCTGGTACTG-3', <i>NdeI</i> recognition site underlined) <i>ndkA</i> -Rev (5'-GTGGATCCTTAGGCGCCGGGAAACCAG <i>Bam</i> HI recognition site underlined)	pET-16b
<b>HSK</b>	<i>thrB</i> Rv1296	<i>thrB</i> -Fwd (5'-GGCATATGGTGACTCAAGCATTG-3', <i>NdeI</i> recognition site underlined) <i>thrB</i> -Rev (5'-GTCTCGAGACCGGGAAGTCTTACTG-3', <i>XhoI</i> recognition site underlined)	pET-20a
<b>AK</b>	<i>ackA</i> Rv0409	<i>ackA</i> -Fwd (5'-GGCATATGGAGTAGCACCGTGCTGGTGATCAAT-3', <i>NdeI</i> recognition site underlined) <i>ackA</i> -Rev (5'-GTGGATCCTTACGCTCGGCGTCC-GCCCAG-3', <i>Bam</i> HI recognition site underlined)	pET-16b
<b>GK</b>	<i>glpK</i> Rv3696c	<i>glpK</i> -Fwd (5'-GGCATATGTCCGACGCCATCCTAG-3', <i>NdeI</i> recognition site underlined) <i>glpK</i> -Rev (5'-CATGTCCGACTTAGGACACGTCAACCCAATCC <i>SalI</i> recognition site underlined)	pET-16b
<b>ThiL</b>	<i>thiI</i> Rv2977c	<i>thiI</i> -Fwd (5'-GGTACATATGACCACTA AAGATCACTC-3', <i>NdeI</i> Recognition site underlined) <i>thiI</i> -Rev (5'-GATCTCGAGTTACCCTAGCGAACCTTG-3', <i>XhoI</i> Recognition site underlined)	pET-28a
<b>RBKS</b>	<i>rbks</i> Rv2436	<i>rbks</i> -Fwd (5'-GTACATATGGCAAACGCCAGTGAG-3', <i>NdeI</i> Recognition site underlined) <i>rbks</i> -Rev (5'-GATCTCGAGTTATGAACCGTTGTG-3', <i>XhoI</i> Recognition site underlined)	pET-28a
<b>AsK</b>	<i>ask</i> Rv3709c	<i>ask</i> alpha-Fwd (5'-GATTACATATGGCGCTCGTCGTGCAG-3', <i>NdeI</i> Recognition site underlined) <i>ask</i> alpha-Rev (5'-GATGTCCGACTTACCGTCCCGTCCCCG-3', <i>SalI</i> Recognition site underlined) <i>ask</i> beta-Fwd (5'-GATCATATGGAAGACCCCATCCTGACCG-3', <i>NdeI</i> Recognition site underlined) <i>ask</i> beta-Rev (3'-GCCCCTGC CCTGCCAGCTGTATG-5', <i>SalI</i> Recognition site underlined)	CDFDuet-1 and pET-26a
<b>SK</b>	<i>aroK</i> Rv2539c	Primers were not designed as the <i>aroK</i> plasmid was received from the laboratory of Chris Abell, University of Cambridge	pET-15b

Table 2-2: Kinase genes and their relevant information

Kinase gene	C or N-terminal 6 His-tag	Antibiotic resistance and concentration used ( $\mu\text{g/ml}$ )	Number of base pairs of gene insert (bp)	Number of base pairs of insert plus vector (bp)	Predicted Molecular weight (kDa) of kinase	Predicted pI of kinase
<b><i>ndkA</i></b> <b>Rv2445c</b>	N-terminal	Amp, 100	415	6114	14.4	6.94
<b><i>thrB</i></b> <b>Rv1296</b>	C-terminal	Amp, 100	952	4538	33.4	5.45
<b><i>ackA</i></b> <b>Rv0409</b>	N-terminal	Amp, 100	1162	6861	43.7	7.3
<b><i>glpK</i></b> <b>Rv3696c</b>	N-terminal	Amp, 100	1558	7262	58.2	5.74
<b><i>thil</i></b> <b>Rv2977c</b>	N-terminal	Kan, 50	1006	6295	36.4	5.31
<b><i>rbks</i></b> <b>Rv2436</b>	N-terminal	Kan, 50	919	6208	32.3	6.64
<b><i>ask</i></b> <b>Rv3709c</b>	No His tag (alpha) C-terminal (beta)	Strep, 50 (alpha) and Kan, 50 (beta)	1268 (alpha) and 520 (beta)	4993 (alpha) and 5750 (beta)	44.4 (alpha) and 19.2 (beta)	4.78 (alpha) and 4.89 (beta)
<b><i>aroK</i></b> <b>Rv2539c</b>	N-terminal	Amp, 100	535	6231	20.7	11.3

### 2.2.1.2 Authentication of template

The template, H37Rv gDNA (~4.4 Mbp), was received from Ian Wiid, University of Stellenbosch. The concentration of the template was diluted to 100 ng/ $\mu\text{l}$  from its initial concentration of 540 ng/ $\mu\text{l}$  and 1  $\mu\text{l}$  of this was loaded onto a 0.8% [w/v] agarose gel containing ethidium bromide and electrophoresed according to the method of agarose gel electrophoresis described in Section 2.2.2.2.

## 2.2.2 DNA amplification

### 2.2.2.1 PCR Amplification

The primers, indicated in Table 2-1, and the genomic DNA from Section 2.2.1.2 were used in PCR to amplify the DNA fragments. Note, that this was not performed for the *aroK* gene encoding SK as this was received already subcloned into a vector. All the amplification reactions were performed in a thermocycler, Eppendorf Mastercycler ep Gradient S PCR machine, in 0.2 ml PCR tubes. Various PCR parameters were tested in order to obtain optimal amplification. The final PCR mixtures, in a total volume of 100  $\mu$ l, contained 0.42 ng/ $\mu$ l of the H37Rv template, distilled water, 1X buffer (GC+ Mg<sub>2</sub>, supplied with *Taq*), 0.3 mM dNTP's, 0.3  $\mu$ M forward primer, 0.3  $\mu$ M reverse primer and 1U DNA polymerase KAPA HiFi (KAPA Biosystems. USA). This polymerase was used as it is thermostable and generates high fidelity amplicons and proof reading activity (KAPA Biosystems. 2014). The PCR cycling profile composed of a 2 minute denaturing step at 95°C. This was then followed by 25 cycles of denaturation at 98°C for 20 seconds, annealing at the appropriate temperature (refer to table 2-3) for 20 seconds and extension at 72°C for 60 seconds. A final extension of 72°C for 5 minutes was conducted and the PCR products were stored at 4°C.

Table 2-3: Kinase genes and their specific annealing temperatures for the PCR reactions

<b>Kinase gene</b>	<b>Annealing temperature (°C)</b>
<i>ndkA</i> Rv2445c	60°C
<i>thrB</i> Rv1296	50°C
<i>ackA</i> Rv0409	50°C
<i>glpK</i> Rv3696c	50°C
<i>thil</i> Rv2977c	58°C
<i>rbks</i> Rv2436	58°C
<i>ask</i> Rv3709c	58°C
<i>aroK</i> Rv2539c	Not applicable

### 2.2.2.2 Agarose gel Electrophoresis

In order to visualize the amplicons, an agarose gel, as described by Sambrook et al. (1989) was utilized. The PCR products were diluted in a 10:1 ratio, with loading dye (10% [w/v] glycerol, 0.09% [w/v] Bromophenol blue, 0.09% [w/v] Xylene cyanol ff, 10 mM Tris pH 7.6 and 10 mM EDTA). These samples were analysed by loading onto an agarose gel (Saarchem-Merck. South Africa), containing 0.8% [w/v] agarose powder, 0.5 µg/ml ethidium bromide, in 100 ml of 1 X TAE buffer (40 mM Tris-HCl, 20 mM NaOAc and 1 mM EDTA; pH 8.5) and electrophoresed at 90 volts through a 0.8% agarose gel using a Power Pac Universal™. A 1 kb DNA ladder was used as a standard molecular weight marker (O'Gene Ruler™, Fermentas. USA) to assess the size of the separated amplicon bands. The gel was viewed on a UV transilluminator, Alpha imager™ 3400 (Alpha Innotech), because the ethidium bromide intercalates DNA and emits fluorescence under UV light (Nicholl. 2008).

### 2.2.2.3 Purification from agarose gel

In order to obtain ultra-pure DNA, a clean scalpel blade was used to excise the correct DNA fragment from the agarose gel before the PCR products, with blunt ends, were purified from the agarose gel using the Zymoclean™ Gel DNA recovery kit (Zymo Research), according to the manufacturer's instructions. The purity and concentrations of the eluted DNA was determined by running 1 µl of DNA on an agarose gel (as in Section 2.2.2.2) together with MassRuler Express High and Low Range markers (Fermentas. USA).

## **2.2.3 Cloning into pGEM®-T Easy vector (Promega. USA)**

### 2.2.3.1 Insertion into pGEM®-T Easy vector (Promega. USA)

The pGEM-T Easy sub-cloning technique is a common, convenient intermediate step used to clone PCR products (Promega. 2010). The blunt end kinase PCR products were A-tailed using the polymerase KAPA 2G Fast enzyme (KAPA Biosystems. USA) as it is a non-proof reading enzyme. This reaction mix consisted of the PCR products, 1 X 2G buffer + Mg<sub>2</sub>, 1.3 mM dATP, and 1 U KAPA 2G Fast enzyme. This was then incubated at 72°C for 5 minutes and then cooled down to 4°C for 5 minutes in the thermocycler. The kinase genes consequently contained 3'-A overhangs, which facilitated their A/T cloning into the suitably treated sites within the

commercial pGEM®-T Easy vector (refer to Appendix B for vector map) according to the manufacturer's instructions (Promega. USA).

#### 2.2.3.2 Ligation of DNA fragments into pGEM®-T Easy vector

The kinase gene PCR products were then ligated into pGEM®-T Easy vector. Ligation is the covalent linking of two ends of DNA with the aid of the ligase enzyme. The purified A-tailed kinase inserts and pGEM®-T Easy vector were combined in a molar ratio of 3:1 (vector: insert). The amount (ng) of insert required was determined by the equation:

$$\text{ng of insert} = [(\text{ng of vector} \times \text{kb size of insert}) / \text{kb size of vector}] \times 3$$

The ligation reactions were performed with the aid of T4 DNA ligase, according to the manufacturer's instructions (Promega. USA). Each ligation reaction consisted of distilled water to a total volume of 10 µl, 25 ng pGEM®-T Easy vector, 1X T4 DNA ligase reaction buffer (10X stock), 1 U T4 DNA ligase and the 3:1 molar excess of kinase insert. The ligation reactions were incubated at 16°C for 16 hours and thereafter inactivated at 70°C for 15 minutes.

#### 2.2.3.3 Preparation of competent cells

*E. coli* cells in general have to be made competent for foreign DNA uptake since these cells are not naturally transformable. Therefore, the preparation of electro-competent *E. coli* cells was carried out. An overnight *E. coli* culture was inoculated into 200 ml sterile LB broth (1% [w/v] NaCl, 0.5% [w/v] yeast extract and 1% [w/v] tryptone; pH 7) and incubated at 37°C until an OD<sub>600</sub> of 0.6 was reached. The culture was subsequently incubated on ice for 30 minutes and the cells were then harvested by centrifugation at 6000 g for 10 minutes in a Sorvall RC-5B centrifuge. The cells were rinsed twice with 50 ml of ice-cold 10% [v/v] glycerol and suspended in 0.6 ml of ice-cold GYT medium (10% [v/v] glycerol, 0.125% [w/v] yeast extract, 0.25% [w/v] tryptone; pH 7.3). Aliquots of 80 µl of the cells were pipette into 1.5 ml Eppendorf tubes and stored at -70°C until further use.

#### 2.2.3.4 Electroporation and Transformation into *E. coli* DH10B cells

Aliquots (80 µl) of competent *E. coli* DH10B cells were thawed on ice, and to each was added 1 µl of the ligation mixtures containing the kinase insert and pGEM®-T Easy plasmid. This was

then transferred to cold electroporation cuvettes with a 0.1 cm electrode gap (Sigma-Aldrich, South Africa). The DNA was introduced into the electro-competent *E. coli* cells by electroporation according to the protocol described by Dower et al (1988). Briefly, the cells were exposed to a single electrical pulse using the Bio-Rad Gene-Pulser™ set at 1.6 kV, 25 µF and 200 Ω. To revive the bacterial cells, this reaction mix was added to 1 ml Super Optimal Catabolite-repression (SOC) media (2% [w/v] tryptone, 0.5% [w/v] yeast extract, 10 mM NaCl, 2.5 mM KCl, 10 mM MgCl<sub>2</sub>, 20 mM MgSO<sub>4</sub> and 20 mM glucose; pH 7) for high transformation efficiency and incubated for 1 hour at 37°C with shaking at 200 rpm. For selection of recombinant clones, 200 µl aliquots of the transformed cells were spread plated on LB agar plates (1% [w/v] NaCl, 0.5% [w/v] yeast extract, 1% [w/v] tryptone and 1.2% [w/v] bacteriological agar; pH 7), 0.1 mM IPTG and 80 µg/ml X-Gal, supplemented with appropriate antibiotics (refer to Table 2-2) to ensure selective growth. The antibiotics were purchased from Sigma-Aldrich. These plates were incubated overnight at 37°C.

## **2.2.4 Identification of successful cloned products**

### **2.2.4.1 PCR screening and inoculation**

The visual indication technique called blue-white screening was used. The white colonies were distinguished as successful cloned products and, therefore, numerous white colonies were PCR screened to quickly test for the presence of the desired gene, without the need to grow and prepare all the colonies. A few of the white colonies were resuspended in 25 µl distilled water and 1 µl of this suspension was added to 9 µl of the colony screen PCR reaction mix. The PCR reaction mix consisted of distilled water, 1X buffer, 0.2 mM dNTP's, 0.5 µM forward primer, 0.5 µM reverse primer and 0.02 U/µl DNA polymerase KAPA 2G Fast enzyme (KAPA Biosystems, USA). The polymerase KAPA 2G Fast enzyme was used as it allows for high speed and processing (KAPA Biosystems, 2014). This was then run on the thermocycler, with the PCR cycling profile composed of a 1 minute denaturing step at 95°C. This was then followed by 30 cycles of denaturation at 95°C for 15 seconds, annealing at 50°C for 15 seconds and extension at 72°C for 15 seconds. A final extension of 72°C for 60 seconds was conducted and the PCR products were stored at 4°C. The PCR products were analysed by agarose gel electrophoresis (as in Section 2.2.2.2) to determine amplification at the correct sized fragments. The positive colonies were dotted onto LB agar plates supplemented with appropriate antibiotics and 2 positive colonies, per kinase, were then inoculated into 5 ml LB broth supplemented with the

appropriate antibiotics (refer to Table 2-2) and incubated overnight at 37°C with shaking at 200 rpm.

#### 2.2.4.2 Restriction enzyme digest for confirmation

The plasmid DNA from the inoculated cultures was prepared using the Zyppy™ Plasmid Miniprep kit according to the manufacturer's instructions (Zymo Research. USA). The eluted plasmid DNA was used to set up a restriction enzyme double digest according to the manufacturer's instructions (Thermo Fisher Scientific Fermentas. USA). Digestion reactions were each set up in a total volume of 25 µl and consisted of approximately 1 to 2 µg of purified DNA, 0.4 U/µl of appropriate restriction endonucleases, distilled water and 1X buffer with the appropriate concentration of salt using the 10X buffer supplied by the manufacturer (Fermentas. USA) (refer to Table 2-4). The reactions were incubated for ±1 hour at 37°C and then stopped by adding loading dye and analysed by electrophoresis through a 0.8% agarose gel (as in Section 2.2.2.2) to confirm the correct sizes.

Table 2-4: Kinase genes and their respective restriction enzymes and buffers used to confirm insert size

<b>Kinase gene</b>	<b>Restriction enzymes</b>	<b>10X buffer</b>
<b><i>ndkA</i> Rv2445c</b>	<i>Bam</i> HI and <i>Nde</i> I	Buffer R <sup>+</sup>
<b><i>thrB</i> Rv1296</b>	<i>Xho</i> I and <i>Nde</i> I	Buffer O
<b><i>ackA</i> Rv0409</b>	<i>Bam</i> HI and <i>Nde</i> I	Buffer R <sup>+</sup>
<b><i>glpK</i> Rv3696c</b>	<i>Sal</i> I and <i>Nde</i> I	Buffer O
<b><i>thil</i> Rv2977c</b>	<i>Xho</i> I and <i>Nde</i> I	Buffer O
<b><i>rbks</i> Rv2436</b>	<i>Xho</i> I and <i>Nde</i> I	Buffer O
<b><i>ask</i> Rv3709c</b>	<i>Nde</i> I and <i>Sal</i> I (alpha) <i>Nde</i> I and <i>Sal</i> I (beta)	Buffer O
<b><i>aroK</i> Rv2539c</b>	Not applicable	Not applicable

### 2.2.4.3 Kinase insert DNA purification

Following the confirmation of the correctly sized plasmid DNA from section 2.2.4.2, a large double digest was set up and, following digestion for 2 hours, the digestion products were run on an agarose gel in order to separate the kinase insert DNA from the pGEM®-T Easy vector. The insert was purified (as in Section 2.2.2.3) using the Zymoclean™ Gel DNA recovery kit. Thereafter, 1 µl of the purified kinase DNA was run on an agarose gel together with the Fermentas MassRuler Express High and Low Range marker to determine their concentrations and assess the purity of the DNA. This was subsequently stored at -20°C for use at a later stage.

## 2.2.5 Cloning into selected pET vector

### 2.2.5.1 Vector preparation

Expression vectors (Novagen, Germany) (refer to Appendix B for vector maps) were selected to allow for in-frame fusion with the C- or N-terminal His-tag, using specific restriction sites. The particular vectors chosen have a lac operon system for recombinant protein expression as well as genes encoding antibiotic resistance (refer to Table 2-2) to ensure selective growth. The expression vectors were purified from inoculated vector cultures using the Zyppy™ Plasmid Miniprep kit. These were then double digested using the selected restriction enzymes (refer to Table 2-5). The use of different flanking restriction enzymes allows for immediate selection of correct orientation of the insert within the vector. This was then run on a 0.8% agarose gel and purified (as in Section 2.2.2.2 and 2.2.2.3) using the Zymoclean™ Gel DNA recovery kit according to the manufacturer's instructions. Subsequently, 1 µl of the purified vector was run on an agarose gel together with the Fermentas MassRuler Express High and Low Range markers to determine their concentrations and assess the purity of the DNA. This was then stored at -20°C for use at a later stage.



Table 2-5: Kinase genes with their vectors and respective restriction enzymes and buffers used for digests

Kinase gene	Vector	Restriction enzymes	10X buffer
<b><i>ndkA</i></b> <b>Rv2445c</b>	pET-16b	<i>Bam</i> HI and <i>Nde</i> I	Buffer R <sup>+</sup>
<b><i>thrB</i></b> <b>Rv1296</b>	pET-20b	<i>Xho</i> I and <i>Nde</i> I	Buffer O
<b><i>ackA</i></b> <b>Rv0409</b>	pET-16b	<i>Bam</i> HI and <i>Nde</i> I	Buffer R <sup>+</sup>
<b><i>glpK</i></b> <b>Rv3696c</b>	pET-16b	<i>Xho</i> I and <i>Nde</i> I	Buffer R <sup>+</sup>
<b><i>thiI</i></b> <b>Rv2977c</b>	pET-28a	<i>Xho</i> I and <i>Nde</i> I	Buffer O
<b><i>rbks</i></b> <b>Rv2436</b>	pET-28a	<i>Xho</i> I and <i>Nde</i> I	Buffer O
<b><i>ask</i></b> <b>Rv3709c</b>	CDFDuet-1 (alpha) and pET-26a (beta)	<i>Nde</i> I and <i>Xho</i> I (alpha) <i>Nde</i> I and <i>Xho</i> I (beta)	Buffer O
<b><i>aroK</i></b> <b>Rv2539c</b>	Not applicable	Not applicable	Not applicable

### 2.2.5.2 Ligation of kinase insert into selected vector

The pure kinase inserts were ligated into the appropriate expression vector with the aid of the FAST-Link™ DNA ligation kit (Epicentre Technologies, USA). The 10 µl ligation reactions consisted of distilled water, 25 ng of the appropriate vector, 1X buffer, 0.15 U/µl DNA FAST-Link™ ligase and kinase insert at the appropriate ratio compared to the vector. The ligation reactions were incubated at 16°C for 16 hours and thereafter inactivated at 70°C for 15 minutes.

### 2.2.5.3 Transformation into *E. coli* DH10B cells

The ligations were transformed by electroporation into *E. coli* DH10B cells as described in Section 2.2.3.4. For selection of recombinant clones, 50 µl of the bacterial cells were spread onto LB agar plates supplemented with appropriate antibiotic before incubating overnight at 37°C. Random colonies were selected for PCR screening and the successful colonies were inoculated into 5 ml LB broth and incubated overnight at 37°C (as in Section 2.2.4.1). The plasmid DNA from the inoculated cultures was prepared using the Zyppy™ Plasmid Miniprep kit, according to the manufacturer's instructions, and eluted in 30 µl and stored at -20°C.

Restriction enzyme digests (refer to Table 2-4) were performed to confirm the successful ligation of the kinase insert DNA in the selected vector (as in Section 2.2.4.2). Glycerol stocks (25% [v/v] glycerol) were made of the correctly cloned cultures and stored at -70°C.

#### 2.2.5.4 Transformation into *E. coli* BL21(DE3)

The final host for the plasmid was *E. coli* BL21 (DE3), as it is well suited for high level protein expression. The DNA from 2.2.5.3 was electroporated (as in Section 2.2.3.4) into *E. coli* BL21 (DE3) cells. For selection of recombinant clones, 50 µl of the bacterial cells were spread onto LB agar plates supplemented with the appropriate antibiotics (refer to Table 2-2). These plates were incubated overnight at 37°C. Thereafter, 2 colonies per kinase were inoculated into 5 ml LB broth and incubated overnight at 37°C (as in Section 2.2.4.1) and purified using the Zyppy™ Plasmid Miniprep kit according to the manufacturer's instructions. Restriction enzyme digests were performed for confirmation (as in Section 2.2.4.2, refer to Table 2-4) and glycerol stocks (25% [v/v] glycerol) were made of the correctly cloned cultures and stored at -70°C. These final restriction enzyme digests were required for an initial screen before being sent for sequencing. This primary screen is to ensure that the constructs sent for sequencing, contain an insert of the correct size (as estimated via the agarose gel), as sequencing is costly and time-consuming.

Table 2-6: A list of kinase genes and their respective restriction enzymes and buffer used to confirm final digestion

<b>Kinase gene</b>	<b>Restriction enzymes</b>	<b>10X buffer</b>
<i>ndkA</i> Rv2445c	<i>Bam</i> HI and <i>Nde</i> I	Buffer R <sup>+</sup>
<i>thrB</i> Rv1296	<i>Xho</i> I and <i>Nde</i> I	Buffer O
<i>ackA</i> Rv0409	<i>Bam</i> HI and <i>Nde</i> I	Buffer R <sup>+</sup>
<i>glpK</i> Rv3696c	<i>Bam</i> HI and <i>Nde</i> I	Buffer O
<i>thiI</i> Rv2977c	<i>Xho</i> I and <i>Nde</i> I	Buffer O
<i>rbks</i> Rv2436	<i>Xho</i> I and <i>Nde</i> I	Buffer O
<i>ask</i> Rv3709c	<i>Xba</i> I and <i>Xho</i> I (alpha) <i>Sma</i> I (beta)	Buffer Tango
<i>aroK</i> Rv2539c	Not applicable	Not applicable

## 2.2.6 Nucleotide sequencing

The recombinant plasmid DNA was submitted to Inqaba Biotechnical Industries for nucleotide sequencing, on an Applied Biosystem® Model 3500XL automated DNA sequencer, to confirm the sequence of the DNA. The nucleotide sequences obtained were analysed with DNAMAN (Lynnon Biosoft) software for verification of the gene sequences and the in-frame fusions with the relevant His-tags.

## 2.3 Results and Discussion

### 2.3.1 Template authentication

A volume of 1  $\mu$ l of the H37Rv template was run on a 0.8% [w/v] agarose gel as described in the Materials and Methods section. This was conducted in order to confirm that the DNA was not degraded due to the DNA being old or stored under incorrect conditions. The agarose gel, presented in Figure 2-1, proved that the DNA was not degraded as a tight band with not much smearing was observed. The size of the template DNA was significantly larger than the largest segment of the molecular marker ladder; however the gel was not used to quantify the DNA, but merely to rapidly check the quality of the template.

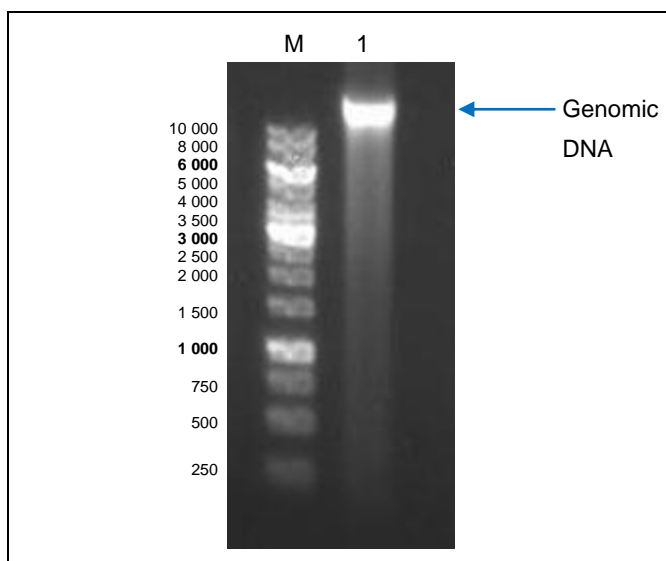


Figure 2-1: Agarose gel electrophoresis of the H37Rv genomic DNA template. The genomic DNA was loaded onto a 0.8% [w/v] agarose gel. M represents the molecular mass marker (O'Gene Ruler™ 1 kb DNA ladder, Fermentas. USA) and the sizes of this marker are indicated to the left of the gel. The blue arrow indicates the genomic DNA template.

### 2.3.2 DNA amplification

Various PCR reactions were prepared using the H37Rv genomic DNA template and primers specific for the amplification of Mtb kinase gene inserts. The sizes of these inserts are shown in Table 2-2 above, as described in Section 2.2.2. As can be noted in Figures 2-2 and 2-3 below, this PCR amplification proved to be specific as DNA bands of the expected sizes were observed in ethidium bromide-stained agarose gels.

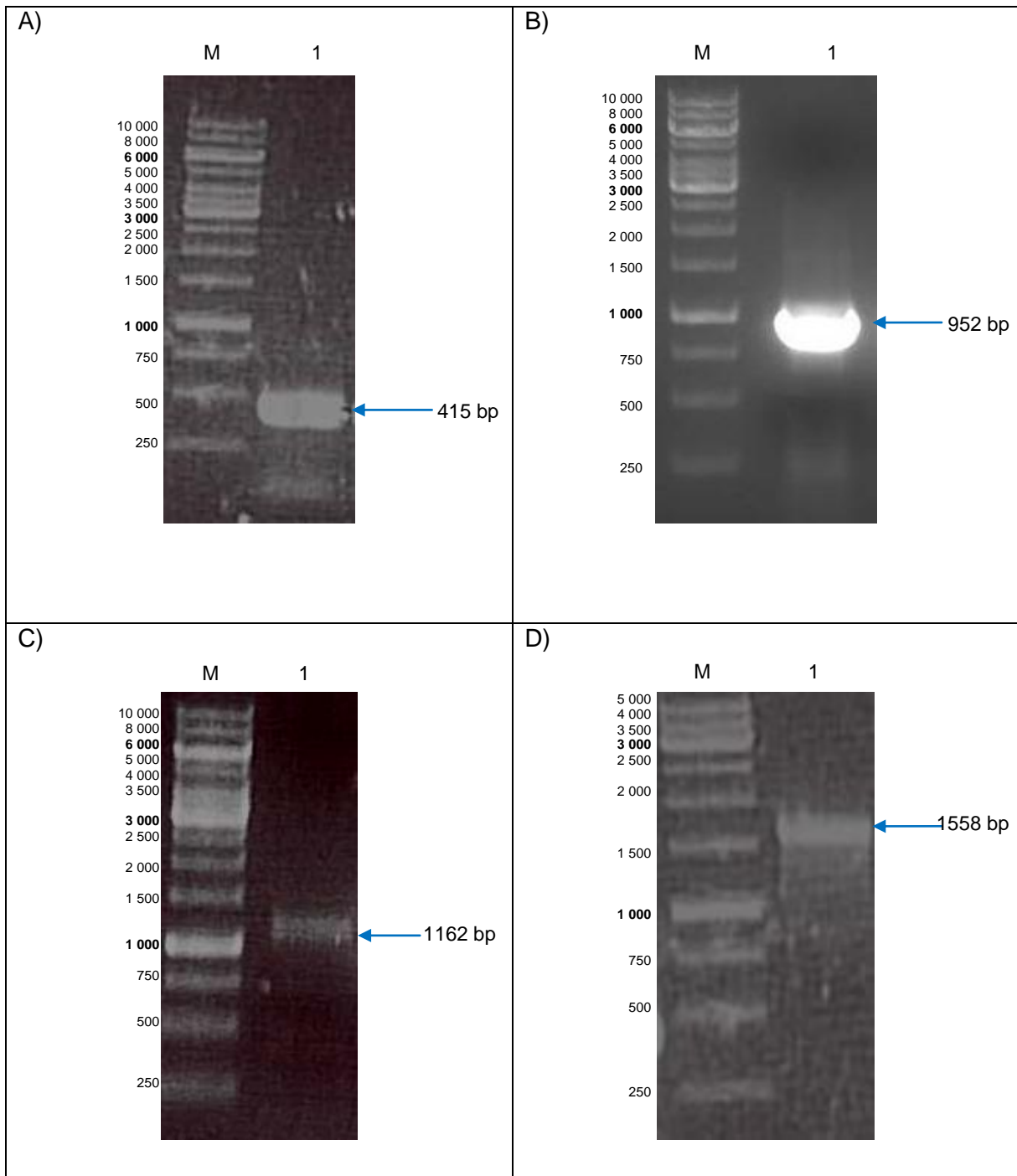


Figure 2-2: Agarose gel electrophoresis of the kinase amplicons obtained by PCR amplification using H37Rv genomic DNA as the template. M represents the molecular mass marker (O'Gene Ruler™ 1 kb DNA ladder, Fermentas, USA) and the sizes of this marker are indicated to the left of the gels. The blue arrow indicates the expected size bands in bp for the amplicons. A) Lane 1 represents the full length *ndkA* amplicon. B) Lane 1 represents the full length *thrB* amplicon. C) Lane 1 represents the full length *ackA* amplicon. D) Lane 1 represents the full length *glpK* amplicon.

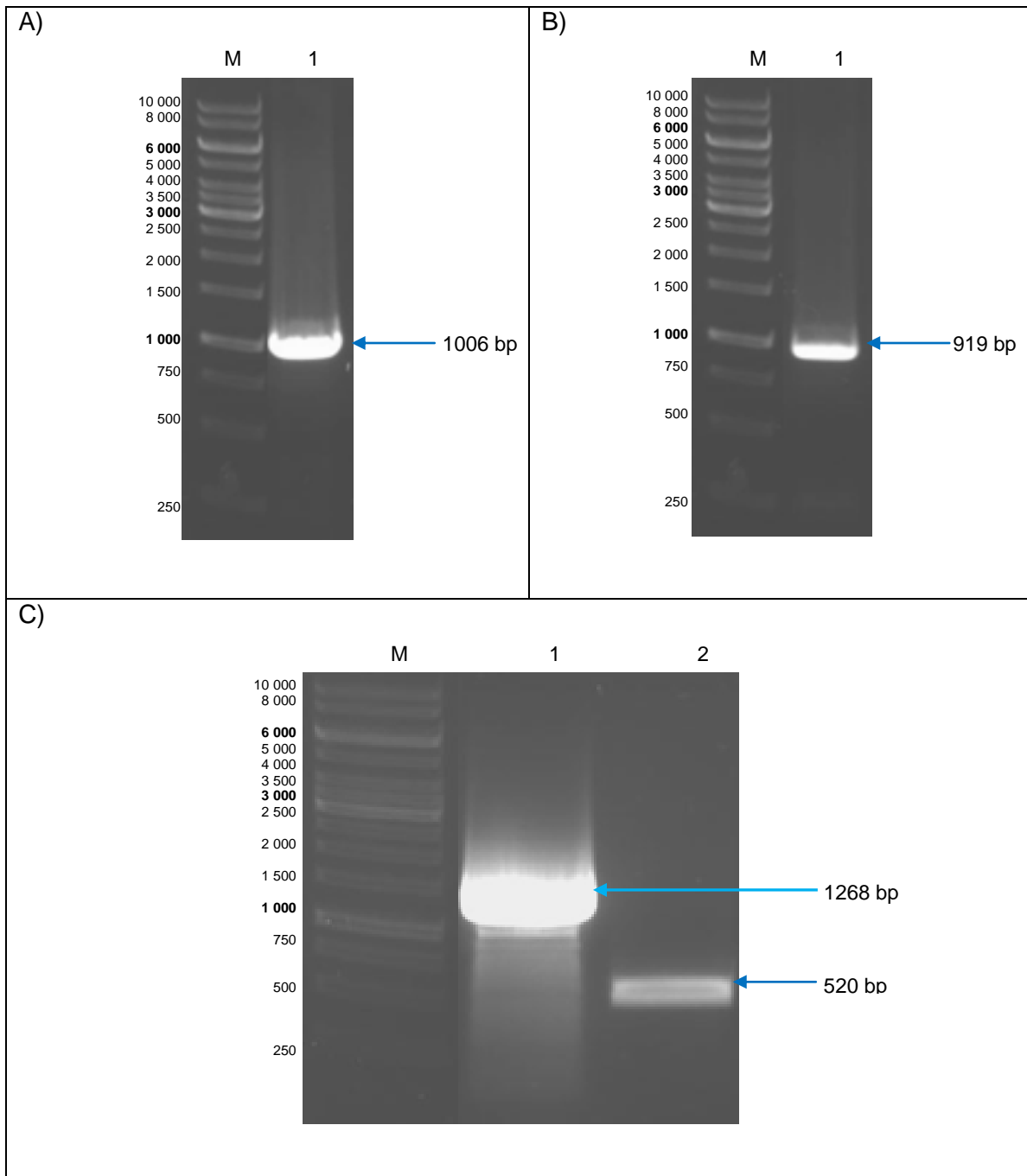


Figure 2-3: Agarose gel electrophoresis of the kinase amplicons obtained by PCR amplification using H37Rv genomic DNA as the template. M represents the molecular mass marker (O'Gene Ruler™ 1 kb DNA ladder, Fermentas. USA) and the sizes of this marker are indicated to the left of the gels. The blue arrow indicates the expected size bands in bp for the amplicons. A) Lane 1 represents the full length *thil* amplicon. B) Lane 1 represents the full length *rbks* amplicon. C) Lane 1 represents the full length *ask* alpha amplicon and lane 2 represents the full length *ask* beta amplicon.

The challenges in gaining optimal amplification were overcome by adjusting annealing temperatures. Amplicons were subjected to gel purifications and thereafter the purified DNA was run on agarose gels together with mass rulers (data not shown) to estimate the DNA concentration for subsequent ligations into vectors as well as to visualize the integrity of the eluted DNA.

### **2.3.3 Plasmid construction**

Kinase gene DNA was first inserted into the pGEM®-T Easy vector system plasmids as described in the Materials and Methods section. The pGEM-T Easy sub-cloning technique proved to be a convenient intermediate step, as it successfully cloned the PCR products (Promega, 2010). The blue-white screening method proved to be effective since it involved the insertional inactivation of the *lac* gene in the presence of the insert which resulted in the formation of white colonies. The *lac* gene encodes for the enzyme  $\beta$ -galactosidase and when there is no insert,  $\beta$ -galactosidase uses X-gal as a synthetic product and IPTG as an inducer and results in the formation of blue colonies. Hence, the white colonies were representatives of positive clones.

The kinase gene DNA that was amplified from H37Rv was cloned into suitable pET vectors (refer to Appendix B). The kinase genes were flanked by restriction endonuclease recognition sequences at the 5' and 3' ends. The genes cloned into its suitable vector, were in-frame with a His-tag at the C- or N-terminal. The complete correct plasmid diagrams are presented in Figures 2-4 and 2-5.

The strong promoter and T7 RNA polymerase favoured the production of the recombinant proteins as described in the following chapters.

The plasmids were verified firstly by PCR amplification of the specific desired gene fragment (as in Section 2.3.2) and secondly by restriction enzyme digestion (refer to Section 2.3.5). The exact amplicons, as well as the accurate digestion fragments were obtained for all plasmids.

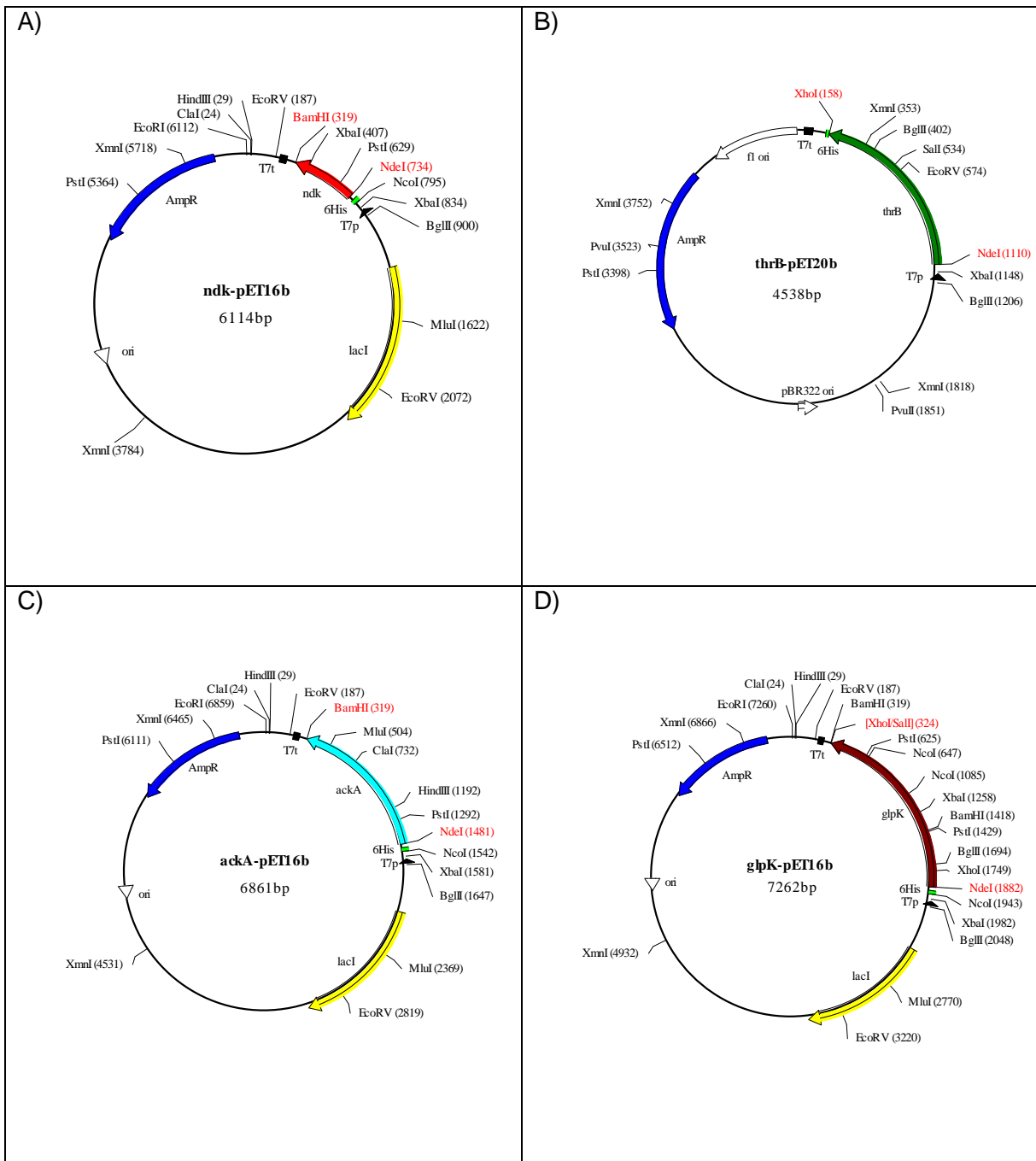


Figure 2-4: Complete plasmid maps. (A) *ndkA*-pET16b, containing the *ndkA* gene Rv2445c in-frame with a N-terminal His-tag. (B) *thrB*-pET20b, containing the Mtb putative *thrB* gene Rv1296 in-frame with a C-terminal His-tag. (C) *ackA*-pET16b, containing the Mtb putative *ackA* gene Rv0409 in-frame with a N-terminal His-tag. (D) *glpK*-pET16b, containing the Mtb putative *glpK* gene Rv3696 in-frame with a N-terminal His-tag.



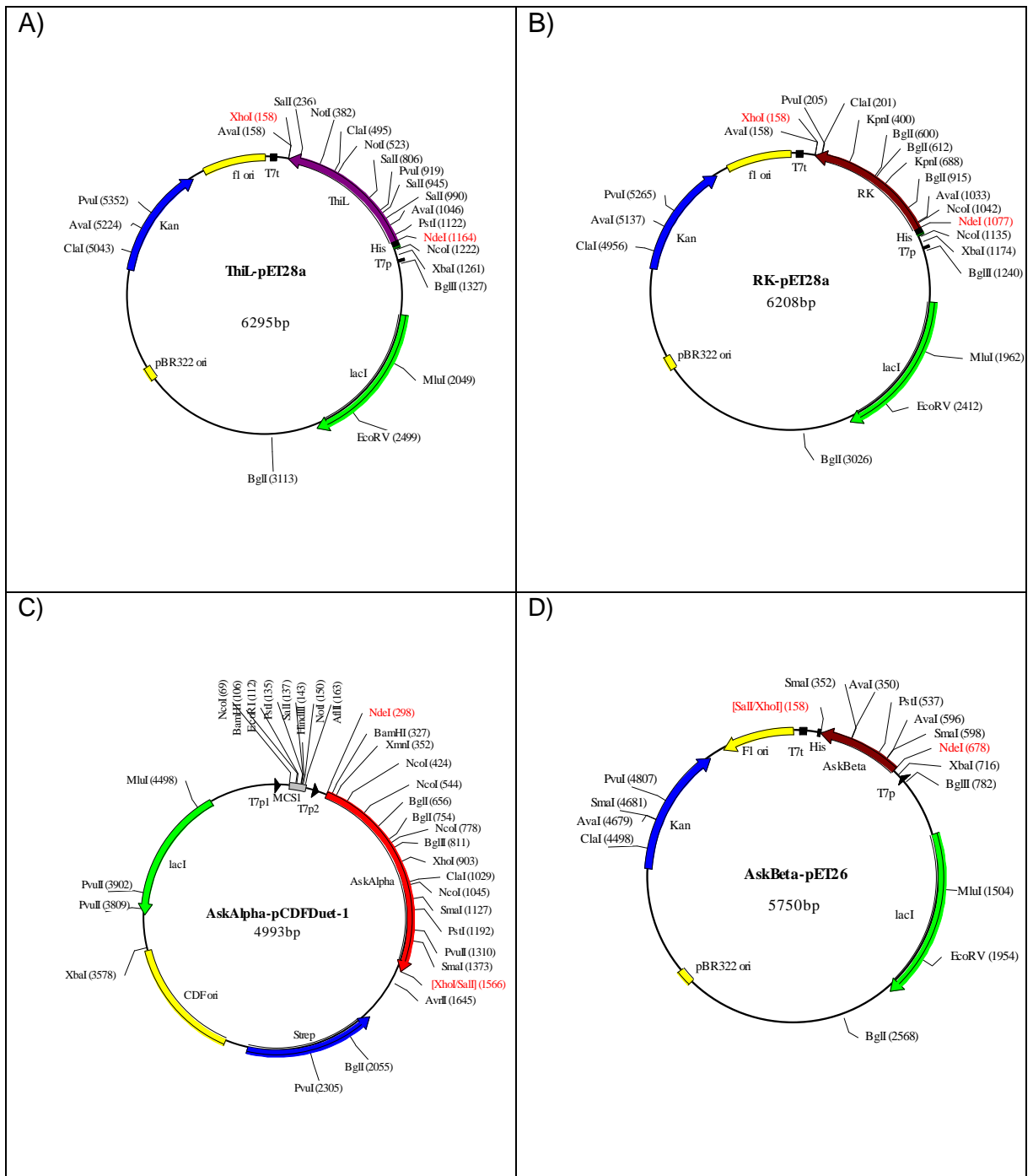


Figure 2-5: Complete plasmids maps. (A) *thiL*-pET28a, containing the Mtb putative *thiL* gene Rv2977c in-frame with a N-terminal His-tag. (B) *rbks*-pET28a, containing the Mtb putative *rbks* gene Rv2436 in-frame with a N-terminal His-tag. (C) *ask alpha*-CDFDuet-1, containing the Mtb putative *ask alpha* gene Rv3709c with no His-tag. (D) *ask beta*-pET26, containing the Mtb putative *ask beta* gene Rv3709c in-frame with a C-terminal His-tag.

### **2.3.4 *E. coli* Transformations**

*E. coli* DH10B competent cells were used as an initial host system throughout the cloning procedures to produce high copy numbers, but *E. coli* BL21 (DE3) was used thereafter as the final expression host for the plasmid as it is well suited and specific for high level protein expression. Throughout the cloning process, the identification of recombinant clones were performed using quick colony PCR screens and only the successful clones, represented by the correct band corresponding to the kinase insert genes, were selected for further procedures. The successful positive recombinants were established by restriction enzyme digestions (refer to Section 2.3.5).

### **2.3.5 Restriction enzyme digests gels**

Digestions were carried out using the appropriate restriction enzymes that flanked the inserts (refer to Section 2.3.3 for the plasmid maps). The results in Figures 2-6 and 2-7 display the correct expected digest sizes on the 0.8% [w/v] agarose gels.

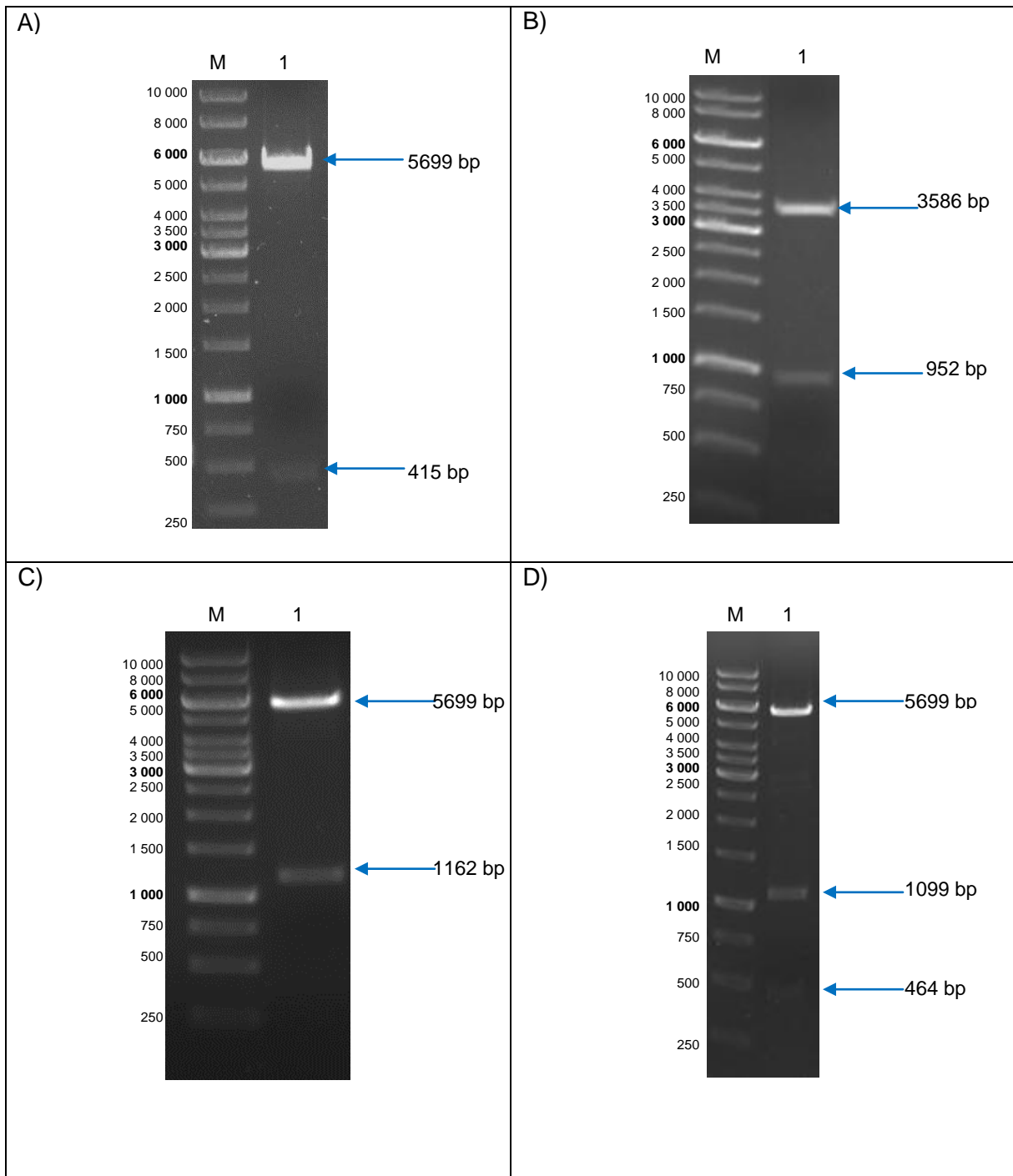


Figure 2-6: Agarose gel electrophoresis of the recombinant vector-kinase inserts eluted from agarose gels following restriction enzyme digestions. M represents the molecular mass marker (O'Gene Ruler™ 1 kb DNA ladder, Fermentas, USA) and the sizes of this marker are indicated to the left of the gels. The blue arrow indicates the expected size bands in bp. A) Lane 1 represents pET16b-*ndkA* DNA digested with *Nde*I and *Bam*HI. B) Lane 1 represents pET20-*thrB* DNA digested with *Nde*I and *Xho*I. C) Lane 1 represents pET16b-*ackA* DNA digested with *Nde*I and *Bam*HI. D) Lane 1 represents pET16b-*glpK* DNA digested with *Nde*I and *Bam*HI.

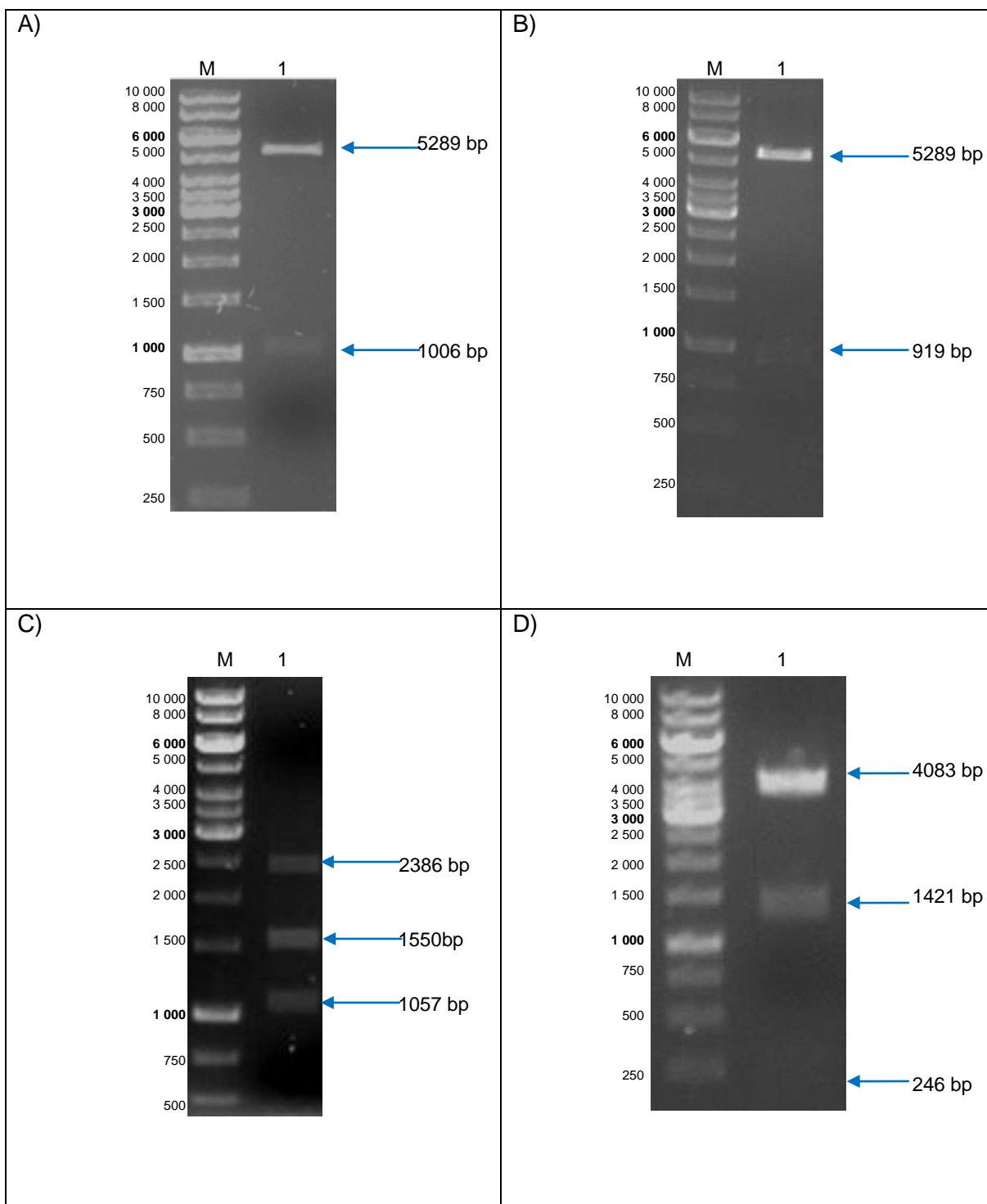


Figure 2-7: Agarose gel electrophoresis of the recombinant vector-kinase inserts following restriction enzyme digestions. M represents the molecular mass marker (O'Gene Ruler™ 1 kb DNA ladder, Fermentas, USA) and the sizes of this marker are indicated to the left of the gels. The blue arrow indicates the expected size bands in bp for the digestions. A) Lane 1 represents pET128a-*thil* DNA digested with *Nde*I and *Xho*I. B) Lane 1 represents pET28a-*rbks* DNA digested with *Nde*I and *Xho*I. C) Lane 1 represents CDFDuet-1-*ask* alpha DNA digested with *Xba*I and *Pst*I. D) Lane 1 represents pET26a-*ask* beta DNA digested with *Sma*I.

### **2.3.6 Nucleotide sequencing**

Sequencing of the genes confirmed that they match identically to the reported Mtb H37Rv genome database. These sequences are indicated in Appendix A below. The fact that the sequences matched to the previously published results (described in Chapter 1: Section 1.3), confirmed the fidelity of the PCR reactions and gene manipulations carried out. This outcome validated the quality of the reagents as well as the methods and technologies applied, which in turn allowed the project to confidently progress into the next stage of research.

### **2.4 Chapter conclusion**

In summation, the aims of this part of the study were to construct expression vectors containing the genes encoding Mtb kinases. The results presented in this chapter indicate that all kinase genes were successfully amplified from Mtb H37Rv genomic DNA and inserted into the chosen expression vectors with either a C- or N-terminal His-tag.

The construction of kinase expression vectors was a preliminary requirement to accomplish the subsequent aims towards the eventual goal of TB drug discovery in order to combat this disease. The kinase expression vectors were then used to produce the kinase proteins in *E. coli*, for purification thereafter. The details regarding this are provided in the following chapter.

# Chapter 3: *E. coli* expression and Protein Purification

---

## 3.1 Introduction

This chapter describes the expression of cloned kinase genes in *E. coli*, and their purification. Protein purification is a sequence of processes used to isolate the protein from a complex mixture such as cells, tissues or organisms, and is fundamental for functional characterization and structure analysis.

Firstly, the cultured cells containing the expressed proteins were broken down by sonication to release the proteins of interest into solution, and then filtered for further purification. Sonication is a mechanical technique that uses high frequency sound energy that disrupts the cell membranes to release the cellular particles for further purification.

Secondly, the solution with the recombinant proteins was purified using appropriate protein purification techniques. Affinity chromatography was utilized, where diverse proteins interact differently with columns packed with various materials, and can, thus, be separated and eluted at different times by altering the chromatography conditions. The purification of soluble his-tagged proteins can be automated with the use of the Bio-Rad Profinia™ System. This method is based on the production of an affinity tag sequence of 6 histidines into the N or C-terminal of the recombinant protein and the attachment of such tagged proteins in nickel-ion affinity columns. The Profinia™ system has convenient Ni-IDA resin-packed cartridges for the ease of purification of his-tagged proteins. Polyhistidine binds strongly to divalent metal ions such as nickel so that as a solution containing his-tagged recombinant proteins is passed through the column containing immobilized nickel ions, all untagged proteins pass through the column whereas the desired protein binds to the column and is subsequently eluted as a result of the addition of imidazole. The imidazole in the elution buffer competes with the polyhistidine tag for binding to the column, which enables the successful elution of the desired protein from the column.

Thirdly, gel electrophoresis via SDS-PAGE (sodium dodecyl sulfate polyacrylamide gel electrophoresis) gels was used to visualize and analyse the purified proteins. This technique is based on the principle that proteins can be separated according to their size or molecular weight through electrophoresis. The theory of electrophoresis relies on the movement of a charged ion in an electric field. The proteins were denatured at 95°C for 5 minutes in a solution containing the detergent, SDS. In these conditions proteins were unfolded and coated with negatively charged SDS detergent molecules. The proteins were separated according to their molecular weight and shape. Each protein migrated as bands through the gel and was easily detected following staining with Coomassie blue dye.

Fourthly, the protein eluates underwent dialysis with specific dialysis buffers that contained appropriate conditions in order to optimize kinase solubilisation and remove the unwanted imidazole. Lastly, the protein eluates were quantified in order to determine the concentration of protein obtained after purification.

Soluble recombinant proteins were easily purified whereas the purification of insoluble recombinant proteins posed problems. The experimental study of insoluble proteins is generally a scientific challenge but many techniques are available to potentially obtain the desired protein from the cell pellet. Hence, the aims and objectives of this part of the study were to express the recombinant genes in *E. coli* effectively and develop optimal protein purification methods for each kinase.

## **3.2 Materials and Methods**

### **3.2.1 *E. coli* expression and cultivation by induction**

Scrapings from the glycerol stocks of the kinase expression vectors in *E. coli* BL21 (DE3) were inoculated into 50 ml LB broth supplemented with the appropriate antibiotic and incubated overnight at 37°C with shaking at 200 rpm. The glycerol stock of the AsK alpha and beta expression vectors was inoculated to be co-expressed. The SK work carried out here has been repeated from previous work conducted by Kenyon et al. (2011) for further investigation in this research study.

Thereafter, 2.5 ml of the overnight cultures was transferred to 250 ml LB broth supplemented with the appropriate antibiotics and incubated at 37°C with shaking at 200 rpm. This was grown to an OD<sub>600</sub> reading of approximately 0.6, measured using spectrophotometry. This culture was then induced with 1 mM Isopropyl β-D-1-thiogalactopyranoside (IPTG) and incubated overnight at 28°C with shaking at 200 rpm.

### **3.2.2 Lysis of cells by sonication**

Each overnight culture was placed in a centrifuge bottle and the cells were sedimented by centrifugation in the Sorvall RC-5B centrifuge at 4 080 *g* for 10 minutes at 4°C. The biomass pellets was then resuspended in 20 ml of 1X binding buffer (1 M NaCl, 20 mM Tris-HCl and 5 mM Imidazole: pH 7.9) and sonicated using a Vibra cell sonicator for 15 minutes on a 100% duty cycle, separated by rest periods of 5 minutes on ice after every 5 minutes of sonication. Samples of 2 ml were collected and centrifuged in the Hettich Mikro 120 centrifuge at 4 080 *g* for 2 minutes at 4°C to recover the cell free extracts (supernatant) and the pellets, containing insoluble proteins and cell debris. The pellets were then resuspended in 2 ml of 1X binding buffer. The remaining culture was centrifuged at 16 300 *g* for 20 minutes at 4°C and stored at -20°C.



### **3.2.3 Sodium Dodecyl Sulfate Polyacrylamide Gel Electrophoresis (SDS-PAGE) analysis**

An SDS-PAGE (Sigma-Aldrich. USA) gel was utilized to analyse the proteins. Samples of 10  $\mu$ l of the cell free extracts as well as resuspended pellets from section 3.2.2 were mixed with an equal volume of 2X protein solvent buffer (2.5% [w/v] SDS, 10% [v/v] glycerol, 5% [v/v] 2-mercaptoethanol, 0.01% [w/v] bromophenol blue, 62.5 mM Tris; pH 6.8) and then denatured for 5 minutes at 95°C. The SDS-PAGE gels (sized 10 cm X 8 cm X 0.5 mm) were made up of a 4% [w/v] acrylamide/bisacrylamide stacking gel (pH 6.8) loaded over a 10% [w/v] acrylamide/bisacrylamide separating gel (pH 8.8). Then 10  $\mu$ l of the denatured samples were loaded on the SDS-PAGE gels and resolved by electrophoresis in a discontinuous gel system, as described by Laemmli (1970). The electrophoresis was performed in a Mini-PROTEAN® Tetra Cell system (Bio-Rad. USA) at 100 volts for  $\pm$ 1 hour in a 1X TGS electrophoresis buffer (0.192 M glycine, 0.1% [w/v] SDS, 0.025 M Tris-HCl; pH 8.3). Following electrophoresis, the gels were stained by gently rotating in a solution containing 0.125% [w/v] Coomassie brilliant blue G-250, 50% [v/v] methanol, 10% [w/v] acetic acid and distilled water for 30 minutes. The gels were then destained in a solution containing 25% [v/v] methanol, 10% [v/v] glacial acetic acid and distilled water, until the protein bands were visible. The staining method depends on the reversible binding by the proteins by a coloured chemical (Fernandez-Patron et al. 1995). The gels were scanned electronically on the Bio-Rad Chemidoc gel imaging system. The sizes of the resolved proteins were estimated by comparison to a readily available molecular mass marker (PageRuler™ Plus Pre-stained Protein Ladder, Fermentas. USA) that was simultaneously run on the gel.

### **3.2.4 Protein Purification**

Depending on the results of the SDS-PAGE gels from 3.2.3, the kinase proteins were determined to be either soluble or insoluble (refer to Table 3-1). NDK, ThiL, RBKS, AsK and SK were soluble, whereas HSK, AK and GK were insoluble. The soluble proteins were purified through the Profinia™ System (refer to section 3.2.4.1), whereas the proteins that were insoluble were further treated with the intention to convert the protein from insoluble to soluble or to retrieve the insoluble protein effectively.

Table 3-1: Recommended purification method according to kinase solubility

NDK	Kinases						
	HSK	AK	GK	ThiL	RBKS	AsK	SK
Soluble	Insoluble	Insoluble	Insoluble	Soluble	Soluble	Soluble	Soluble
Profinia™ System	Solubility studies & Denature & AKTA Ni-IDA Purification	Solubility studies & Denature & MagReSyn Purification	Solubility studies & Denature & MagReSyn Purification	Profinia™ System	Profinia™ System	Profinia™ System	Profinia™ System

#### 3.2.4.1 Purification of soluble his-tagged proteins using the automated Bio-Rad Profinia™ System

Each of the cell free extracts of the soluble kinases (from section 3.2.2) was filtered through a 0.45 µm syringe filter to remove any particles present. The cell free extract was loaded onto the Bio-Rad Profinia™ System with appropriate buffers and reagents (refer to Appendix C) and a 1 ml column containing nickel-iminodiacetic acid (Ni-IDA) resin. The Standard Native conditions and protocols were followed according to the manufacturer's instructions (Bio-Rad. USA). This system purified the proteins on the basis of immobilized metal ion affinity chromatography (IMAC) technology by using IDA resin packed cartridges available for his-tagged proteins. The fraction lines collected the flowthrough, wash 1, wash 2 and elution fractions. The insoluble particles (pellets) and the soluble cell free extracts (supernatants) obtained after sonication and centrifugation in Section 3.2.2, as well as the fractions obtained from the Profinia column were analysed by SDS-PAGE gels as described in Section 3.2.3 and the elution fraction was dialysed overnight in dialysis buffer (refer to Section 3.2.5).

#### 3.2.4.2 Solubility studies

Protein solubility studies were conducted for the insoluble HSK, AK and GK kinases by using different buffers at a variety of pH's to determine the optimal purification buffer. Other purification methods that were tested included the use of and transformation of Origami (DE3)

competent cells instead of BL21 (DE3), co-expression of chaperone proteins using the Chaperone Plasmid Set (Clone Tech Laboratories, TaKaRa, USA) consisting of pG-KJE8, pGro7, pKJE7, pG-Tf2 and pTf16 plasmids for refolding assistance, and adding the dipeptide glycylglycine to the cell culture medium to increase the solubility of the expressed recombinant proteins. These protocols were all evaluated by SDS-PAGE gels as described in Section 3.2.3.

#### 3.2.4.3 Denaturation

When the solubility studies indicated above indicated no increase in solubility of the expressed HSK, AK and GK kinases, urea denaturation of these insoluble kinases was attempted.

The HSK kinase was purified using the AKTA Avant with packed Tricorn™ 5/50 columns (GE Healthcare Life Sciences, Italy). Then its biomass pellet was resuspended in 40 ml denaturation solubilisation buffer (50 mM NaH<sub>2</sub>PO<sub>4</sub>, 300 mM NaCl, 8 M urea; pH 7.9) and was incubated for 2 hours at 37°C with shaking at 50 rpm. This was then sonicated (as in section 3.2.2) and centrifuged in the Sorvall RC-5B centrifuge at 4 080 g for 10 minutes at 4°C. The supernatant was clarified through a 0.45 µm syringe filter and loaded onto a 25 ml bed volume Ni-NTA (nickel-nitrilotriacetic acid) column on the AKTA Avant, pre-equilibrated with denaturation solubilisation buffer. After loading, the column was washed with denaturation buffer. The HSK was refolded on the column using a linear gradient from 100% Denaturation Solubilisation Buffer to 100% of the urea-free Lysis Equilibration Buffer (50 mM NaH<sub>2</sub>PO<sub>4</sub>, 300 mM NaCl; pH 7.9) before being eluted off the resin using Elution Buffer (50 mM NaH<sub>2</sub>PO<sub>4</sub>, 300 mM NaCl, and 250 mM Imidazole; pH 8.0). The eluates were concentrated five times through a Vivaspin 10 kDa MWCO column by centrifugation at 4 080 g for 30 minutes at 4°C in the Sorvall RC-5B centrifuge.

For AK and GK, the biomass pellets obtained from section 3.2.2 were resuspended in 40 ml denaturation lysis buffer (50 mM KH<sub>2</sub>PO<sub>4</sub>, 300 mM NaCl, 6 M urea, 5 mM Imidazole; pH 8.0) and sonicated (as in section 3.2.2). After centrifugation at 4 080g for 10 minutes at 4°C, the supernatant was clarified through a 0.45 µm syringe filter and loaded onto the Profinia™ System, with a 1 ml Ni-IDA cartridge, using the Denaturing IMAC protocol according to the manufacturer's instructions. The denaturing Elution Buffer contained 50 mM KH<sub>2</sub>PO<sub>4</sub>, 300 mM NaCl, 3 M urea, 250 mM Imidazole at pH 8.0. Matrix-assisted refolding techniques as described for HSK and the Protino® Ni-TED and Ni-IDA (Macherey-Nagel) drip columns with buffers were

also tested, according to the manufacturer's instructions (Macherey-Nagel, Germany). Samples were analysed by SDS-PAGE gels and the eluates were dialysed overnight (refer to section 3.2.5).

#### 3.2.4.4 MagReSyn™ NTA Purification

The denaturation of AK and GK as described above subsequently showed that the denatured protein precipitated during dialysis, and that the enzymes were not functional. Therefore, the native MagReSyn™ NTA purification method was attempted for AK and GK. MagReSyn™ is a magnetic microsphere support designed for Ni-affinity capture to purify and recover his-tagged proteins.

The biomass pellets (from section 3.2.2) were resuspended in 20 ml 1X binding buffer and sonicated as described in section 3.2.2. The scaled-up protocol was followed and the reagents were used according to the manufacturer's instructions (MagReSyn™ Biosciences, South Africa). Samples of the fractions were taken throughout for analysis by SDS-PAGE gels as described in section 3.2.3.

#### 3.2.5 Dialysis

The protein eluates were placed in dialysis tubing (Pierce snakeskin 10 kDa MWCO) and the sealed tubing was then placed in appropriate dialysis buffers and stirred at 4°C overnight. For details of the dialysis buffers, please refer to Table 3-2. The selected buffers were shown to contain the appropriate conditions to optimize kinase solubilisation. The proteins were then removed from the dialysis tubing and aliquots of 55 µl were pipetted into 1.5 ml Eppendorf tubes. The Eppendorf tubes with the protein were placed in liquid nitrogen to snap-freeze the protein and subsequently stored at -70°C for further use at a later stage. The AK and GK kinases were not placed in liquid nitrogen to snap-freeze, but rather the aliquots of 50 µl of the dialysed protein were pipetted into 1.5 ml Eppendorf tubes and 50% [v/v] Glycerol-50% was added and subsequently stored at -70°C for use at a later stage. Samples were run on SDS-PAGE gels to confirm the presence and size of the protein.

Table 3-2: Dialysis buffers used to solubilise NDK, HSK, AK, GK, ThiL, RBKS, AsK and SK kinase proteins

<b>A) NDK</b>	<b>B) HSK</b>	<b>C) AK &amp; GK</b>
50 mM Tris pH 8.0 100 mM KCl 1 mM DTT 1 mM MgCl <sub>2</sub> ·6H <sub>2</sub> O	50 mM MOPS pH 8.0 150 mM NaCl 1 mM DTT 10 mM MgCl <sub>2</sub> ·6H <sub>2</sub> O	50 mM Tris pH 7.5 150 mM NaCl 1 mM DTT 5 mM MgCl <sub>2</sub> ·6H <sub>2</sub> O
<b>D) ThiL &amp; RBKS</b>	<b>E) AsK</b>	<b>F) SK</b>
50 mM MOPS pH 7.6 150 mM NaCl 1 mM DTT 10 mM MgCl <sub>2</sub> ·6H <sub>2</sub> O	50 mM Tris pH 6.0 200 mM NaCl 1 mM DTT 10 mM MgCl <sub>2</sub> ·6H <sub>2</sub> O	50 mM Tris pH 7.5 1 M NaCl

### 3.2.6 Protein Quantitation

The concentration of the protein stored at -70°C was determined using the Basic Qubit Fluorometric Quantitation kit as recommended by the manufacturers (Life Technologies. USA). This technique was based on the detection and accurate measurement of specific target molecules using highly sensitive fluorescence-based assays. The fluorescent dye used in the assays emitted signals when bound to the target protein, which minimized the effects of contaminants, and accurately quantified the target protein. Various dilutions of the proteins were added to the working solutions made up of protein buffer and Qubit fluorescent dye. These mixtures were thoroughly vortexed for 10 seconds before being incubated at room temperature for 15 minutes. The Qubit® 2.0 Fluorometer (Life Technologies. USA) was then used to calculate the estimated protein concentration.

### **3.3 Results and Discussion**

#### **3.3.1 *E. coli* expression**

*E. coli* remains the favoured choice for the expression of recombinant proteins as it provides the simplicity of use, low cost, high speed and high level protein production. Cells such as BL21 (DE3) were used because the pET system requires a host strain lysogenised by a DE3 phage segment, which encodes the T7 RNA polymerase, and regulated by the IPTG inducible lac promoter. The addition of IPTG at an OD<sub>600</sub> reading of ~0.6, the mid log phase, is a crucial point to activate the lac operon. The cultivation and expression of the proteins was shown to be successful.

#### **3.3.2 Protein production evaluation**

The Profinia™ Protein Purification system successfully purified the NDK, ThiL, RBKS, AsK and SK proteins based on the principle of immobilized metal ion affinity chromatography (IMAC) technology. This convenient automated system was highly efficient for the purification of the his-tagged proteins.

Initial protein purification indicated that HSK, AK and GK were insoluble under native conditions. The incidence of insoluble proteins could be because it is a membrane-bound protein that is hydrophobic or misfolded when over-expressed in the host (Tripmin & Brizzard. 2009). As protein solubility depends on the binding buffer, different buffers with different conditions and modifications were tested. However, initial solubilisation experiments resulted in no major improvement on kinase solubility.

After testing different buffers and purification methods, optimal purification of HSK, AK and GK kinase proteins was shown following their denaturation with urea. In addition, active HSK enzyme was obtained using this method, as described in the following chapter. The AKTA Avant was used for the on-column refolding, by gradually reducing the urea concentration from 8 M to 0 M. This showed that it was possible to purify an insoluble recombinant protein by denaturation and then refolding the protein to the native conformation.

However, denaturation and on-column refolding did not work optimally for the AK and GK kinases. This could be due to incorrect folding of the protein during renaturation. The best results were obtained using the MagReSyn™ NTA purification method as it had an optimal capacity for binding of the protein and resulted in the purification of active enzyme.

### **3.3.3 SDS-PAGE analysis of purified protein**

The screening of all the proteins was carried out using SDS-PAGE analysis. Protein fractions resulting from various stages in the purification steps are displayed in Figures 3-1 and 3-2. In Figures 3-1 and 3-2, the total protein is the protein fraction after sonication, prior to centrifugation. The insoluble protein is the pellet obtained after centrifugation which contains the insoluble protein and cell debris. The lane labelled loaded, is the cell free extract obtained after centrifugation that is loaded onto the system. The flowthrough, wash 1, wash 2 and elution fractions are the fraction lines collected during protein purification. Refer to Appendix C for the buffers and reagents used at the various stages. The presence in the eluate lane of a concentrated protein band of the anticipated size for each kinase indicates the successful purification of the kinase proteins. Contaminated proteins were present in HSK, AK, GK and AsK, but visual purity was estimated at 90-95%.

The technique involving the use of SDS-PAGE and 10% acrylamide gels was shown to be successful to sequentially screen kinase purification products. This method was shown to be simple, effective and reproducible.

Different affinity tags have different sizes and properties but ideally a tag should be small in order to have a negligible effect on the structure and activity of the eluted protein (Qiagen. 2004). A 6 x His-tag has a small size of just 0.84 kDa and generally according to other studies, hardly ever obstructs the protein construction and function (Qiagen. 2004). Thus, using a 6 X His-tag was shown to be simple and suitable in the purification of the 8 kinase proteins.

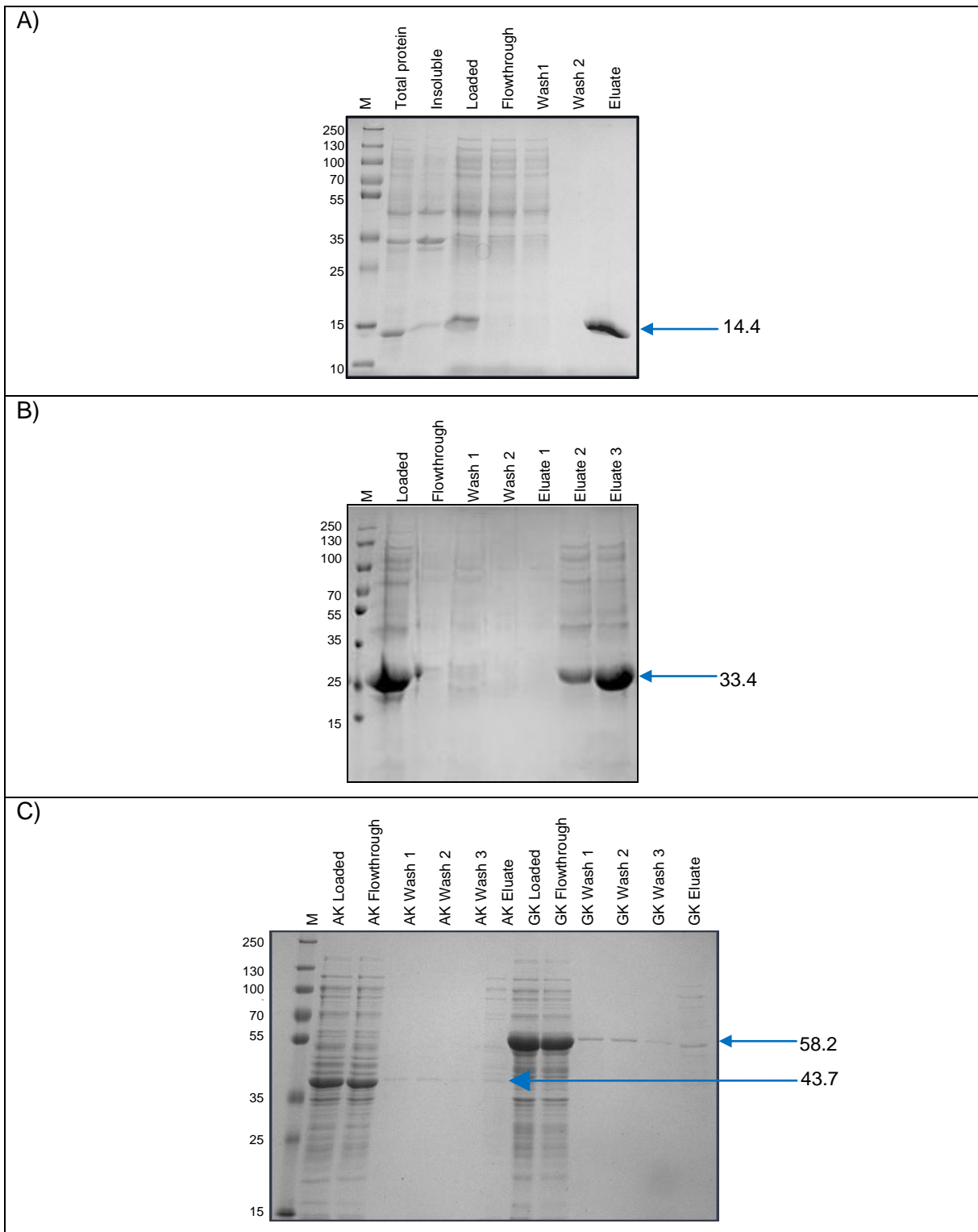


Figure 3-1: SDS-PAGE gels of the Mtb his-tagged kinases purified from *E. coli* BL21 (DE3). The fractions were loaded on a 10% [w/v] gel. A) NDK protein fractions using the Ni-IDA resin on the Profinia™. B) HSK protein fractions using the Ni-IDA resin on the AKTA. C) AK and GK protein fractions using MagReSyn™. M represents the molecular mass marker (PageRuler™ Plus Pre-stained Protein Ladder, Fermentas) and the sizes of this marker are indicated to the left of the gels. The blue arrows indicate the expected size bands in kDa for the purified protein eluates.



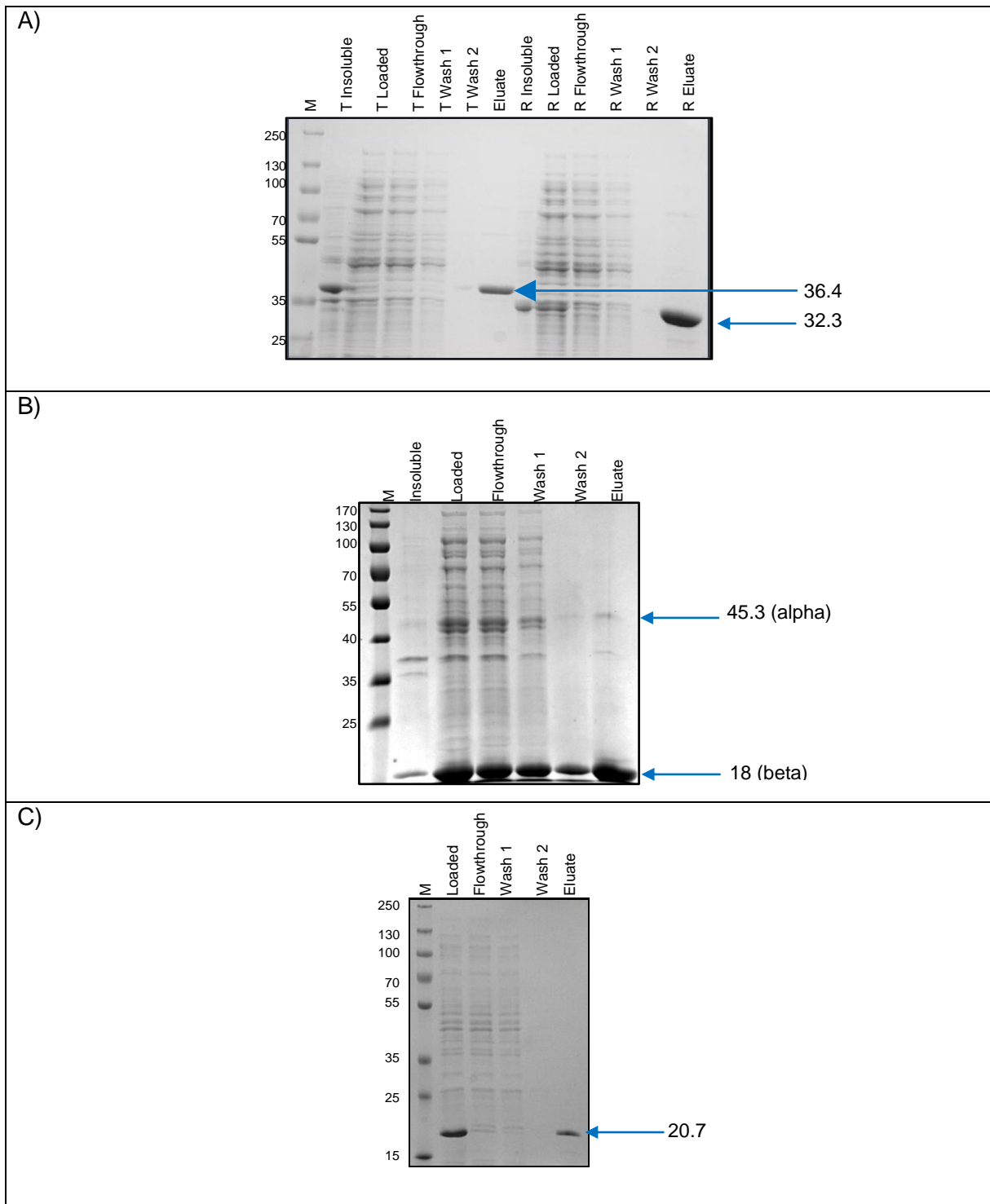


Figure 3-2: SDS-PAGE gels of the Mtb his-tagged kinases purified from *E. coli* BL21 (DE3). The fractions were loaded on a 10% [w/v] gel. A) ThiL (T) and RBKS (R) protein fractions using the Ni-IDA resin on the Profinia™. B) Ask protein fractions using the Ni-IDA resin on the Profinia™. C) SK protein fractions using the Ni-IDA resin on the Profinia™. M represents the molecular mass marker (PageRuler™ Plus Pre-stained Protein Ladder, Fermentas, USA) and the sizes of this marker are indicated to the left of the gels. The blue arrows indicate the expected size bands in kDa for the purified protein eluates.

### 3.3.4 Determination of Protein Quantitation

The Qubit® 2.0 Fluorometer quantitated the purified proteins swiftly and accurately (Life Technologies. USA). This molecular technique provided a simple way to determine the concentration of the available protein for further analysis. The results are presented in Table 3-3. The total enzyme concentration is displayed, as well as the estimated recombinant protein concentration by visual purity estimation.

Table 3-3: Concentration of purified kinase proteins (presented in µg/ml)

<b>Kinase</b>	<b>Total Enzyme Concentration (µg/ml)</b>	<b>Estimated Recombinant protein concentration (µg/ml)</b>
<b>NDK</b>	1480	1480
<b>HSK</b>	935	841.5
<b>AK</b>	390	370.5
<b>GK</b>	348	330.6
<b>ThiL</b>	755	755
<b>RBKS</b>	800	800
<b>AsK</b>	1128	1071.6
<b>SK</b>	2030	2030

The use of sequential purification techniques were intended to generate smaller amounts of purer active protein. The concentration levels of protein expression obtained through these sequential protein purification techniques and systems were suitable for further functional analysis and screening protocols.

HPLC enzyme assays are routinely used as the final test for determination of the purity and activity of the protein. The subsequent chapter was necessary in order to determine and confirm if the purified protein obtained was indeed functional, and did not unfold or aggregate during the various purification techniques performed in this chapter.

### **3.4 Chapter conclusion**

In summary, the expression of the recombinant kinase genes in *E. coli* was successful. As observed, the purification of the proteins thereafter was complex, but various different methods and techniques were explored to obtain sufficient amounts of pure protein for further analysis.

The purification of recombinant kinase proteins was necessary to progress towards the eventual detection of possible TB drug targets. The functional characterization of the purified kinases was then evaluated through enzyme assays. The particulars regarding this are described in the following chapter.

# Chapter 4: Functional characterization of enzymes

---

## 4.1 Introduction

This research chapter describes the functional analysis of the kinases by examining the enzyme activity subsequent to protein purification. Enzyme activity is studied for many reasons, but in this area of research, the fundamental interest is for practical applications such as potential drug target discovery.

Reaction kinetics is the general biochemical tool used to study the rates of chemical processes which is ultimately used to investigate molecular interactions within biological systems. More specifically, the basic experiment employed to study the enzyme activity during reactions is the measurement of the amount of substrate converted to product over time, under specific reaction conditions. This method of study is termed an enzyme assay. Enzymes must be assayed under controlled conditions because time, concentrations, pH and temperature alter the activity (Haas. 2005). It is important to unravel the intrinsics of enzymatic chemical reactions as it can reveal the rates of the catalysed reactions, the specificity of the enzymes and the outcome of varying the conditions of the reactions (Muljadi. 2011).

The survival and growth of the Mtb organism depends on complex networks of chemical reactions (Tomioka et al. 2008). Some of these reactions are mediated by the action of their kinase enzymes as described in Chapter 1. Thus, the study of the activity of the Mtb kinase enzymes is crucial in understanding the biochemistry of this infectious agent, as it allows us to study the processes within the cells of this microorganism, particularly those critical processes that allow the survival of these microbes.

Kinases use ATP to transfer the phosphate to the protein, which implies that kinases rely mostly on ATP during catalysis (Kenyon et al. 2011, Cheek et al. 2002 and Cheek et al. 2005). Thus, the investigation to establish the effects of varying conditions of ATP concentrations on the enzymes activity is also essential.

Therefore, the aims and objectives of this section were to develop and optimize validated assays for the assessment of the enzymes activity in order to determine the functionality for each kinase, as well as to establish the reaction effects of varying concentrations of ATP.

## 4.2 Materials and Methods

### 4.2.1 Enzyme activity analysis by High Performance Liquid Chromatography (HPLC)

The kinase protein samples from the -70°C freezer were allowed to thaw on ice prior to setting up the enzyme High Performance Liquid Chromatography (HPLC) assays. HPLC is used to separate components in a mixture, to identify each component and quantify each component (Horvath et al. 1967). The assays performed were based on the principle of measuring the product formation and substrate reduction, by separation of the reaction mixture into its components following their movement through a HPLC column.

The HPLC assay reactions were carried out in 100 µl volumes and incubated at 37°C. These assay reactions consisted of tubes of 90 µl of the prepared reaction mixture with either 10 µl of enzyme, prepared in triplicate or 10 µl distilled water, prepared in duplicate, served as a control blank. The reaction was then stopped with 5% [v/v] 200 mM EDTA.2Na.2H<sub>2</sub>O and subsequently loaded onto an Agilent 1100 HPLC to measure the adenosine diphosphate (ADP) product formation and the reduction of the adenosine triphosphate (ATP) substrate.

All the kinases were assayed using the HPLC system which automatically injected 0.2 µl of each sample reaction mix onto a Phenomenex 5 µ LUNA C18 column with the mobile phase containing PIC A® (Waters Corporation. USA), 250 ml acetonitrile and 7 g KH<sub>2</sub>PO<sub>4</sub> per litre of water. The flow rate of the mobile phase was 1 ml/minute and the separated reactants were detected using a UV detector to measure absorbance at a wavelength of 259 nm.

An AMP, ADP and ATP standard was used to calibrate the HPLC and the levels of ADP in each sample were determined by using Agilent ChemStation (Revision B.02.01) software (Agilent Technologies. USA). The ADP blank control consisted of reactions where enzyme was substituted with distilled water. Absorbance values obtained for this control were subtracted from the enzyme reactions.

Standard optimizations, not included in this dissertation, were carried out on parameters such as enzyme concentration, buffer, pH, salt concentration and incubation times. These enzymes were optimized as part of the published data (Kenyon et al. 2011 and Kenyon et al. 2012) and only the optimized conditions are stated. Favourable enzyme activity, in this study, was defined

by achieving linearity to demonstrate a constant rate, as well as attaining percentage conversions (of ATP to ADP) within the range of 5-15% (Wu et al. 2003). Another criterion for confirming favourable activity of the enzyme was to acquire data that is reproducible. ATP and  $MgCl_2$  concentrations were always kept at a 1:1 ratio (Walaas et al. 1962). The SK work performed in this chapter has been repeated from previous work conducted by Kenyon et al. (2011) to be further investigated in this research study.

#### **4.2.2 ATP concentration gradient assays**

Enzyme assays were optimised according to the deduced specific reagents and concentrations, with differing ATP concentration gradients as shown in Table 4-1. The incubation times stipulated in table 4-1 were chosen subsequent to various optimization tests conducted during this study.

The reaction mixtures were incubated at 37°C before being stopped with the addition of a chelating agent - 5% [v/v] 200 mM EDTA.2Na.2H<sub>2</sub>O. An aliquot (0.2 µl) was subsequently loaded onto the HPLC system for measurement of ADP production.

Table 4-1: Kinase enzymes with their respective enzyme activity assay conditions

<b>Enzyme</b>	<b>Assay reaction mixtures</b>	<b>Incubation time</b>
<b>NDK</b>	100 mM K-PO <sub>4</sub> buffer (pH 6.8), 250 mM KCl 5 nM enzyme, 0.2 M TDP 0.25 – 1.5 mM ATP and 0.25 – 1.5 mM MgCl <sub>2</sub>	40 minutes
<b>HSK</b>	50 mM HEPES buffer (pH 7.0), 450 mM KCl 704 nM enzyme, 10 mM Homoserine 0.25 – 2.5 mM ATP and 0.25 – 2.5 mM MgCl <sub>2</sub>	4 hours
<b>AK</b>	100 mM Tris buffer (pH 7.0), 250 mM KCl 223 nM enzyme, 10 mM Na acetate 0.25 – 4 mM ATP and 0.25 – 4 mM MgCl <sub>2</sub>	24 hours
<b>GK</b>	100 mM Tris buffer (pH 7.0), 250 mM KCl 208.6 nM enzyme, 100 mM Glycerol 0.25 – 2.5 mM ATP and 0.25 – 2.5 mM MgCl <sub>2</sub>	24 hours
<b>ThiL</b>	100 mM Tris buffer (pH 8.0), 250 mM KCl 2074 nM enzyme, 1 mM TMP 0.25 – 2.5 mM ATP and 0.25 – 2.5 mM MgCl <sub>2</sub>	5 hours
<b>RBKS</b>	100 mM Tris buffer (pH 7.2), 100 mM KCl 250 nM enzyme, 10 mM D-ribose 0.25 – 4 mM ATP and 0.25 – 4 mM MgCl <sub>2</sub>	4 hours
<b>AsK</b>	100 mM Tris-HCl buffer (pH 7.5), 178.2 nM enzyme 10 mM L-Aspartic acid 0.25 – 2.5 mM ATP and 0.25 – 2.5 mM MgCl <sub>2</sub>	6 hours
<b>SK</b>	100 mM K-PO <sub>4</sub> buffer (pH 6.8), 500 mM KCl 10 nM enzyme, 8 mM shikimic acid 0.5 – 10 mM ATP and 0.5 – 10 mM MgCl <sub>2</sub>	20 minutes



## **4.3 Results and Discussion**

### **4.3.1 Determination of enzyme activity**

To evaluate the enzyme activity, the quantity of ATP converted into ADP by the action of the kinases was analysed. The specific substrate and product reactions measured for each kinase is shown in Table 4-2. The automated HPLC tool allowed for a fast analysis. This technique swiftly separates the components of the enzyme assay through high pressures, to identify and quantify each component (Horvath et al. 1967). Each component interacted slightly differently with the mobile phase and the Phenomenex 5  $\mu$  LUNA C18 column, which resulted in varied retention of the reaction mix components in the column. This is shown by different flow rates of reactants from the column. The quantitative analysis was examined using a sensitive UV HPLC detector, which generates a signal relative to the amount of sample from the output of the column (Horvath et al. 1967). The data were processed and displayed efficiently by the HPLC Agilent ChemStation (Revision B.02.01) software. The enzyme assays and HPLC analysis was performed and assessed in triplicate to ensure that the results were reliable.

Validated assays with ideal conditions as indicated in Table 4-1 above were established in order to attain optimum enzyme activity for each kinase. The optimum enzyme activity was authenticated by the fact that the data depicted linearity on the shape of the graphs and the percentage conversions of ATP to ADP, calculated from the assays, were within the required range of 5-15% (Wu et al. 2003). The ideal conditions established and its supporting data were validated because the data was reproducible. These ideal conditions were then used for further enzyme activity analysis by ATP concentration gradient assays, which are interpreted in the following section.

Table 4-2: Reactions of kinases

Kinase	Enzyme Concentration (µg/ml)
<b>NDK</b>	nucleoside diphosphate + ATP $\rightleftharpoons$ ADP + nucleoside triphosphate
<b>HSK</b>	L-homoserine + ATP $\rightarrow$ O-phospho- L-homoserine + ADP
<b>AK</b>	Acetate + ATP $\rightarrow$ Acetyl-phosphate + ADP
<b>GK</b>	Glycerol + ATP $\rightarrow$ Glycerol-3-phosphate + ADP
<b>ThiL</b>	Thiamine monophosphate + ATP $\rightarrow$ Thiamine diphosphate + ADP
<b>RBKS</b>	D-ribose + ATP $\rightarrow$ D-ribose 5-phosphate + ADP
<b>AsK</b>	L-aspartate + ATP $\rightarrow$ 4-phospho-L-aspartate + ADP
<b>SK</b>	Shikimate + ATP $\rightarrow$ Shikimate-3-phosphate + ADP

#### 4.3.2 ATP concentration gradient assay outcome

ATP is known as the primary energy source for all living organisms (Bergman. 1999). In this field of enzyme research, the chemical energy available in the phosphate bond of ATP is required to drive the kinase-dependent phosphorylation reactions in order to modify the activity of specific proteins. These specific protein kinases are required to facilitate and control metabolic and signaling pathways (Kenyon et al. 2012). This basic chemical reaction was explored to deduce functionality.

The dephosphorylation of ATP to produce ADP was observed immediately upon addition of the enzyme to the reaction mix ( $T_0$ ). The ADP levels measured in the blank controls (no enzyme) were subtracted from the final ADP concentration (absolute value) measured at the completion of the reaction. The resulting net ADP levels, as well as the blank ADP levels and the ADP levels at time zero, were plotted against the ATP concentrations with error bars. The error bars are as a result of the assays being done in triplicate. The results represented by line graphs are shown in Figure 4-1 to 4-8.

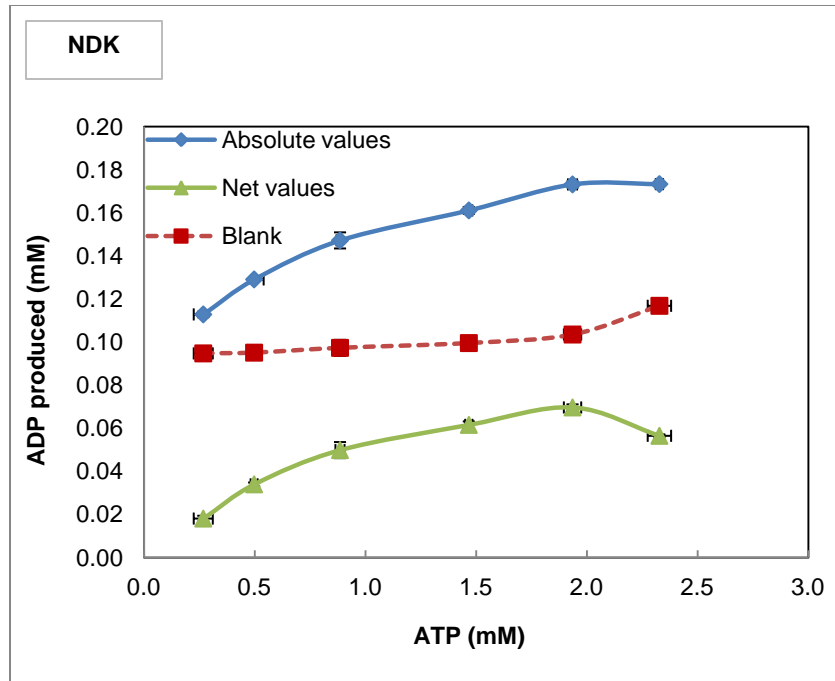


Figure 4-1: ADP production by His-NDK as a measure of TDP phosphorylating activity. The 40 minute assay contained 100 mM K-PO<sub>4</sub> buffer (pH 6.8), 250 mM KCl, 5 nM enzyme, 0.2 M TDP and 0.25 – 2.5 mM ATP and MgCl<sub>2</sub>. The net value of ADP production for this reaction was obtained by subtracting the corresponding blank value from the absolute value.

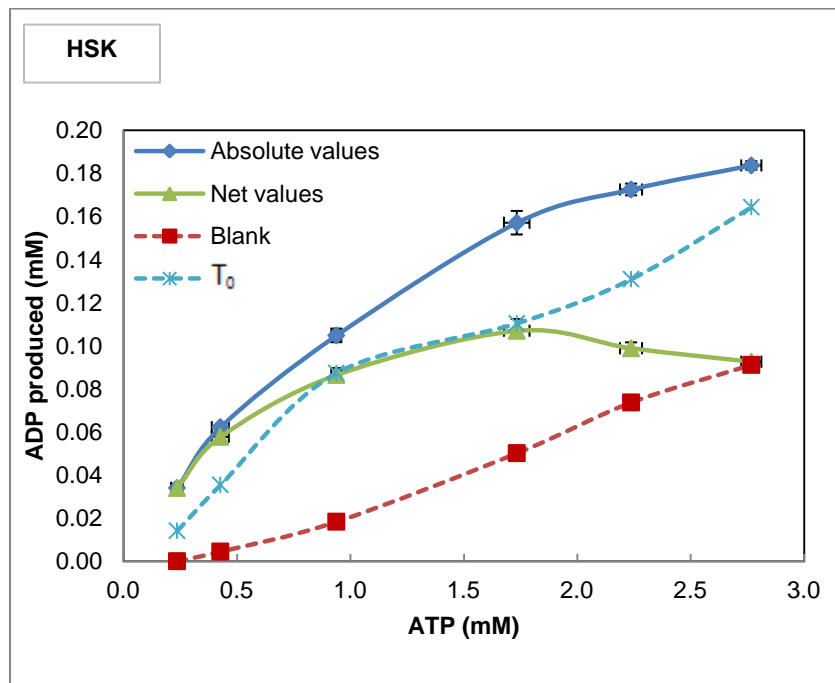


Figure 4-2: ADP production by His-HSK as a measure of homoserine phosphorylating activity. The 4 hour assay contained 50 mM HEPES buffer (pH 7.0), 450 mM KCl, 704 nM enzyme, 10 mM Homoserine and 0.25 – 2.5 mM ATP and MgCl<sub>2</sub>. The net value of ADP production for this reaction was obtained by subtracting the corresponding blank value from the absolute value. The ADP levels at time zero were also plotted.

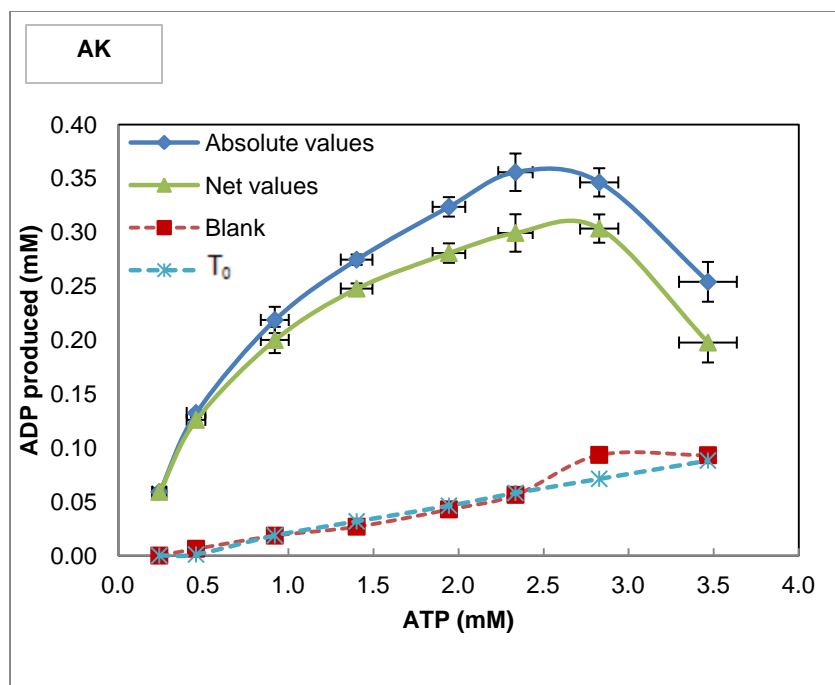


Figure 4-3: ADP production by His-AK as a measure of Na-acetate phosphorylating activity. The 24 hour assay contained 100 mM Tris buffer (pH 7.0), 250 mM KCl, 223 nM enzyme, 10 mM Na acetate and 0.25 – 4 mM ATP and MgCl<sub>2</sub>. The net value of ADP production for this reaction was obtained by subtracting the corresponding blank value from the absolute value. The ADP levels at time zero were also plotted.

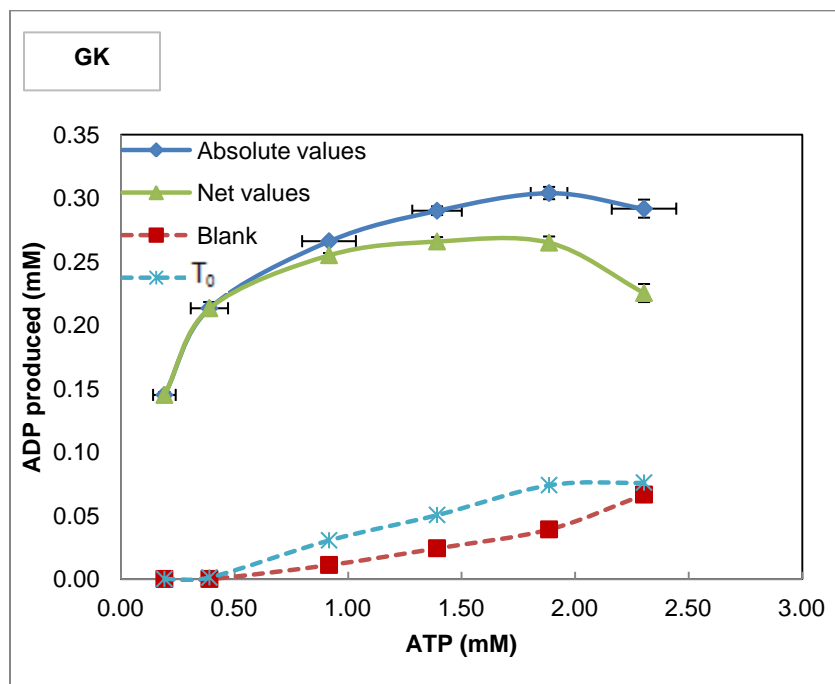


Figure 4-4: ADP production by His-GK as a measure of glycerol phosphorylating activity. The 24 hour assay contained 100 mM Tris buffer (pH 7.0), 250 mM KCl, 208.6 nM enzyme, 100 mM Glycerol and 0.25 – 2.5 mM ATP and MgCl<sub>2</sub>. The net value of ADP production for this reaction was obtained by subtracting the corresponding blank value from the absolute value. The ADP levels at time zero were also plotted.

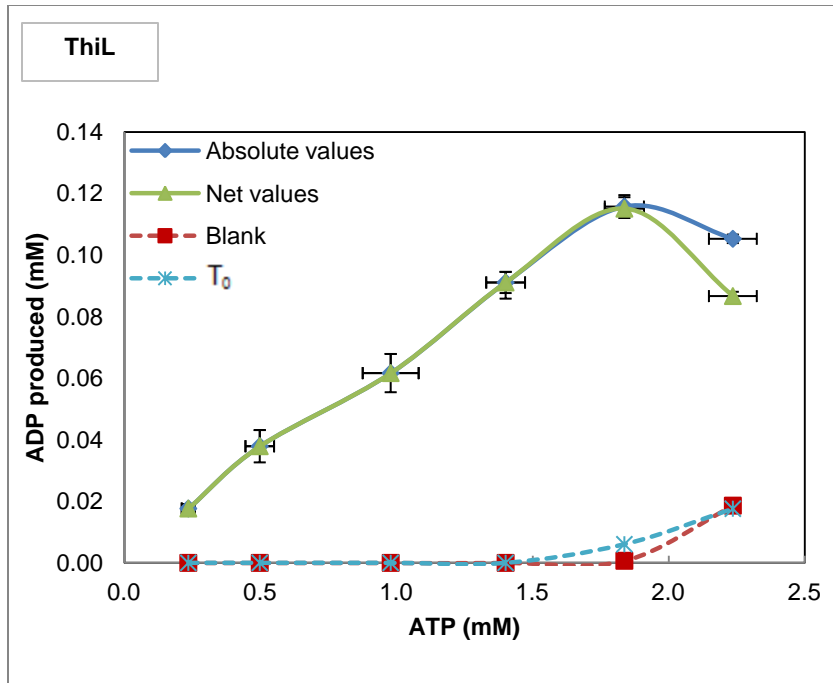


Figure 4-5: ADP production by His-ThiL as a measure of TMP phosphorylating activity. The 5 hour assay contained 100 mM Tris buffer (pH 8.0), 250 mM KCl, 2074 nM enzyme, 1 mM TMP and 0.25 – 2.5 mM ATP and MgCl<sub>2</sub>. The net value of ADP production for this reaction was obtained by subtracting the corresponding blank value from the absolute value. The ADP levels at time zero were also plotted.

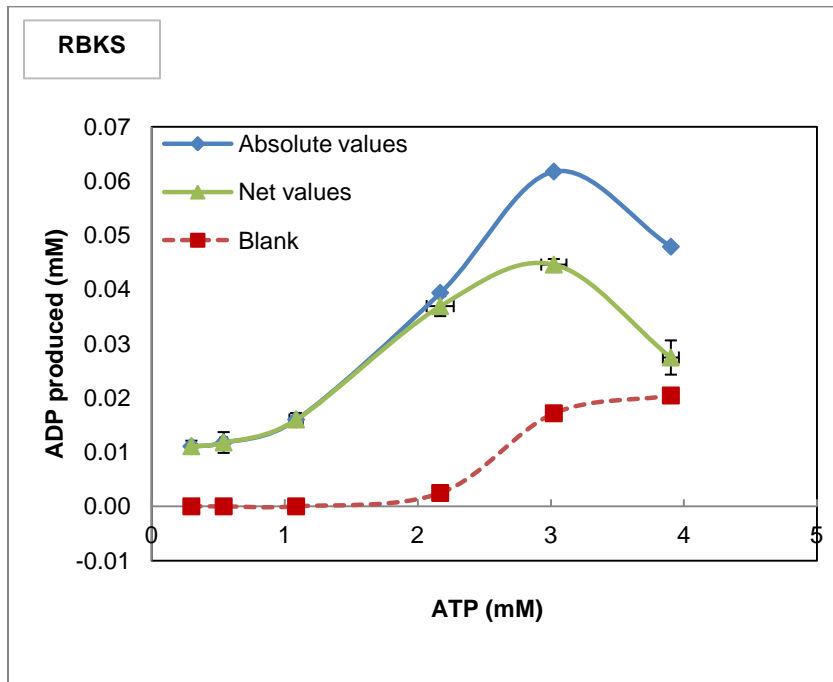


Figure 4-6: ADP production by His-RBKS as a measure of D-ribose phosphorylating activity. The 4 hour assay contained 100 mM Tris buffer (pH 7.2), 100 mM KCl, 250 nM enzyme, 10 mM D-ribose and 0.25 – 4 mM ATP and MgCl<sub>2</sub>. The net value of ADP production for this reaction was obtained by subtracting the corresponding blank value from the absolute value.

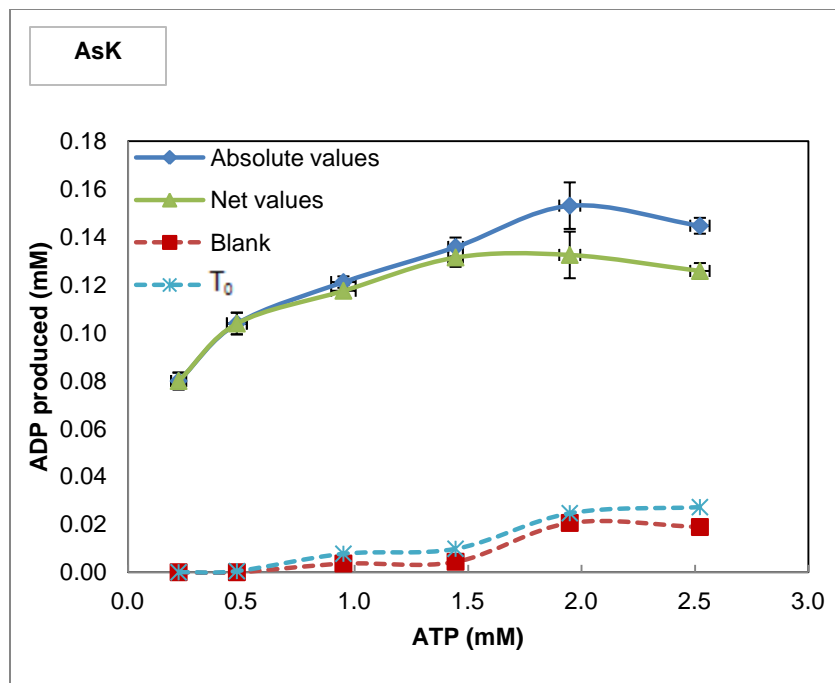


Figure 4-7: ADP production by His-AsK as a measure of aspartate phosphorylating activity. The 6 hour assay contained 100 mM Tris-HCl buffer (pH 7.5), 178.2 nM enzyme, 10 mM L-Aspartic acid and 0.25 – 2.5 mM ATP and MgCl<sub>2</sub>. The net value of ADP production for this reaction was obtained by subtracting the corresponding blank value from the absolute value. The ADP levels at time zero were also plotted.

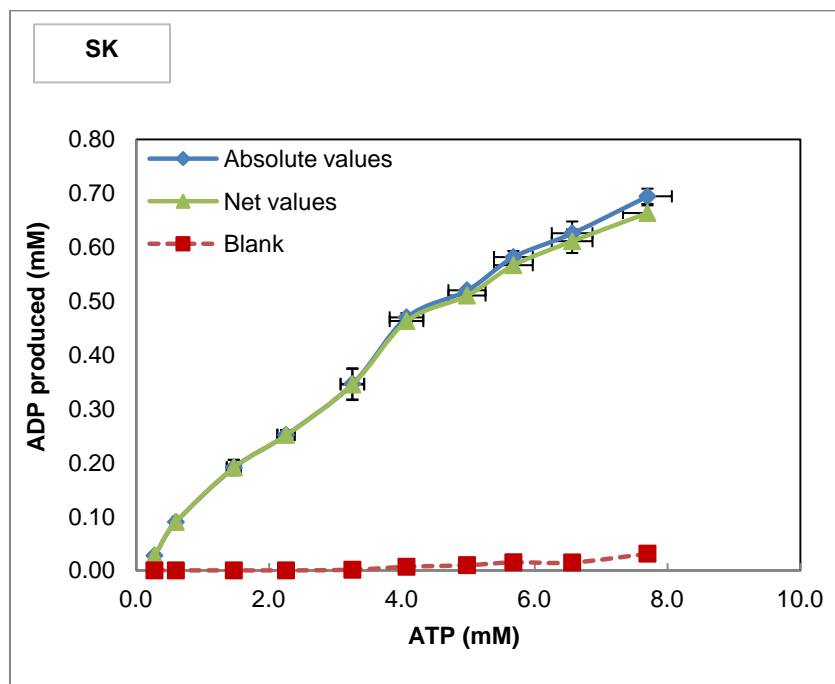


Figure 4-8: ADP production by His-SK as a measure of shikimic acid phosphorylating activity. The 20 minute assay contained 100 mM K-PO<sub>4</sub> buffer (pH 6.8), 500 mM KCl, 10 nM enzyme, 8 mM shikimic acid and 0.5 – 10 mM ATP and MgCl<sub>2</sub>. The net value of ADP production for this reaction was obtained by subtracting the corresponding blank value from the absolute value.

From the figures above, it shows that the ADP product is produced even at low ATP concentrations and that there was a corresponding gradual increase in ADP concentrations in reactions containing sequentially higher ATP concentrations. The NDK, Ask and, to a lesser extent, GK enzymes were shown to be particularly active due to the relatively high starting concentration of ADP even at low ATP concentration. This means that NDK used ATP to transfer a phosphate to the TDP protein substrate. This demonstrates phosphorylating activity similar to previous studies conducted by Kumar et al (2004). The main function of HSK is to catalyze the phosphorylation of L-homoserine to L-homoserine phosphate. The results here confirmed this functionality, as in studies completed by Rees et al (1992). However, the ADP levels at time zero ( $T_0$ ), for HSK were high. This could perhaps be caused by the reactants in the assay mixture that exhibit reagent instability. The ADP levels for the blank reactions (no enzyme) for the NDK and HSK assays are observed to be high, and this could perhaps be due to autophosphorylation or a result of contaminated ATP as the concentration is increased. The results of the AK and GK enzyme assays showed the successful conversion of substrate to product which reflects the presence of activity. The activities of ThiL investigated by an enzyme assay confirmed the transfer of the phosphate of ATP which is essentially the conversion of thiamine monophosphate to thiamine diphosphate (McCulloch et al. 2008). The characterization of RBKS was verified by an assay that detected the transformation of D-ribose into D-ribose 5-phosphate as per studies by Yang et al (2011), with slight modification of the assay reactants. The ADP formation determined by the HPLC during the AsK and SK enzyme assays provided evidence that the enzymes were active. The results overall indicated that the enzymes were indeed functional.

#### **4.4 Chapter conclusion**

In conclusion, assays have been optimised and developed for each kinase. The objective to determine the enzyme functionality was achieved as it was evident that the purified proteins demonstrated validated enzyme activity. The ATP concentration gradient assay information was needed to elucidate the action of ATP on the function and regulation of the mechanisms involved in the phosphoryl transfer amongst the selected eight kinases.

The investigation of the overall enzyme functionality of the kinases was required in order to further study, by comparison, the potential enzyme inhibition by the medicinal plant, *Pelargonium sidoides*, which is fully explained in Chapter 5.



# Chapter 5: Screening of the effect of extracts of *Pelargonium sidoides* on Mtb kinase activity

---

## 5.1 Introduction

The classic treatment of TB is the administration of 4 antibiotics for 2 months, followed by 2 antibiotics for another 4 months (World Health Organisation. 2014). During this long period of treatment, the waxy, hydrophobic cell wall of Mtb is able to survive against acids, detergents, oxidative bursts and antibiotics (Dartmouth Undergraduate Journal of Science. 2009). TB is a major health threat because Mtb penetrates the body's own immune system, can survive for weeks outside the body, and has adaptive abilities to resist most of the standard antibiotics resulting in the development of multi-drug resistance, as well as co-infection with HIV patients (Dartmouth Undergraduate Journal of Science. 2009, Yang et al. 2011). The WHO has tried to execute a new system, called directly observed treatment short-course (DOTS), which monitors TB patients closely in order to assist in the absolute eradication of the infection as well as to prevent multi-drug resistance (World Health Organisation. 2008). Therefore, considering the fact that TB is a public health concern, it is imperative to find new effective drug compounds.

The treatment of human diseases has, since the beginning of human civilization, consisted of the use of natural products such as plants, animals and minerals (Lahlou. 2013, Patwardhan et al. 2004). In particular, the use of plants has been a significant source for medical remedies. The widespread use of plants has, over time, led to the development of many modern medical therapies (Patwardhan et al. 2004). Unfortunately, research gaps still exist between traditional plant medication and modern pharmaceuticals. Hence, the extensive examination and analysis of medically valuable plants has become a vital area of research for the discovery and development of novel drugs in the pharmaceutical industry (Lahlou. 2013).

*Pelargonium sidoides* has been used by traditional healers many years ago to treat coughs, chest problems and TB, by the administration of a concoction of the plants root (Helmstadter. 1996). Although this medicinal plant has been extensively used and broadly researched, there is

still a lack of understanding of this plant's scientific curative effect (Kayser & Kolodziej. 1995). The biologically active compounds from this plant, and their key targets, have not been thoroughly investigated. Thus, in an effort to find new lead compounds for TB treatment, the final stage of this study focused on the basic screening of the TB kinases against a root extract of *P. sidoides*.

Firstly, harvesting and extraction methodologies were carried out on the *P. sidoides* plant to obtain crude plant extracts of the root. Secondly kinase activity was determined, in the presence of the *P. sidoides* plant extract, using the chromatography technique of HPLC to measure reaction analytes. The application of these two essential processes, carried out in this section of the study, was ultimately to evaluate and assess the possible inhibitory effect of the plant extract on the eight Mtb kinases, giving an indication of the presence of a possible natural plant kinase inhibitor. Lastly, the results obtained were plotted on graphs to obtain dose-response curves. Once the dose response curves were attained, the  $IC_{50}$ , which is the half maximum inhibition value, was calculated as it is a quantitative measure of the effectiveness of the plant extract in inhibiting the kinases' activity (Wu et al. 2003).

Hence, the central objective of this last segment of research was to screen each purified Mtb kinase against an extract prepared from *P. sidoides*, to determine any inhibitory effects by the plant extract.

## 5.2 Materials and Methods

### 5.2.1 Plant Harvesting and Extraction

The *P. sidoides* fresh plant material was supplied to the Natural Plants and Agroprocessing (NPA) division of CSIR Biosciences from the CSIR Enterprise Creation for Development (ECD) division. The roots of the plant material underwent a series of plant preparation and extraction procedures which were carried out by the NPA staff.

The plant material was ground and then extracted in 43% (m/v) ethanol in water at 60°C, followed by an evaporation step to remove the ethanol. The resulting powder was then freeze-dried and the resulting refined product, of dry plant crude extract, was placed in a plastic bottle and subsequently stored at 4°C. These methodologies were required for the chemical separation of the plant substances.

### 5.2.2 Plant inhibitory screens

The eight kinases stored at -70°C were allowed to thaw on ice in order to set up plant inhibition screens by means of HPLC-based activity assays.

Prior to the setup of the assays, stocks of the *P. sidoides* plant extract were prepared. The dry plant crude extract stored at 4°C, was weighed out in 100 mg per 1 ml of distilled water and stored in a sterile 2 ml microcentrifuge tube. This was then subsequently used to set up six 1 ml 10-fold serial dilutions in distilled water, ranging from  $1 \times 10^{-5}$  mg/ml to  $1 \times 10^1$  mg/ml, before being stored at -20°C.

The HPLC enzyme assays were set up according to the designed and optimized validated assays described in Chapter 4 with the addition of varying concentrations of the *P. sidoides* plant extract. The *P. sidoides* dilution stocks, stored at -20°C, were used to set up the plant extract concentration gradient assay for each kinase. A control assay of 0 mg/ml of plant extract (i.e. water) was also run in parallel, in order to serve as a negative control for activity comparison analysis.

The reagents and conditions of these HPLC assay reaction mixtures are presented in Table 5-1. The assay reactions were each carried out in 100 µl volumes with 10 µl of the varying plant extract concentrations. These assay reactions consisted of tubes of 90 µl of the prepared reaction mixture with either 10 µl of enzyme, prepared in triplicate or 10 µl distilled water, prepared in duplicate, served as a control blank. These assays were allowed to incubate at 37°C for a specific amount of time, stipulated in Table 5-1, and thereafter stopped with 5% [v/v] 200 mM EDTA.2Na.2H<sub>2</sub>O. The reactions were subsequently loaded onto the HPLC system for the measurement of ADP production (as per HPLC process in section 4.2.1). The resulting data was then displayed by the HPLC Agilent ChemStation (Revision B.02.01) software.

The resulting data displayed were then processed and thereafter plotted on graphs to obtain dose-response curves with error bars. The ADP values were plotted against the plant extract concentration gradient, ranging from  $1 \times 10^{-6}$  mg/ml to  $1 \times 10^0$  mg/ml, represented by LOGS. The absolute ADP values were subtracted by the blank values (assay with no enzyme) to give the net value of the ADP production. The ADP levels at time zero were also plotted.

The IC<sub>50</sub> values were calculated, with the aid of GraphPad Prism 5 (GraphPad Software Inc. USA), from the compiled results of the dose-response curves.

Table 5-1: Details of kinase reactions in the presence of various dilutions of plant root extract

Enzyme	Assay reaction mixtures	Incubation time
<b>NDK</b>	100 mM K-PO <sub>4</sub> buffer (pH 6.8), 250 mM KCl 5 nM enzyme, 0.2 M TDP 1 mM ATP and 1 mM MgCl <sub>2</sub> 0-1 mg/ml <i>P. sidoides</i> plant extract	40 minutes
<b>HSK</b>	50 mM HEPES buffer (pH 7.0), 450 mM KCl 704 nM enzyme, 10 mM Homoserine 1 mM ATP and 1 mM MgCl <sub>2</sub> 0-1 mg/ml <i>P. sidoides</i> plant extract	4 hours
<b>AK</b>	100 mM Tris buffer (pH 7.0), 250 mM KCl 223 nM enzyme, 10 mM Na acetate 1 mM ATP and 1 mM MgCl <sub>2</sub> 0-1 mg/ml <i>P. sidoides</i> plant extract	24 hours
<b>GK</b>	100 mM Tris buffer (pH 7.0), 250 mM KCl 208.6 nM enzyme, 100 mM Glycerol 1 mM ATP and 1 mM MgCl <sub>2</sub> 0-1 mg/ml <i>P. sidoides</i> plant extract	24 hours
<b>ThiL</b>	100 mM Tris buffer (pH 8.0), 250 mM KCl 2074 nM enzyme, 1 mM TMP 1 mM ATP and 1 mM MgCl <sub>2</sub> 0-1 mg/ml <i>P. sidoides</i> plant extract	5 hours
<b>RBKS</b>	100 mM Tris buffer (pH 7.2), 100 mM KCl 250 nM enzyme, 10 mM D-ribose 1 mM ATP and 1 mM MgCl <sub>2</sub> 0-1 mg/ml <i>P. sidoides</i> plant extract	4 hours
<b>AsK</b>	100 mM Tris-HCl buffer (pH 7.5), 178.2 nM enzyme 10 mM L-Aspartic acid 1 mM ATP and 1 mM MgCl <sub>2</sub> 0-1 mg/ml <i>P. sidoides</i> plant extract	6 hours
<b>SK</b>	100 mM K-PO <sub>4</sub> buffer (pH 6.8), 500 mM KCl 10 nM enzyme, 8 mM shikimic acid 1 mM ATP and 1 mM MgCl <sub>2</sub> 0-1 mg/ml <i>P. sidoides</i> plant extract	20 minutes

## 5.3 Results and Discussion

### 5.3.1 Plant material

The harvesting and extraction methodologies for *P. sidoides* were successfully conducted by the NPA staff.

### 5.3.2 *Pelargonium sidoides* concentration gradient assay outcome

The experiment conducted was to simply observe any potential inhibition by the plant extract. This elemental assessment was successfully carried out by HPLC-based assays, which were swift and validated. As indicated above, HPLC is a widely used technique for the isolation and detection of biological compounds (Horvath et al. 1967). The inhibitory activity was determined by the measurement of the kinase enzymatic activity, in comparison to the enzymatic activity of the kinase exposed to the plant extract. Each assay point was conducted in triplicate in order to obtain reliable results.

The resulting graphs of the ADP production by the kinases as a measure against a LOG concentration gradient of the plant extract, ranging from  $1 \times 10^{-6}$  –  $1 \times 10^0$  mg/ml, are shown in Figures 5-1 to 5-8, with error bars. The error bars are as a result of the assays being done in triplicate. The calculated  $IC_{50}$  values are tabulated in Table 5-2.

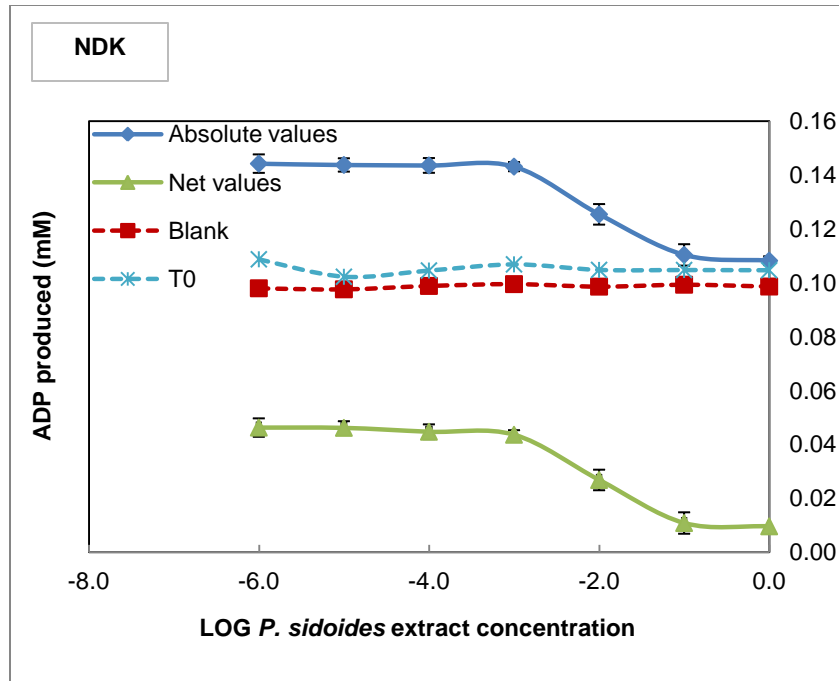


Figure 5-1: ADP production by His-NDK as a measure against a LOG concentration gradient of *P. sidoides* extract. The 40 minute assay contained 100 mM K-PO<sub>4</sub> buffer (pH 6.8), 250 mM KCl, 5 nM enzyme, 0.2 M TDP, 1 mM ATP, 1 mM MgCl<sub>2</sub> and 1 x 10<sup>-6</sup> mg/ml to 1 x 10<sup>0</sup> mg/ml *P. sidoides* plant extract. The varying concentrations of *P. sidoides* plant extract are represented by LOGS.

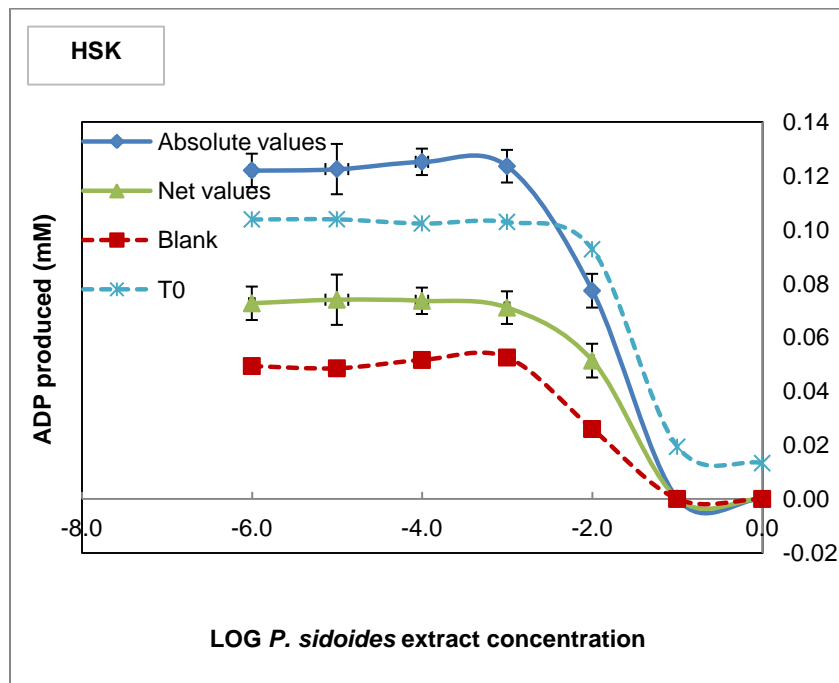


Figure 5-2: ADP production by His-HSK as a measure against a LOG concentration gradient of *P. sidoides* extract. The 4 hour assay contained 50 mM HEPES buffer (pH 7.0), 450 mM KCl, 704 nM enzyme, 10 mM Homoserine and 1 mM ATP, 1 mM MgCl<sub>2</sub> and 1 x 10<sup>-6</sup> mg/ml to 1 x 10<sup>0</sup> mg/ml *P. sidoides* plant extract. The varying concentrations of *P. sidoides* plant extract are represented by LOGS.

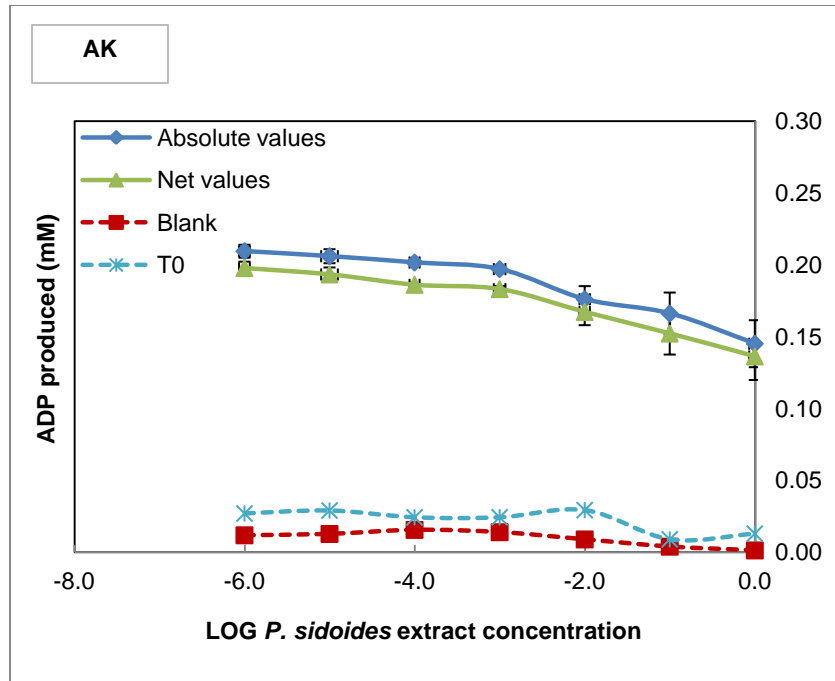


Figure 5-3: AK - ADP production by His-AK as a measure against a LOG concentration gradient of *P. sidoides* extract. The 24 hour assay contained 100 mM Tris buffer (pH 7.0), 250 mM KCl, 223 nM enzyme, 10 mM Na acetate and 1 mM ATP, 1 mM MgCl<sub>2</sub> and 1 x 10<sup>-6</sup> mg/ml to 1 x 10<sup>0</sup> mg/ml *P. sidoides* plant extract. The varying concentrations of *P. sidoides* plant extract are represented by LOGS.

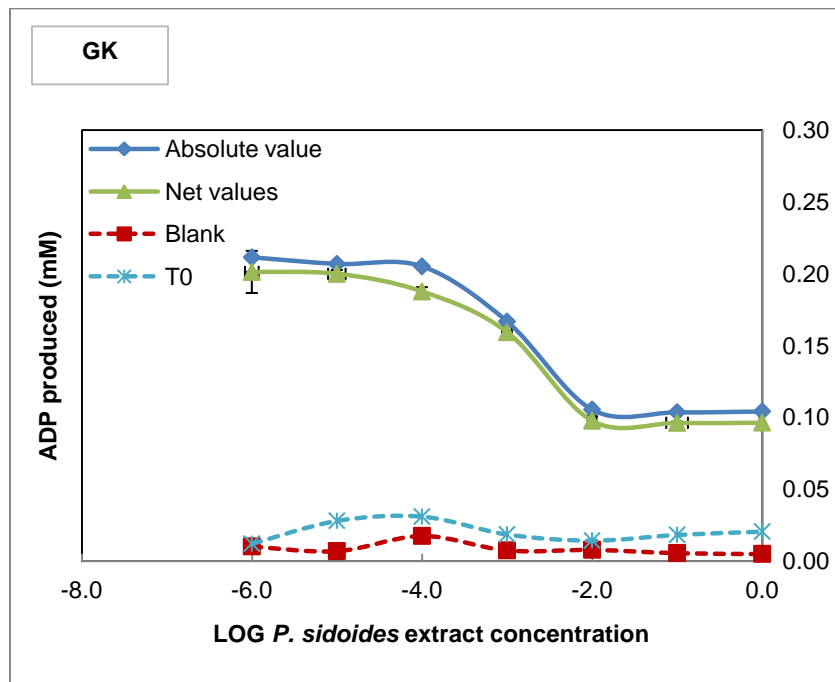


Figure 5-4: GK - ADP production by His-GK as a measure against a LOG concentration gradient of *P. sidoides* extract. The 24 hour assay contained 100 mM Tris buffer (pH 7.0), 250 mM KCl, 208.6 nM enzyme, 100 mM Glycerol and 1 mM ATP, 1 mM MgCl<sub>2</sub> and 1 x 10<sup>-6</sup> mg/ml to 1 x 10<sup>0</sup> mg/ml *P. sidoides* plant extract. The varying concentrations of *P. sidoides* plant extract are represented by LOGS.



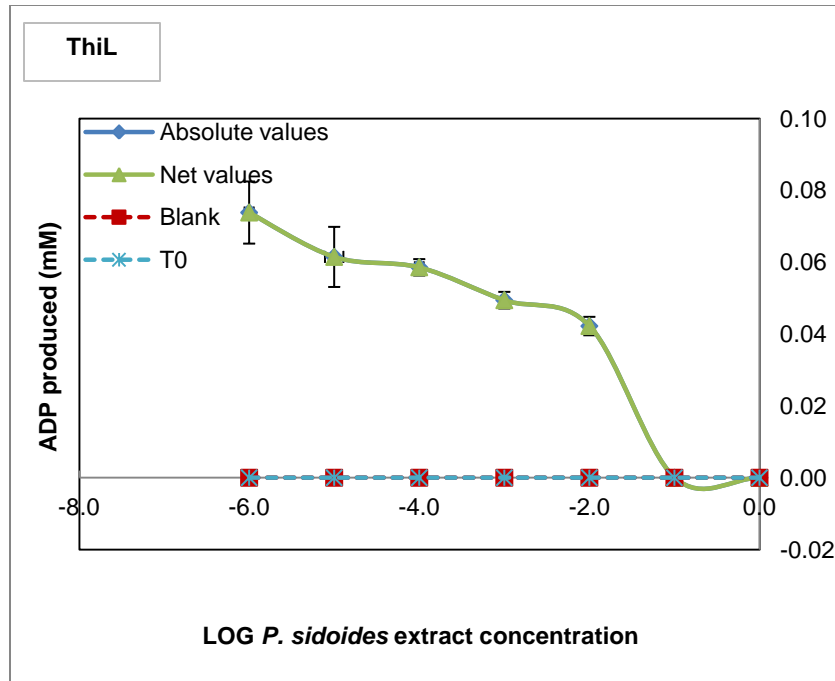


Figure 5-5: ADP production by His-ThiL as a measure against a LOG concentration gradient of *P. sidoides* extract. The 5 hour assay contained 100 mM Tris buffer (pH 8.0), 250 mM KCl, 2074 nM enzyme, 1 mM TMP and 1 mM ATP, 1 mM MgCl<sub>2</sub> and 1 x 10<sup>-6</sup> mg/ml to 1 x 10<sup>0</sup> mg/ml *P. sidoides* plant extract. The varying concentrations of *P. sidoides* plant extract are represented by LOGS.

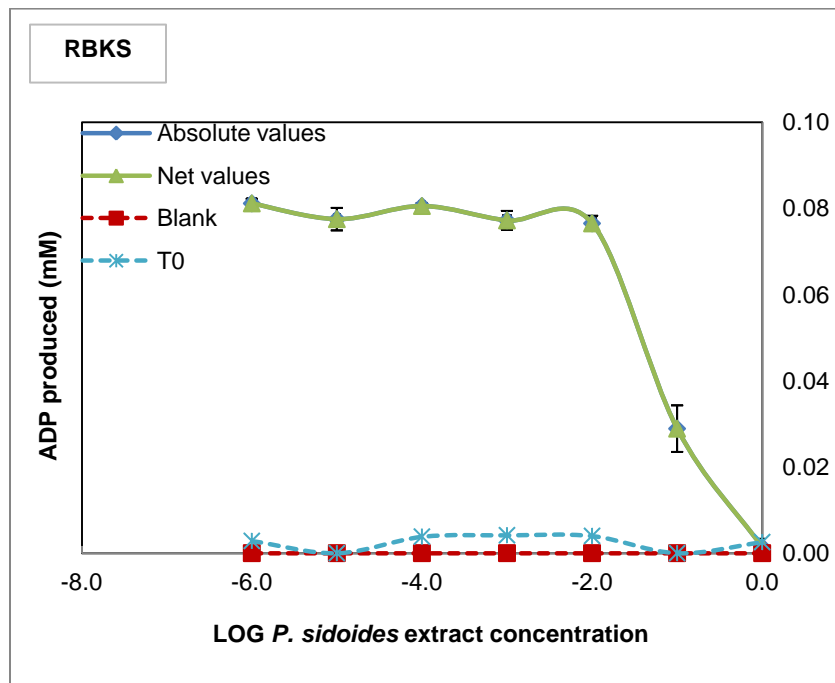


Figure 5-6: ADP production by His-RBKS as a measure against a LOG concentration gradient of *P. sidoides* extract. The 4 hour assay contained 100 mM Tris buffer (pH 7.2), 100 mM KCl, 250 nM enzyme, 10 mM D-ribose and 1 mM ATP, 1 mM MgCl<sub>2</sub> and 1 x 10<sup>-6</sup> mg/ml to 1 x 10<sup>0</sup> mg/ml *P. sidoides* plant extract. The varying concentrations of *P. sidoides* plant extract are represented by LOGS.

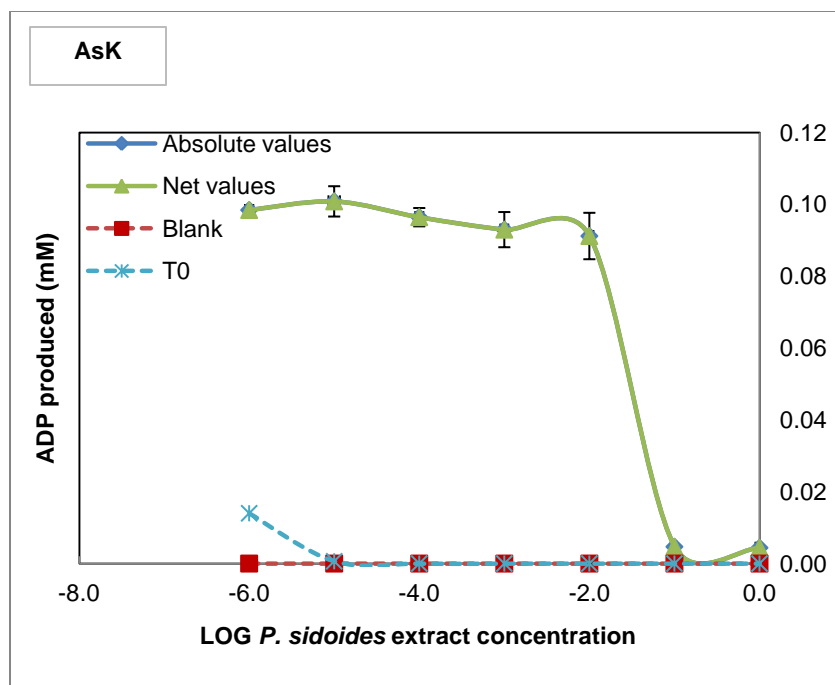


Figure 5-7: ADP production by His-AsK as a measure against a LOG concentration gradient of *P. sidoides* extract. The 6 hour assay contained 100 mM Tris-HCl buffer (pH 7.5), 178.2 nM enzyme, 10 mM L-Aspartic acid and 1 mM ATP, 1 mM MgCl<sub>2</sub> and 1 x 10<sup>-6</sup> mg/ml to 1 x 10<sup>0</sup> mg/ml *P. sidoides* plant extract. The varying concentrations of *P. sidoides* plant extract are represented by LOGS.

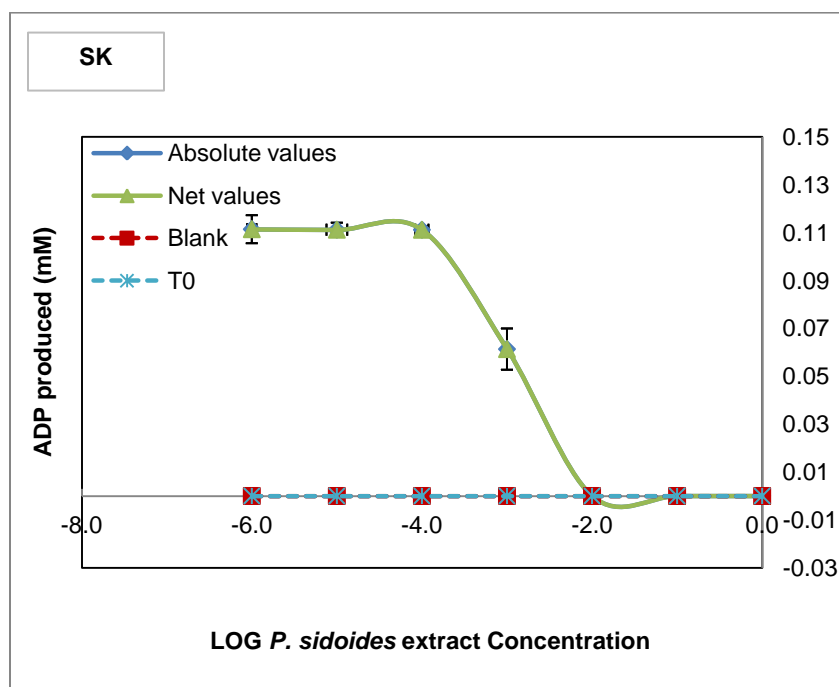


Figure 5-8: ADP production by His-SK as a measure against a LOG concentration gradient of *P. sidoides* extract. The 20 minute assay contained 100 mM K-PO<sub>4</sub> buffer (pH 6.8), 500 mM KCl, 10 nM enzyme, 8 mM shikimic acid and 1 mM ATP, 1 mM MgCl<sub>2</sub> and 1 x 10<sup>-6</sup> mg/ml to 1 x 10<sup>0</sup> mg/ml *P. sidoides* plant extract. The varying concentrations of *P. sidoides* plant extract are represented by LOGS.

Table 5-2: Kinases and their respective IC<sub>50</sub> values derived from the dose-response curves

Kinase	IC <sub>50</sub> value (mM)
NDK	0.00952
HSK	0.02
AK	0.01168
GK	0.01023
ThiL	0.01668
RBKS	0.07589
AsK	0.03388
SK	0.001170

With regard to the graphs displayed in Figure 5-1 to 5-8, it can be seen that the enzyme's activity was generally constant at low levels of plant extract and then began to decrease in the presence of higher concentrations of plant extract. The blank and time zero values were high for NDK and HSK as seen in Figure 5-1 and 5-2 respectively. This is consistent with the results obtained from the ATP concentration gradient assay graphs in Chapter 4. At this stage, it cannot be certain that the inhibition displayed for HSK at the higher concentrations was caused by the plant only, as it could also be changes in the assay conditions which affected the activity.

The IC<sub>50</sub> values essentially represent the concentration of a drug that is required for 50% inhibition. The lower the IC<sub>50</sub> value, the more potent the potential drug is. At this initial point in the study, the SK enzyme inhibitory assay showed the lowest IC<sub>50</sub> value in comparison to the other enzymes.

### 5.3.3 Plant inhibitory screens evaluation

The data, from the biochemical analysis of the serial dilutions of *P. sidoides* extract, were also presented on bar graphs displayed in Figures 5-9 to 5-16, with error bars. These visual graphs were prepared to easily observe the effect of the plant extract concentration gradient, ranging from 0 to 1 x 10<sup>0</sup> mg/ml, on the activity of the various kinases.

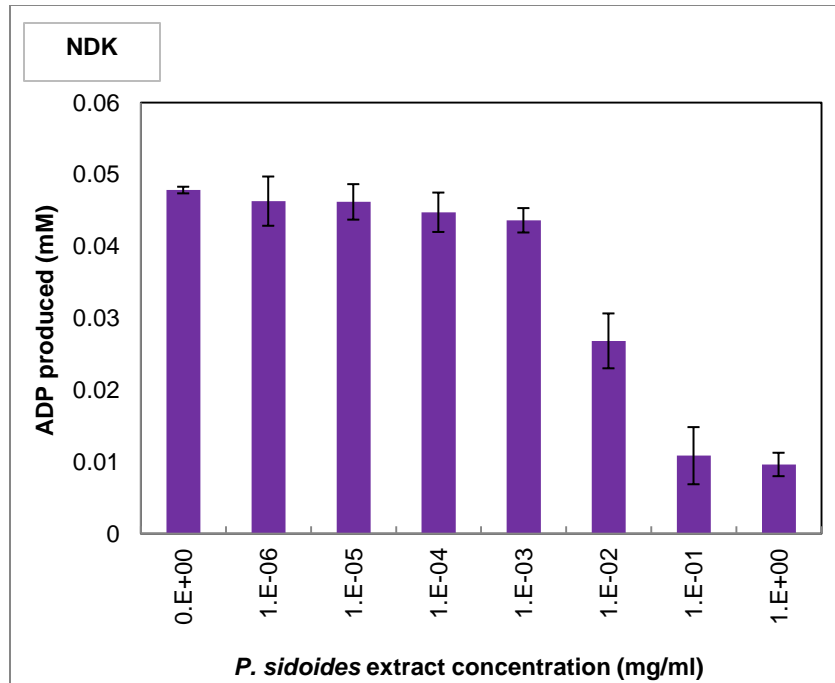


Figure 5-9: Bar graph of ADP production by His-NDK as measured against a concentration gradient of *P. sidoides* plant extract. The varying concentrations of 0 to  $1 \times 10^0$  mg/ml of *P. sidoides* plant extract are represented by scientific numbers.

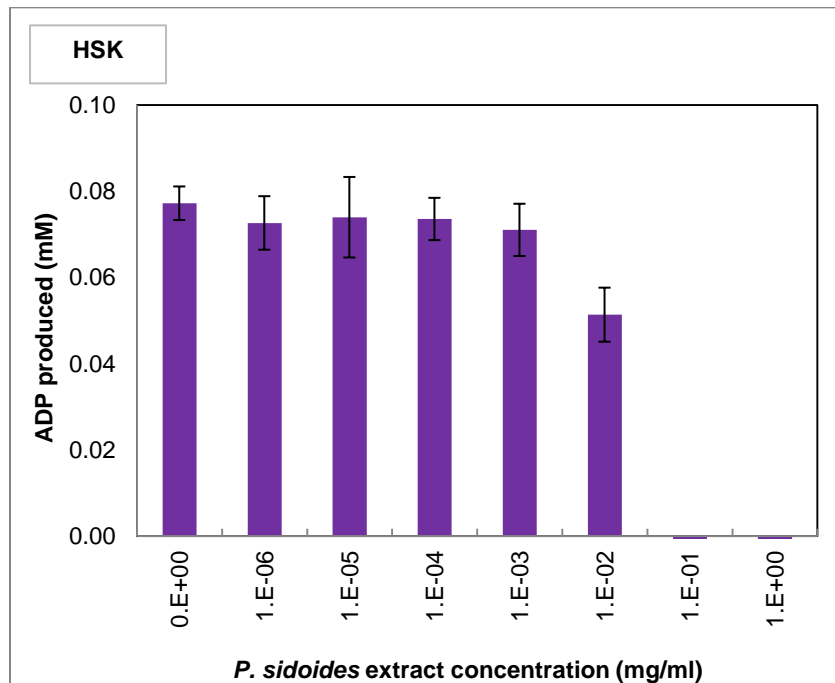


Figure 5-10: Bar graph of ADP production by His-HSK as measured against a concentration gradient of *P. sidoides* plant extract. The varying concentrations of 0 to  $1 \times 10^0$  mg/ml of *P. sidoides* plant extract are represented by scientific numbers

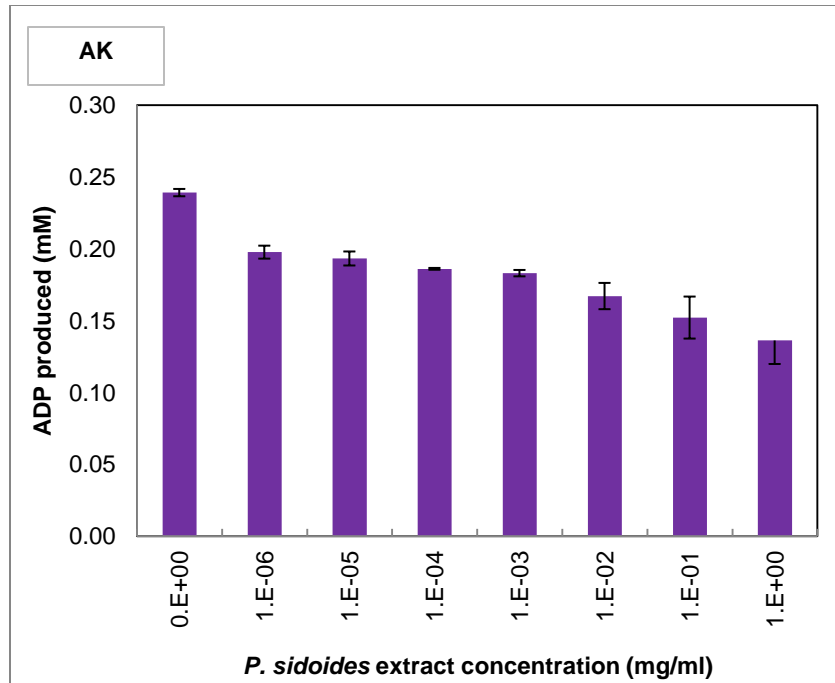


Figure 5-11: Bar graph of ADP production by His-AK as measured against a concentration gradient of *P. sidoides* plant extract. The varying concentrations of 0 to  $1 \times 10^0$  mg/ml of *P. sidoides* plant extract are represented by scientific numbers.

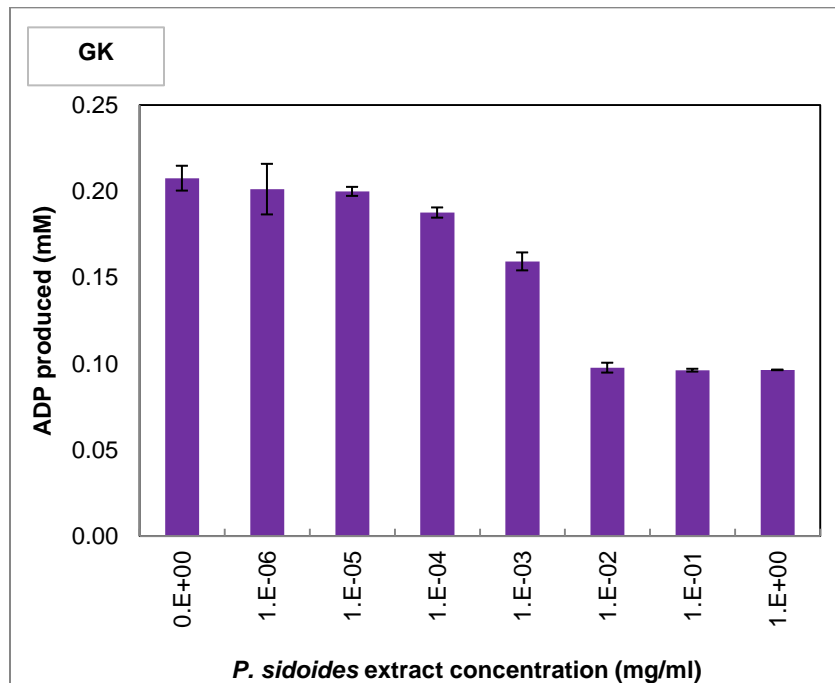


Figure 5-12: Bar graph of ADP production by His-GK as measured against a concentration gradient of *P. sidoides* plant extract. The varying concentrations of 0 to  $1 \times 10^0$  mg/ml of *P. sidoides* plant extract are represented by scientific numbers.

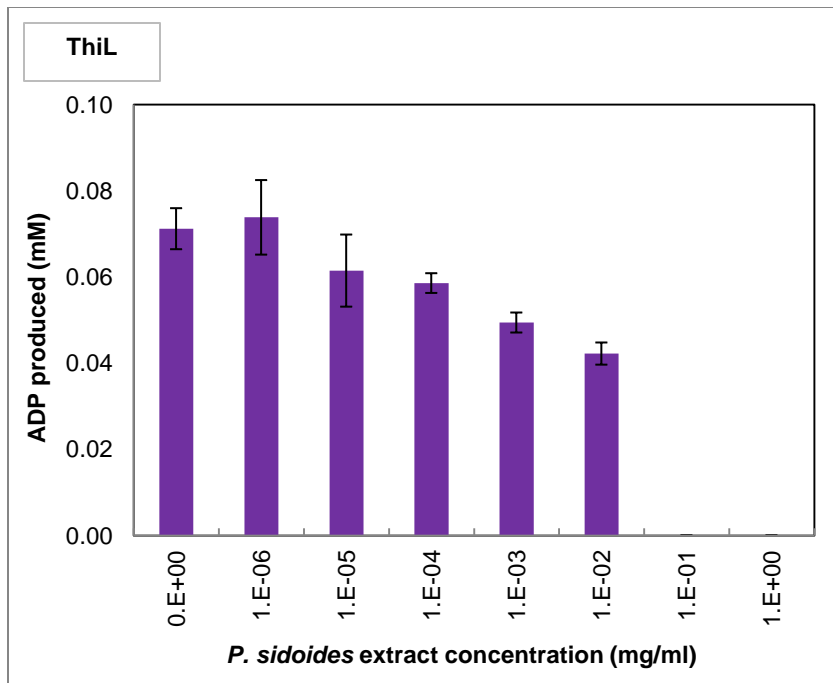


Figure 5-13: Bar graph of ADP production by His-ThiL as measured against a concentration gradient of *P. sidoides* plant extract. The varying concentrations of 0 to  $1 \times 10^0$  mg/ml of *P. sidoides* plant extract are represented by scientific numbers.

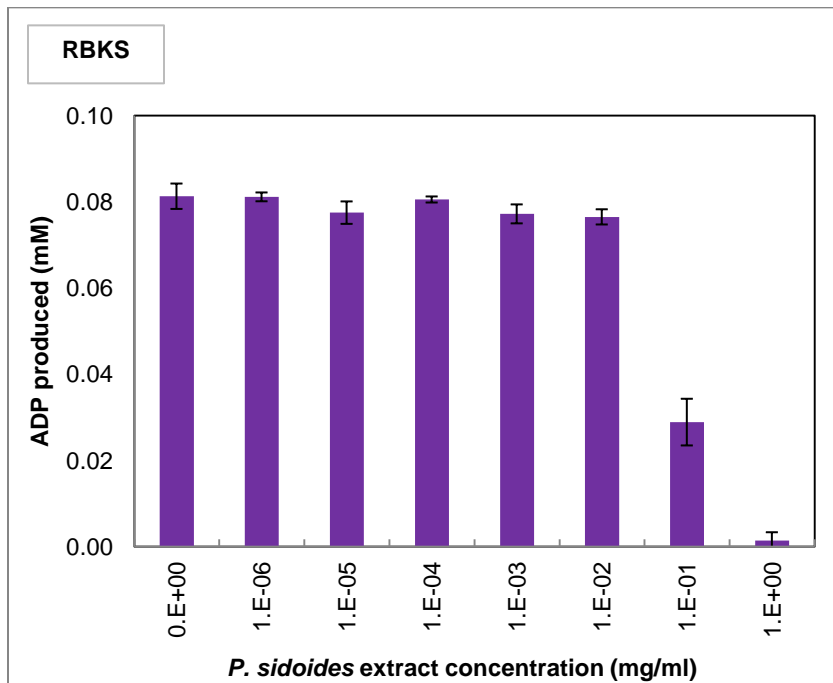


Figure 5-14: Bar graph of ADP production by His-RBKS as measured against a concentration gradient of *P. sidoides* plant extract. The varying concentrations of 0 to  $1 \times 10^0$  mg/ml of *P. sidoides* plant extract are represented by scientific numbers.

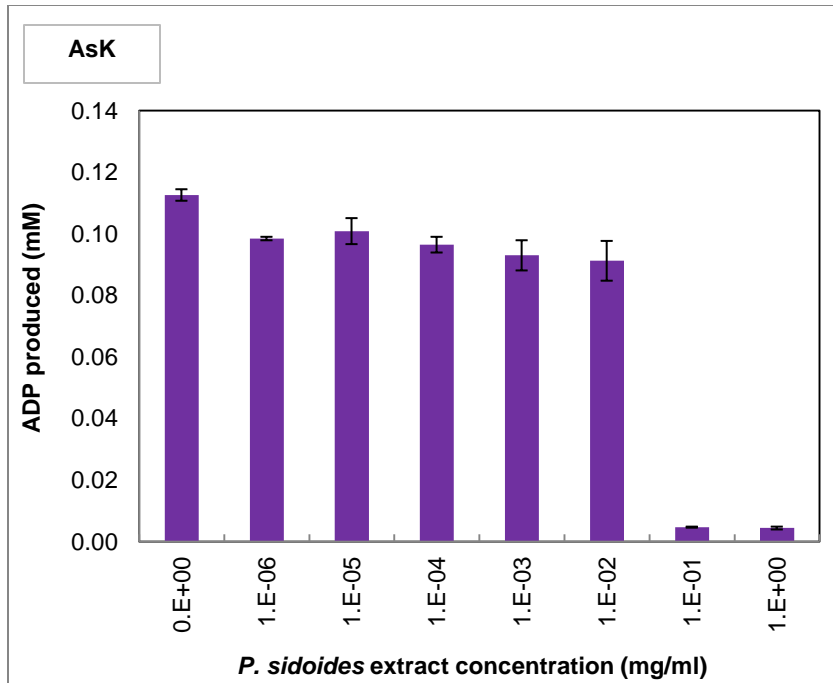


Figure 5-15: Bar graph of ADP production by His-AsK as measured against a concentration gradient of *P. sidoides* plant extract. The varying concentrations of 0 to  $1 \times 10^0$  mg/ml of *P. sidoides* plant extract are represented by scientific numbers.

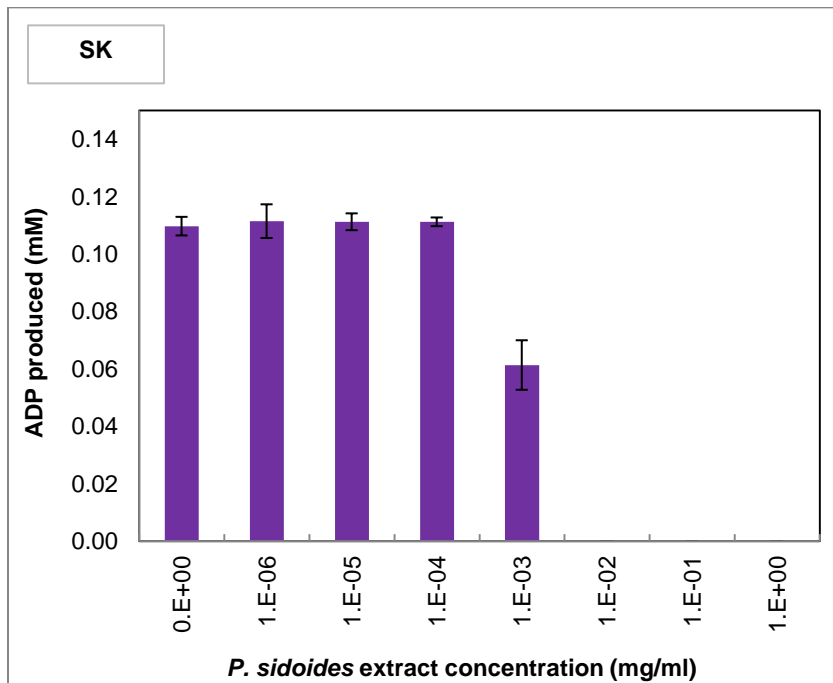


Figure 5-16: Bar graph of ADP production by His-SK as measured against a concentration gradient of *P. sidoides* plant extract. The varying concentrations of 0 to  $1 \times 10^0$  mg/ml of *P. sidoides* plant extract are represented by scientific numbers.

The resulting data provided information regarding the inhibitory action of the *P. sidoides* against the eight kinases. The determination of plant extract-enzyme interactions was established by assessing the changes in the kinase activity.

The results revealed in Figure 5-9 demonstrated that the NDK activity was relatively constant at low plant extract concentrations before starting to decrease at higher plant extract concentrations points of  $1 \times 10^{-2}$ ,  $1 \times 10^{-1}$  and  $1 \times 10^0$  mg/ml. The activity of HSK and AsK was stable and then decreased rapidly at the last two concentration points, as seen in Figure 5-10 and 5-15, respectively. The graph displaying the inhibitory screen results of the AK enzyme in Figure 5-11 does not exhibit noteworthy inhibition, as there appeared to be no significant reduction of activity. The GK activity portrayed in Figure 5-12 showed a gradual reduction in activity and then a drop in activity over the last three points. Figure 5-14, demonstrating the ADP production by the RBKS enzyme against the plant extract, revealed consistent activity and thereafter a notable decrease at the  $1 \times 10^{-1}$  mg/ml plant extract point until reaching a low ADP value at  $1 \times 10^0$  mg/ml plant extract. The activity of the ThiL enzyme, presented in Figure 5-13, illustrates a regular reduction in ADP production and a plummet to no ADP production at all at the last two concentration points. Yet on the other hand, the measurement of the SK enzyme activity, illustrated in Figure 5-16, has reduced significantly more than the other enzymes. There was absolutely no activity present at the last three plant extract concentration points.

This substantial ten-fold reduction of SK activity, compared to the other inhibited enzymes, suggests that this enzyme is a potential drug target. This notion, of SK being a potential target to develop antimicrobial agents, is in agreement with the authors Gu et al (2002) and Pereira et al (2004). This remarkable observation validates that this kinase could be a potential lead candidate for drug discovery.



## 5.4 Chapter conclusion

In conclusion, the main intention of this study was to compare TB kinase activity under normal conditions alongside proteins treated with a potential inhibitor. The inhibition of the enzymes occurred at the higher concentrations of *P. sidoides* extract at a low level. However, the SK enzyme results presented a significantly higher inhibition and the lowest IC<sub>50</sub> value, in comparison to the other kinases, which makes this kinase an attractive drug target against TB.

This research conducted has increased the quality of information available in this field of study. These interesting results, proposing SK as a potential target, can be a starting point to extend this research and possibly contribute towards the discovery of curing TB.

# Chapter 6: Concluding discussion and future recommendations

---

## 6.1 Concluding discussion

### 6.1.1 Insights into combating TB

As previously mentioned, TB is a major health risk and the emergence of multi-drug resistance against existing therapeutics, as well as HIV co-infection, has become problematic (Yang et al. 2011). TB is a disease that has the potential to be curable and preventable, provided that efficient medication, at a low cost, is constantly accessible for all infected patients worldwide. Therefore new competent TB drugs are needed immediately to treat and manage this critical disease. Hence, the identification of potential drug targets against Mtb is currently a crucial field of research.

Mtb is able to establish persistent infections in the macrophage cells, which would normally be responsible for destroying foreign microorganisms in the body (Flynn & Chaney. 2003). This strategy used by Mtb makes this organism highly pathogenic and successful. The eradication of this disease has been stalled due to insufficient information pertaining to Mtb, and its processes and mechanisms (Yang et al. 2011). As a result, the complete genome sequence of the Mtb H37Rv strain has been established (Cole et al. 1998) to help scientists gain new insights into this organism at a molecular level.

This research conducted, made use of the application of available genomic techniques, as well as systems biology, to provide further information regarding this organism, with the eventual goal of creating better medication to eliminate this lethal disease.

### 6.1.2 Using kinases as potential drug targets

Protein kinases are molecular switches that regulate biological functions, as they play a critical role in numerous metabolic and signaling pathways (Kenyon et al. 2011). Mtb kinases transmit signals through phosphorylation, which present many potential targets for innovative remedies

(Grundner et al. 2005). Therefore, the further understanding of kinases, as molecules, is essential in determining possible drug targets.

The Mtb species differs from other bacteria, as a large proportion of its coding capacity is assigned to the production of enzymes (Cole et al. 1998). Mtb has a few isolated kinase and regulatory genes, as well as a phosphorelay system (Cole et al. 1998), which suggests that there is perhaps a requirement of multiple kinases at various points in Mtb metabolism.

A characteristic virulent feature of Mtb is its slow growth and dormancy. The conversion from dormancy to reactivation is assumed to be genetically programmed and to involve intracellular signaling pathways (Cole et al. 1998). Given that kinases are involved in signaling, the inactivation of critical kinases could jeopardize these pathways, as perhaps Mtb requires back-up kinases for critical phosphorylation reactions.

The aim of this study was to firstly construct expression vectors containing the genes encoding Mtb kinases. The 8 kinase genes were successfully amplified from the Mtb H37Rv genomic DNA and inserted into selected expression vectors with a His-tag at either the C- or N-terminal. The reliability of the PCR reactions and gene manipulations conducted, were confirmed through restriction enzyme digests displayed visually on agarose gels. The accuracy of the gene sequences were validated by nucleotide sequencing. These authenticated results obtained, facilitated the progression into the next phase of study.

The next objective was to express the recombinant kinase genes in *E. coli* for protein purification. The purification of the proteins was challenging, but a variety of different techniques were investigated in order to acquire sufficient amounts of pure protein. The resulting purified protein products were effectively confirmed through SDS-PAGE gels. In summation, the expression and purification of the recombinant kinase proteins was successfully accomplished, which was necessary for further analysis.

HPLC enzyme assays were carried out to assess the functional characterization of the purified kinase proteins. Validated assays were set up and optimized for each kinase. The main purpose, to establish that the enzymes were indeed functional, was achieved as the proteins demonstrated apparent enzyme activity. The ATP concentration gradient assay results provided preliminary information that was required to clarify the action of ATP, as well as its role,

regulation and mechanism, during the phosphoryl transfer process. The overall enzyme functionality information was a pre-requisite for executing further plant screening comparison studies.

### **6.1.3 The gap between traditional *P. sidoides* usage and modern pharmaceuticals**

The traditional use of the plant root of *P. sidoides* has been used to treat coughs, chest problems and TB. However, there is still a major research breach between traditional practice and modern therapies.

According to the evaluation of *P. sidoides* antibacterial activity, conducted by Kolodziej (2007), the data provided positive responses from the infected cells, as oppose to the noninfected cells. This provided support to validate the medicinal use of *P. sidoides*. However, the remedial effects are not yet associated to biochemical defined principles and therefore further studies is required in order to investigate and analyse this medically significant plant (Lahlou. 2013).

Other studies show that *P. sidoides* has a wide range of antibacterial activity on gram positive and gram negative organisms. Phytochemical studies show the presence of a large number of secondary metabolites in the plant such as tannins, coumarins, phenolic acids, phenylpropanoid derivatives and other chemical constituents (Brendler & Van Wyk. 2008). The exploration for the actual compound responsible is imperative. The main goal is to define the responsible antibacterial compound and recondition and enhance these activities (Taylor. 2004) for a cost-effective remedy.

The most important objective of this study was to contrast TB kinase activity under normal conditions against proteins treated with the possible plant inhibitor. The results revealed some inhibition of the enzymes only at the higher concentrations of the *P. sidoides* extract. *P. sidoides* exhibit remarkable diversity and complexity (Kolodziej. 2007), with broad inhibitory activity that perhaps promotes a general phosphorylation shut down.

On the other hand, the SK enzyme results displayed a significantly higher inhibition compared to the other enzymes, as well as the lowest IC<sub>50</sub> value of 0.001170. This noteworthy ten-fold reduction of SK activity validates and recommends that this enzyme is an attractive potential drug target. Another advantage is that SK, and other enzymes involved in the shikimate

pathway, are great potential targets for creating harmless antimicrobial agents because the pathway is essential for Mtb but is not present in mammals (Pereira et al. 2004). This perception, of SK being a lead candidate to develop antibacterial medication, has also been previously described by Gu et al (2002) and Pereira et al (2004).

This study carried out has improved the value of information available in this specific field of study. These remarkable results, suggesting SK as a probable target, can be the starting point to expand this investigation further. These preliminary results could also facilitate in bridging the gap between traditional *P. siddoides* practice and modern therapies in addition to help contribute to the development of effective TB remedy.

## 6.2 Future recommendations

The essential biologically active compound, within the *P. sidoides* plant extract, that is responsible for the inhibitory effects, is most likely concealed in the multi-component mixture. Thus, the separation, detection and analysis of this multi-component mixture must be carried out in order to utilize these natural resource compounds effectively (Lahlou. 2013).

Fractionation of the plant material can be carried out, and the resulting isolated fractions can be tested through HPLC assays for the detection of enzyme inhibition (Tu et al. 2010). The fractions of the plant that demonstrate inhibitory activity can then be further dried, weighed and reformatted for screening. Subsequently, the evaluation of the fractions for the identification of the actual molecules responsible for the inhibition can be conducted. These molecules will then have to be purified, by using a variety of purification techniques, to further isolate these particular bioactive compounds for structure elucidation (Tu et al. 2010). Automated and high-throughput methods can also be used throughout to rapidly prepare and evaluate various plant fractions to provide a more detailed and accurate study (Tu et al. 2010).

Once these fractionation studies are established, they can be used as a platform for advanced studies in the pharmacological sector. Pharmacological methods can be applied for the ultimate production and assessment of medically effective TB drugs. This research will allow the development and design of novel TB drugs and as a consequence, unlock opportunities for new drug systems.

# Appendices

---

## Appendix A

### 1) Nucleoside diphosphokinase

```
1      ATGGGCCATCATCATCATCATCATCATCATCACAGCAGCGGCCATATCGAAGGTCGT
1      M G H H H H H H H H H S S G H I E G R

61     CATATGACCGAACGGACTCTGGTACTGATCAAGCCGGATGGCATCGAAAGGCAGCTGATC
21     H M T E R T L V L I K P D G I E R Q L I

121    GGCGAGATCATCAGCCGCATCGAGCGCAAAGGCCTCACCATCGCTGCGCTGCAGCTCAGG
41     G E I I S R I E R K G L T I A A L Q L R

181    ACCGTCAGCGCGGAGTTGGCCAGCCAGCACTACGCCGAACATGAAGGCAAACCATTCTTT
61     T V S A E L A S Q H Y A E H E G K P F F

241    GGATCGTTGCTGGAGTTCATCACGTCGGGTCCGGTGGTAGCGGCATCGTGGAGGGAACC
81     G S L L E F I T S G P V V A A I V E G T

301    CGAGCCATCGCGGCGGTTTCGCCAACTCGCCGGCGGCACCGACCCGGTGCAGGCGGCGGCG
101    R A I A A V R Q L A G G T D P V Q A A A

361    CCCGGCACAATCCGGGGCGACTTCGCTCTAGAGACGCAGTTCAACCTGGTGCACGGGTCT
121    P G T I R G D F A L E T Q F N L V H G S

421    GATTCGGCCGAATCCGCGCAGCGCGAAATCGCGCTCTGGTTTTCCCGGCGCCTAA
141    D S A E S A Q R E I A L W F P G A *
```

## 2) Homoserine kinase

1 ATGGTGACTCAAGCATTGTTGCCTTCTGGGCTGGTGGCCAGTGCGGTGGTGGCGGCGTCC  
1 M V T Q A L L P S G L V A S A V V A A S

61 AGTGCAAACCTGGGCCCCGGGCTTCGACAGTGTCCGTTTGGCGCTGAGTCTCTACGACGAG  
21 S A N L G P G F D S V G L A L S L Y D E

121 ATCATCGTCGAGACAACAGATTCCGGCTTGACGGTGACTGTAGACGGCGAGGGCGGCGAC  
41 I I V E T T D S G L T V T V D G E G G D

181 CAGGTGCCGCTGGGCCCCGAGCACCTCGTGGTCCGCGCCGTGCAGCACGGGTTACAGGCA  
61 Q V P L G P E H L V V R A V Q H G L Q A

241 GCGGGGGTTCAGCGCCGCGGCGCTGGCGGTGCGCTGCCGCAACGCCATCCCGCACTCCCGC  
81 A G V S A A G L A V R C R N A I P H S R

301 GGCCTCGGCTCCTCCGCGGCAGCAGTTGTGGGCGGTCTTGCGGCCGTTAACGGTCTTGTG  
101 G L G S S A A A V V G G L A A V N G L V

361 GTACAAACGGATTTCGTCACCATCGAGCGATGCTGAGCTGATTTCAGTTGGCTTCGGAGTTC  
121 V Q T D S S P S S D A E L I Q L A S E F

421 GAGGGTTCATCCCGACAACGCGGCGGCGCGGTTTTGGGTGGTGGCGTGGTTCGTTGGACT  
141 E G H P D N A A A A V L G G A V V S W T

481 GACCACAGTGGTGACCGGCCCAACTATTCGGCCGTATCACTGCGGCTTCATCCCGATATC  
161 D H S G D R P N Y S A V S L R L H P D I

541 CGCCTGTTCACTGCGATTCCCGAGCAGCGTTTCGTCGACCGCGGAAACGCGGGTGCTATTG  
181 R L F T A I P E Q R S S T A E T R V L L

601 CCCGCGCAGGTTAGTCACGACGACGCACGGTTCAATGTCAGTCGCGCGGCGCTGCTGGTG  
201 P A Q V S H D D A R F N V S R A A L L V

661 GTTGGCTCACCGAACGGCCGATCTGCTGATGGCGGCCACCGAAGATCTGCTTCATCAG  
221 V A L T E R P D L L M A A T E D L L H Q

721 CCGCAACGTGCCGCGGCAATGACAGCCTCCGCGGAATATCTTCGGCTGTTGCGGCGTCAT  
241 P Q R A A A M T A S A E Y L R L L R R H

781 AACGTGGCAGCAGCACTGTCCGGGGCAGGTCTTCGTTGATCGCCCTGAGTACAGATTCA  
261 N V A A A L S G A G P S L I A L S T D S

841 GAGTTGCCGACCGACGCGGTGGAGTTCGGAGCCGCAAAGGGATTTGCCGTTACCGAGCTG  
281 E L P T D A V E F G A A K G F A V T E L

901 ACTGTTGGCGAGGCGGTTTCGCTGGAGCCCGACAGTAAGAGTTCCCGGTCTCGAGCACCAC  
301 T V G E A V R W S P T V R V P G L E H H

961 CACCACCACCTGA  
321 H H H H \*



### 3) Acetate kinase

1 ATGGGCCATCATCATCATCATCATCATCATCATCACAGCAGCGGCCATATCGAAGGTCGT  
1 M G H H H H H H H H H S S G H I E G R

61 CATATGAGTAGCACCGTGTGGTATCAATTCCGGCTCGTTCGCTGAAGTTCAGCTC  
21 H M S S T V L V I N S G S S S L K F Q L

121 GTCGAGCCGGTCCCGGCATGTACAGTGCCCGGGATTGTGAGCGGATCGGCGAGCGG  
41 V E P V A G M S R A A G I V E R I G E R

181 TCATCCCCGTTGCCGATCACGCCAGGCGCTGCATCGCGCATTCAAGATGTTGGCCGAG  
61 S S P V A D H A Q A L H R A F K M L A E

241 GACGGAATTGACCTGCAGACCTGCGGGCTGGTGGCGGTCGGACACCGGGTGGTCCACGGC  
81 D G I D L Q T C G L V A V G H R V V H G

301 GGCACGGAGTTTACCAGCCGACGCTGCTGGATGACACGGTGCATCGGCAAGCTTGAGGAG  
101 G T E F H Q P T L L D D T V I G K L E E

361 CTGTGCGGCGTGGCCCCGTTGCACAACCCGCCGGGTTACTGGGCATCAAGGTGGCACGC  
121 L S A L A P L H N P P A V L G I K V A R

421 AGATTGCTGGCCAATGTGCGGCACGTGCGGGTGTTCGATACGGCCTTTTTCCATGACTTG  
141 R L L A N V A H V A V F D T A F F H D L

481 CCCCCGGCGCCGCGACCTATGCCATCGACCGCGACGTGCGCCGACAGATGGCATATCCGC  
161 P P A A A T Y A I D R D V A D R W H I R

541 CGCTACGGATTTTCATGGCACTTACACCAATACGTGAGCGAGCGGGCCCGCCTTCCCTG  
181 R Y G F H G T S H Q Y V S E R A A A F L

601 GGCCGCCGCTCGACGGTTTGAATCAGATTGTGCTGCATCTGGGTAACGGTGCCTCCGCC  
201 G R P L D G L N Q I V L H L G N G A S A

661 TCGGCGATTGCCCGCGCCGCGGGTGGAAACGTGATGGGCCTGACACCGCTTGAGGGC  
221 S A I A R G R P V E T S M G L T P L E G

721 TTGGTGATGGGCACCCGAGTGGCGACCTGGACCCGGGCGTCATCAGCTACTTGTGGCGC  
241 L V M G T R S G D L D P G V I S Y L W R

781 ACCGCGAGGATGGGTGTGAGGACATCGAATCGATGCTCAACCATCGGTCCGGGATGTTG  
261 T A R M G V E D I E S M L N H R S G M L

841 GGGTTGGCGGGGAGCGGGATTTTCGCCGTCTACGACTAGTGATCGAAACCGGGGACAGG  
281 G L A G E R D F R R L R L V I E T G D R

901 TCAGCACAATTGGCGTATGAGGTGTTTCATCCACCGGTTGCGCAAGTACCTTGGTGCCTAT  
301 S A Q L A Y E V F I H R L R K Y L G A Y

961 CTGGCGGTGTTGGGCCACACCGATGTGGTGAGCTTTACCGCCGGGATCGGCGAAAACGAT  
321 L A V L G H T D V V S F T A G I G E N D

1021 GCGGCGGTGCGGCGGGACGCGTTGGCTGGCCTTACGGGGCTAGGTATCGCACTCGACCAA  
341 A A V R R D A L A G L Q G L G I A L D Q

1081 GACCGCAACCTGGGCCCCGGGCACGGCGCCCGGGGATTTCGTGAGACGATTCACCGATC  
361 D R N L G P G H G A R R I S S D D S P I

1141 GCCGTGCTGGTGGTTCACGAAATGAAGAACTGGCCATCGCCCGGATTGCCTGAGGGTG  
381 A V L V V P T N E E L A I A R D C L R V

1201 CTGGGCGGACGCCGAGCGTAA  
401 L G G R R A \*

#### 4) Glycerol kinase

1 ATGGGCCATCATCATCATCATCATCATCATCATCACAGCAGCGGCCATATCGAAGGTCGT  
1 M G H H H H H H H H H H S S G H I E G R

61 CATATGTCCGACGCCATCCTAGGAGAGCAATTGGCCGAGTCCTCGGATTTTCATAGCCGCC  
21 H M S D A I L G E Q L A E S S D F I A A

121 ATCGACCAGGGCACCACCAGCACCCGCTGCATGATCTTCGATCACCACGGTGCCGAGGTG  
41 I D Q G T T S T R C M I F D H H G A E V

181 GCCCGCCACCAGCTCGAGCACGAGCAGATCCTGCCCGGGCCGGCTGGGTGGAGCACAAC  
61 A R H Q L E H E Q I L P R A G W V E H N

241 CCGGTTCGAGATCTGGGAGCGCACCCGCTCGGTGTTGATCTCGGTGCTCAACGCCACCAAC  
81 P V E I W E R T A S V L I S V L N A T N

301 CTATCGCCGAAAGATATTGCCGCGTTGGGGATTACCAACCAACGTGAGACGACGCTGGTA  
101 L S P K D I A A L G I T N Q R E T T L V

361 TGGAATCGGCACACCCGACGGCCCTACTACAACGCGATTGTATGGCAGGATACCCGACCC  
121 W N R H T G R P Y Y N A I V W Q D T R T

421 GACCGCATCGCGTCGGCGCTGGATCGAGACGGTCGTGGAAACCTGATCCGCCCAAGGCG  
141 D R I A S A L D R D G R G N L I R R K A

481 GGCCTGCCCGCGCAACTTATTTCTCTGGCGGCAAGCTGCAGTGGATCCTGGAAAATGTC  
161 G L P P A T Y F S G G K L Q W I L E N V

541 GATGGAGTCCGCGCGGCCCGGAGAACGGCGACGCATTGTTCCGGCACACCCGGACACCTGG  
181 D G V R A A A E N G D A L F G T P D T W

601 GTGTTGTGGAATCTGACCGGCGGGCCGCGGGGGGGTGTGCATGTCACCGATGTAACCAAC  
201 V L W N L T G G P R G G V H V T D V T N

661 GCCAGCCGGACCATGTTGATGGATCTAGAGACGCTGGACTGGGACGACGAGCTGTTGTGCG  
221 A S R T M L M D L E T L D W D D E L L S

721 TTGTTTTCGATACCTCGGGCCATGCTGCCCGAGATCGCATCGTCGGCGCCGTCGGAGCCT  
241 L F S I P R A M L P E I A S S A P S E P

781 TACGGTGTACGCTGGCGACCGGGCCTGTGCGCGGTGAGGTGCCGATCACCGGAGTTCTC  
261 Y G V T L A T G P V G G E V P I T G V L

841 GGTGATCAGCATGCGGCCATGGTCGGTCAAGTCTGTCTGGCCCCAGGGGAGGCGAAAAAC  
281 G D Q H A A M V G Q V C L A P G E A K N

901 ACCTATGGGACCGGCAATTTTCTGCTGCTGAACACCGGTGAAACGATCGTGCGATCGAAT  
301 T Y G T G N F L L L N T G E T I V R S N

961 AACGGCCTGCTAACCACGGTGTGCTACCAATTCGGGAACGCTAAACCCGTGTACGCGCTT  
321 N G L L T T V C Y Q F G N A K P V Y A L

1021 GAAGTTTCGATCGCGGTGACCGGCTCGGCGGTGCAGTGGCTACGCGATCAGCTGGGCATC  
341 E G S I A V T G S A V Q W L R D Q L G I

1081 ATCAGCGGGCGCCGCACAGAGTGAGGCGCTGGCCCCGCCAGGTCCCCGACAACGGCGGCATG  
361 I S G A A Q S E A L A R Q V P D N G G M

1141 TATTTTCGTGCCGGCGTTTTCCGGGCTGTTTCGCGCCATACTGGCGGTCCGATGCGCGCGGC  
381 Y F V P A F S G L F A P Y W R S D A R G

1201 GCGATCGTCGGGTTGTTCGCGGTTCAACACCAACGCGCACCTGGCGCGCGCAACGCTGGAG  
401 A I V G L S R F N T N A H L A R A T L E

1261 GCGATCTGCTACCAGAGCCGCGATGTGGTGGACGCCATGGAAGCAGACTCCGGTGTTCGC  
421 A I C Y Q S R D V V D A M E A D S G V R

1321 CTGCAGGTGTTGAAGGTGGATGGCGGGATCACCGGCAACGACCTGTGTATGCAGATCCAG  
441 L Q V L K V D G G I T G N D L C M Q I Q

1381 GCCGACGTGTTGGGTGTGGATGTGGTGC GGCCGGTGGTGC GCCGAGACCACCGCACTAGGT  
461 A D V L G V D V V R P V V A E T T A L G

1441 GTGGCCTACGCGGCGGGCTTGGCGGTTCGGGTTCTGGGCGGCTCCGTCCGATCTGCGGGCC  
481 V A Y A A G L A V G F W A A P S D L R A

1501 AACTGGCGAGAGGACAAGCGGTGGACACCGACGTGGGACGACGACGAGCGTGCCGCGGGT  
501 N W R E D K R W T P T W D D D E R A A G

1561 TATGCCGGCTGGCGCAAGGCGGTGCAGCGGACCCTGGATTGGGTTGACGTGTCCTAA  
521 Y A G W R K A V Q R T L D W V D V S \*

**5) Thiamine monophosphate kinase**

1 ATGGGCAGCAGCCATCATCATCATCACAGCAGCGGCCTGGTGCCGCGCGGCAGCCAT  
1 M G S S H H H H H S S G L V P R G S H

61 ATGACCACTAAAGATCACTCACTTGCAACGGAGTCCCCGACGCTGCAGCAGCTCGGCGAG  
21 M T T K D H S L A T E S P T L Q Q L G E

121 TTCGCCGTGATCGACCGGCTGGTGCGGGGGCGCCGACAACCCGCCACGGTACTGCTCGGG  
41 F A V I D R L V R G R R Q P A T V L L G

181 CCCGGCGACGATGCCGCGCTGGTGTCTGCCGGCGATGGTCGCACTGTGGTGTGACGGAC  
61 P G D D A A L V S A G D G R T V V S T D

241 ATGCTGGTGCAAGATAGTCACTTCCGGCTGGACTGGTCGACACCGCAGGACGTCGGCCGC  
81 M L V Q D S H F R L D W S T P Q D V G R

301 AAGGCGATCGCCCAGAATGCCGCCGACATCGAGGCGATGGGGGCGGGGCCACCGCGTTC  
101 K A I A Q N A A D I E A M G A R A T A F

361 GTGGTCCGGCTTTGGAGCACCCGCTGAGACGCCGGCGCGCAGGCGAGCGGTTGGTTCGAC  
121 V V G F G A P A E T P A A Q A S A L V D

421 GGAATGTGGGAGGAGGCGGGGCGCATTGGTGCCGGCATCGTCGGCGGCGATCTGGTCAGC  
141 G M W E E A G R I G A G I V G G D L V S

481 TGCCGGCAGTGGGTGGTGTGCGGTCACCGCGATTGGTGACCTTGACGGTCGTGCCCGGTG  
161 C R Q W V V S V T A I G D L D G R A P V

541 CTGCGCTCCGGGGCGAAGGCCGGCTCGGTGCTGGCCGTCGTCGGTGAGCTGGGCCGCTCG  
181 L R S G A K A G S V L A V V G E L G R S

601 GCTGCTGGCTATGCGCTGTGGTGAACGGGATTGAAGACTTCGCCGAAGTGCGCCGCCGC  
201 A A G Y A L W C N G I E D F A E L R R R

661 CATTGGTGCCCGCAGCCGCCCTACGGCCACGGCGCGGCGGCGGCTGTGCGGGCTCAA  
221 H L V P Q P P Y G H G A A A A A V G A Q

721 GCGATGATCGATGTCTCCGACGGGCTGCTCGCCGATCTGCGGCACATCGCCGAGGCATCC  
241 A M I D V S D G L L A D L R H I A E A S

781 GGCGTGCGCATCGACCTGTCCGCCGCGGCGTTGGCCGCTGACCGCGACGCTTTGACTGCG  
261 G V R I D L S A A A L A A D R D A L T A

841 GCCGCAACCGCTCTGGGCACCGACCCCTGGCCGTGGGTGCTAAGCGGGGTGAAGATCAT  
281 A A T A L G T D P W P W V L S G G E D H

901 GCCCTGGTCGCTGTTTCGTCGGTCCGGTGCCGGCCGGGTGGCGCACCATTTGGCCGGGTT  
301 A L V A C F V G P V P A G W R T I G R V

961 CTCGACGGGCCGGCTAGGGTGTGGTGTGACGGCGAGGAGTGGACTGGATACGCGGGCTGG  
321 L D G P A R V L V D G E E W T G Y A G W

1021 CAATCGTTTGGGGAGCCAGACAATCAAGTTTCGCTAGGGTAA  
341 Q S F G E P D N Q G S L G \*

**6) Ribokinase**

1 ATGGGCAGCAGCCATCATCATCATCACAGCAGCGGCCTGGTGCCGCGCGGCAGCCAT  
1 M G S S H H H H H S S G L V P R G S H

61 ATGGCAAACGCCAGTGAGACTAACGTGCGCCCCATGGCGCCCCGGGTGTGCGTGGTAGGC  
21 M A N A S E T N V G P M A P R V C V V G

121 AGCGTGAACATGGACCTGACGTTTCGTGGTGGACGCGCTTCCGCGCCCCGGCGAGACGGTG  
41 S V N M D L T F V V D A L P R P G E T V

181 CTTGCGGCGTCGTTGACCCGAACGCCAGGCGGGAAGGGCGCCAACCAGGCGGTGGCCGCA  
61 L A A S L T R T P G G K G A N Q A V A A

241 GCGCGCGCAGGCGCGCAGGTACAGTTCTCCGGTGCATTCGGCGACGATCCAGCCGCCGCC  
81 A R A G A Q V Q F S G A F G D D P A A A

301 CAGCTGCGGGCCACCTGCGCGCCAACGCCGTTGGACTGGACAGGACCGTACGGTGCCC  
101 Q L R A H L R A N A V G L D R T V T V P

361 GGACCGAGCGGGACGGCGATTATCGTGGTTCGATGCCAGCGCCGAGAACCAGTGTGGTG  
121 G P S G T A I I V V D A S A E N T V L V

421 GCGCCGGGTGCCAATGCACATCTGACTCCGGTACCCTCGGCCGTCGCCAACTGCGATGTA  
141 A P G A N A H L T P V P S A V A N C D V

481 CTGTTGACCCAGTTGGAGATTCTGTTGCAACCGCGCTGGCAGCCGCGGGCAGCCCAG  
161 L L T Q L E I P V A T A L A A A R A A Q

541 TCGGCCGATGCGGTTGTCATGGTCAACGCCTCCCCAGCCGGCCAGGATCGAAGCTCCTTG  
181 S A D A V V M V N A S P A G Q D R S S L

601 CAGGACTTGGCCGCTATCGCCGACGTGGTGTGATCGCCAACGAGCATGAGGCAAACGACTGG  
201 Q D L A A I A D V V I A N E H E A N D W

661 CCGTCGCCACCAACACATTTTCGTGATCACCTGGGTGTGCGCGGTGCCCGGTACGTCGGC  
221 P S P P T H F V I T L G V R G A R Y V G

721 GCGGACGGGGTGTTGAGGTACCCGCCCAACGGTAACGCCAGTGGATAACCGCCGGCGCC  
241 A D G V F E V P A P T V T P V D T A G A

781 GGCGACGTATTTGCCGGGGTCTTGTCTGCGAATTGGCCGCGCAACCCAGGTTGCGCGGCC  
261 G D V F A G V L A A N W P R N P G S P A

841 GAGCGACTGCGCGCATTGCGGCGGGCCTGCGCTGCGGGTTCGCTGGCAACTTTGGTGTCC  
281 E R L R A L R R A C A A G A L A T L V S

901 GGTGTCGGCGACTGCGCACCGGCCCGCCGCGATCGATGCGGCCCTGCGAGCCAACCGC  
301 G V G D C A P A A A A I D A A L R A N R

961 CACAACGGTTCATAA  
321 H N G S \*

**7a) Aspartokinase-alpha**

1 ATGGCGCTCGTTCGTGCAGAAGTACGGCGGATCCTCGGTGGCCGACGCCGAACGGATTTCGC  
1 M A L V V Q K Y G G S S V A D A E R I R

61 CGCGTCGCCGAACGCATCGTTCGCCACCAAGAAGCAAGGCAATGACGTCGTTCGTTCGTTCGC  
21 R V A E R I V A T K K Q G N D V V V V V

121 TCTGCCATGGGGGATAACCACCGACGACCTGCTGGATCTGGCTCAGCAGGTGTGCCCGGGC  
41 S A M G D T T D D L L D L A Q Q V C P A

181 CCGCCGCTCGGGAGCTGGACATGCTGCTTACCGCCGGTGAACGCATCTCGAATGCGTTG  
61 P P P R E L D M L L T A G E R I S N A L

241 GTGGCCATGGCCATCGAGTCGCTCGGCGCGCATGCCCGGTTCGTTACCGGTTTCGCAGGCC  
81 V A M A I E S L G A H A R S F T G S Q A

301 GGGGTGATCACCACCGGCACCCACGGCAACGCCAAGATCATCGACGTCACGCCGGGGCGG  
101 G V I T T G T H G N A K I I D V T P G R

361 CTGCAAACCGCCCTTGAGGAGGGGCGGGTCTTTTTGGTGGCCGGATTCCAAGGGGTCAGC  
121 L Q T A L E E G R V V L V A G F Q G V S

421 CAGGACACCAAGGATGTCACGACGTTGGGCCGCGGGCTCGGACACCACCGCCGTTCGCC  
141 Q D T K D V T T L G R G G S D T T A V A

481 ATGGCCGCGCGCTGGGTGCCGATGTCTGTGAGATCTACACCGACGTGGACGGCATCTTC  
161 M A A A L G A D V C E I Y T D V D G I F

541 AGCGCCGACCCGCGCATCGTTCGCAACGCCCGAAAGCTCGACACCGTGACCTTCGAGGAA  
181 S A D P R I V R N A R K L D T V T F E E

601 ATGCTCGAGATGGCGGCCTGCGGCGCCAAGGTGCTGATGCTGCGCTGCGTGAATACGCT  
201 M L E M A A C G A K V L M L R C V E Y A

661 CGCCGCCATAATATTCCGGTGCACGTCCGGTTCGTCGTACTIONCGACAGACCGGGCACCGTC  
221 R R H N I P V H V R S S Y S D R P G T V

721 GTTGTGCGATCGATCAAGGACGTACCCATGGAAGACCCATCCTGACCGGAGTCGCGCAC  
241 V V G S I K D V P M E D P I L T G V A H

781 GACCGCAGCGAGGCCAAGGTGACCATCGTTCGGGCTGCCCGACATCCCCGGGTATGCGGCC  
261 D R S E A K V T I V G L P D I P G Y A A

841 AAGGTGTTTAGGGCGGTGGCCGACGCCGACGTCAACATCGACATGGTGCTGCAGAACGTC  
281 K V F R A V A D A D V N I D M V L Q N V

901 TCCAAGGTTCGAGGACGGCAAGACCGACATCACCTTCACCTGCTCCCGCGACGTCGGGGCC  
301 S K V E D G K T D I T F T C S R D V G P

961 GCCGCCGTGGAAAACTGGACTCGCTCAGAAACGAGATCGGCTTCTCACAGCTGCTGTAC  
321 A A V E K L D S L R N E I G F S Q L L Y

1021 GACGACCACATCGGCAAGGTATCGCTGATCGGTGCCGGCATGCGCAGCCACCCCGGGGTC  
341 D D H I G K V S L I G A G M R S H P G V

1081 ACCGCGACGTTCTGTGAGGCGCTGGCGGGCGGTGGGGGTCAACATCGAGCTGATCTCCACC

361 T A T F C E A L A A V G V N I E L I S T  
1141 TCGGAGATCAGGATCTCGGTGTTGTGCCGCGACACCGAACTGGACAAGGCCGTGGTTCGCG  
381 S E I R I S V L C R D T E L D K A V V A  
1201 CTGCATGAAGCGTTCGGGCTCGGCGGCGACGAGGAGGCCACGGTGTACGCGGGGACGGGA  
401 L H E A F G L G G D E E A T V Y A G T G  
1261 CGGTAA  
421 R \*

**7b) Aspartokinase-beta**

```
1      ATGGAAGACCCCATCCTGACCGGAGTCGCGCACGACCGCAGCGAGGCCAAGGTGACCATC
1      M E D P I L T G V A H D R S E A K V T I

61     GTCGGGCTGCCCCGACATCCCCGGGTATGCGGCCAAGGTGTTTAGGGCGGTGGCCGACGCC
21     V G L P D I P G Y A A K V F R A V A D A

121    GACGTCAACATCGACATGGTGTCTGCAGAACGTCTCCAAGGTCGAGGACGGCAAGACCGAC
41     D V N I D M V L Q N V S K V E D G K T D

181    ATCACCTTCACCTGCTCCCGCGACGTCGGGCCCCGCCCGCTGGAAAACTGGACTCGCTC
61     I T F T C S R D V G P A A V E K L D S L

241    AGAAACGAGATCGGCTTCTCACAGCTGCTGTACGACGACCACATCGGCAAGGTATCGCTG
81     R N E I G F S Q L L Y D D H I G K V S L

301    ATCGGTGCCGGCATGCGCAGCCACCCCGGGGTCACCGCGACGTTCTGTGAGGCGCTGGCG
101    I G A G M R S H P G V T A T F C E A L A

361    GCGGTGGGGGTCAACATCGAGCTGATCTCCACCTCGGAGATCAGGATCTCGGTGTTGTGC
121    A V G V N I E L I S T S E I R I S V L C

421    CGCGACACCGAACTGGACAAGGCCGTTGGTCGCGCTGCATGAAGCGTTTCGGGCTCGGCGGC
141    R D T E L D K A V V A L H E A F G L G G

481    GACGAGGAGGCCACGGTGTACGCGGGGACGGGACGGGTCGAGCACCACCACCACCACCAC
161    D E E A T V Y A G T G R V E H H H H H H

541    TGA
181    *
```



## 8) Shikimate kinase

1 ATGGGCAGCAGCCATCATCATCATCACAGCAGCGGCCTGGTGCCGCGGGCAGCCAT  
1 M G S S H H H H H S S G L V P R G S H

61 ATGGCACCCAAAGCGGTTCTCGTCGGCCTGCCGGGCTCCGGCAAGTCCACCATCGGGCGC  
21 M A P K A V L V G L P G S G K S T I G R

121 CGGCTGGCCAAGGCGCTCGGGGTCGGCCTGCTCGACACCGACGTCGCGATCGAGCAGCGG  
41 R L A K A L G V G L L D T D V A I E Q R

181 ACCGGACGCAGCATCGCCGACATCTTCGCCACCGACGGGGAGCAGGAGTTCCGACGTATC  
61 T G R S I A D I F A T D G E Q E F R R I

241 GAGGAGGACGTGGTGCGCGGGCACTGGCCGACCACGACGGTGTGCTGTGCTCGGCGGC  
81 E E D V V R A A L A D H D G V L S L G G

301 GGCGCGGTGACCAGCCCCGGTGTGCGCGGGCGCTGGCCGGCCACACCGTCGTCTACCTG  
101 G A V T S P G V R A A L A G H T V V Y L

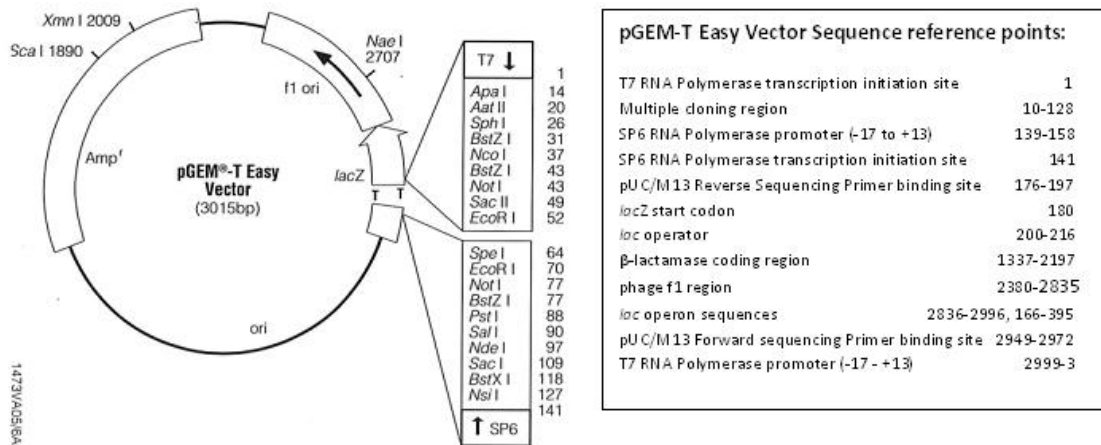
361 GAGATCAGCGCCCGAGGGCGTGCGCCGACCGGGCAACACCGTGCGCCCACTGCTG  
121 E I S A A E G V R R T G G N T V R P L L

421 GCCGGCCCCGACCGCGCCGAAAAATACCGCGCGCTGATGGCCAAGCGGGCACCCTGTAC  
141 A G P D R A E K Y R A L M A K R A P L Y

481 CGGCGCGTCGCGACCATGCGAGTGGACACCAATCGCCGCAACCCCGGGGCGGTGGTCCGC  
161 R R V A T M R V D T N R R N P G A V V R

541 CATATCCTGTGCGGGCTGCAGGTTCCAGCCCCAGCGAGGCGGCCACATGA  
181 H I L S R L Q V P S P S E A A T \*

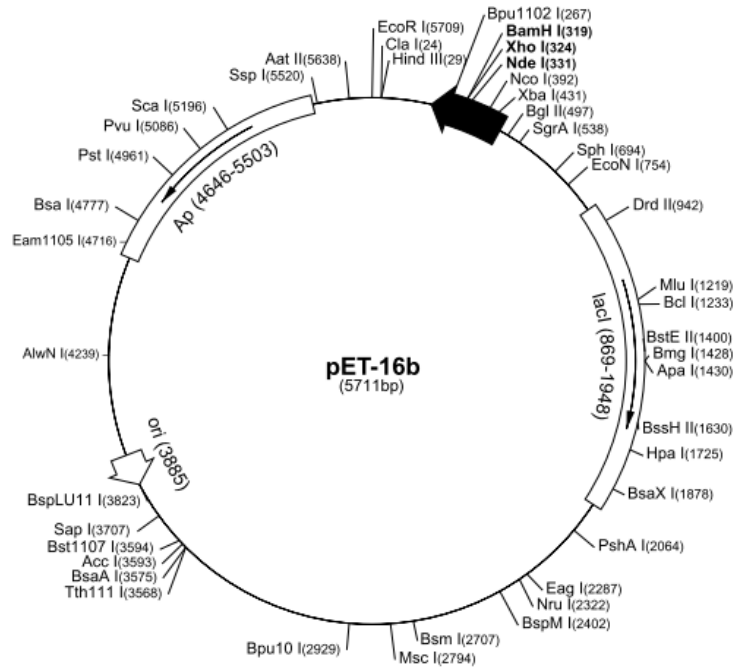
## Appendix B



Map of pGEM®-T Easy vector (Promega. 2010)

**pET-16b sequence landmarks**

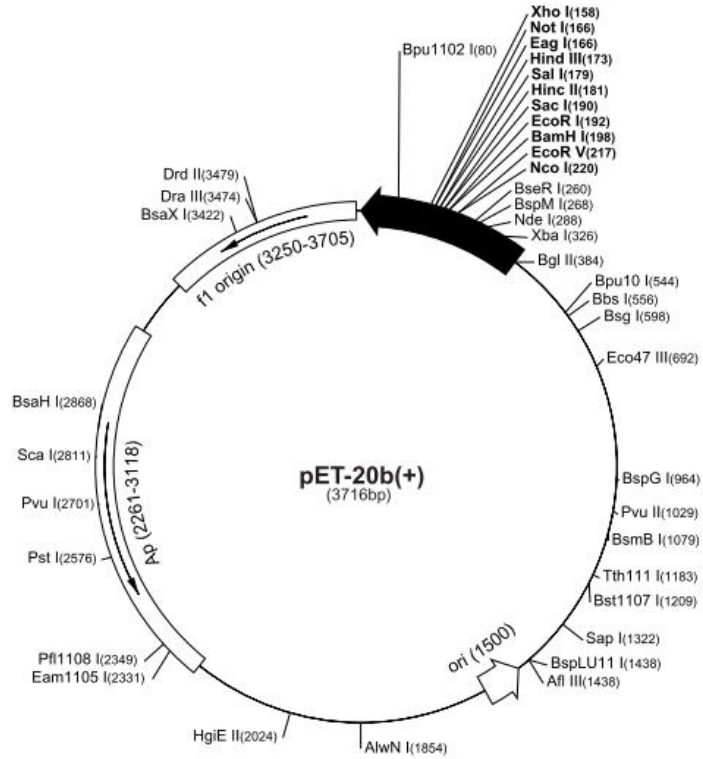
T7 promoter	466-482
T7 transcription start	465
His <sup>+</sup> tag coding sequence	360-389
Multiple cloning sites (Nde I -BamH I)	319-335
T7 terminator	213-259
<i>lacI</i> coding sequence	869-1948
pBR322 origin	3885
<i>bla</i> coding sequence	4646-5503



Map of pET-16b vector (EMD Millipore. 2013)

**pET-20b(+) sequence landmarks**

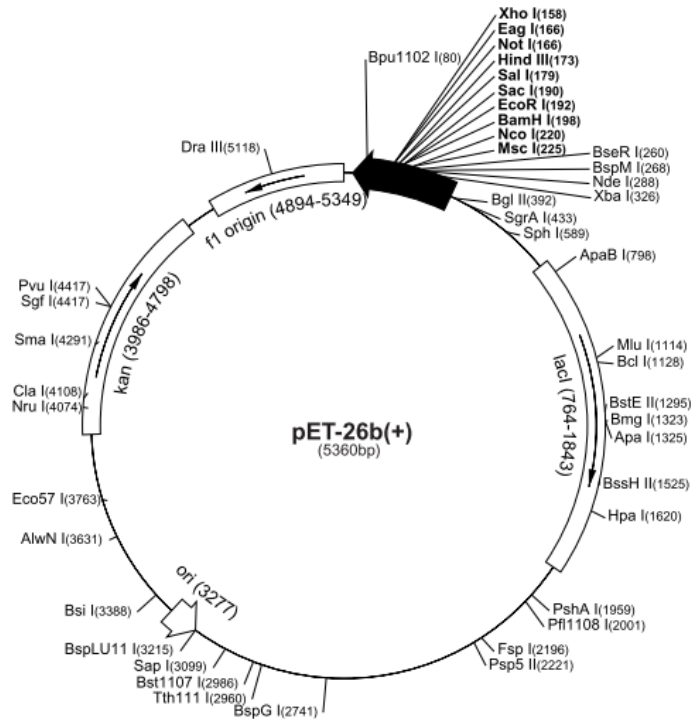
T7 promoter	353-369
T7 transcription start	352
pelB coding sequence	224-289
Multiple cloning sites (Nco I - Xho I)	158-225
His <sup>+</sup> T ag coding sequence	140-157
T7 terminator	26-72
pBR322 origin	1500
bla coding sequence	2261-3118
f1 origin	3250-3705



Map of pET-20b vector (EMD Millipore. 2013)

**pET-26b(+) sequence landmarks**

T7 promoter	361-377
T7 transcription start	360
pelB coding sequence	224-289
Multiple cloning sites (Nco I - Xho I)	158-225
His <sup>+</sup> T ag coding sequence	140-157
T7 terminator	26-72
lacI coding sequence	764-1843
pBR322 origin	3277
Kan coding sequence	3986-4798
f1 origin	4894-5349

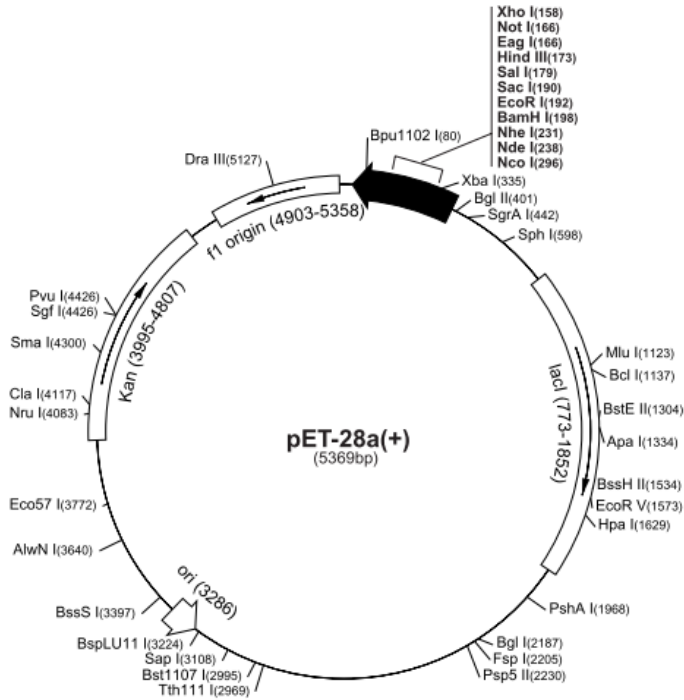


Map of pET-26b vector (EMD Millipore. 2013)

**pET-28a(+) sequence landmarks**

T7 promoter	370-386
T7 transcription start	369
His•Tag coding sequence	270-287
T7•Tag coding sequence	207-239
Multiple cloning sites (BamH I - Xho I)	158-203
His•Tag coding sequence	140-157
T7 terminator	26-72
<i>lacI</i> coding sequence	773-1852
pBR322 origin	3286
Kan coding sequence	3995-4807
f1 origin	4903-5358

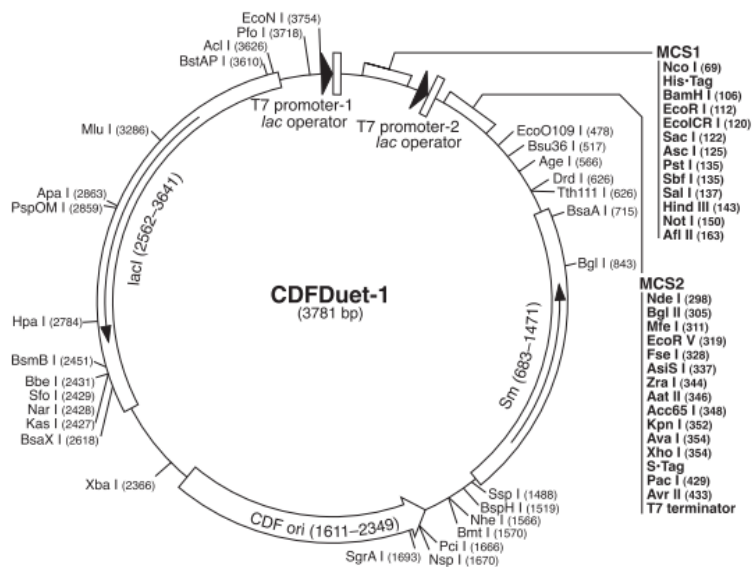
The maps for pET-28b(+) and pET-28c(+) are the same as pET-28a(+) (shown) with the following exceptions: pET-28b(+) is a 5368bp plasmid; subtract 1bp from each site beyond BamH I at 198. pET-28c(+) is a 5367bp plasmid; subtract 2bp from each site beyond BamH I at 198.



Map of pET-28a vector (EMD Millipore. 2013)

**pCDFDuet-1 sequence landmarks**

T7 promoter-1	3765-3781
T7 transcription start-1	1
His•Tag <sup>®</sup> coding sequence	83-100
Multiple cloning sites-1 (Nco I - Afl II)	69-168
T7 promoter-2	214-230
T7 transcription start-2	231
Multiple cloning sites-2 (Nde I - Avr II)	297-438
S•Tag <sup>™</sup> coding sequence	366-410
T7 terminator	462-509
<i>aadA</i> (SmR) coding sequence	683-1471
CDF origin	1611-2349
<i>lacI</i> coding sequence	2562-3641



Map of CDFDuet-1 vector (EMD Millipore. 2013)

## **Appendix C: Profinia Buffers**

### **BUFFER 1 (Wash Buffer 1, 2x), 250 ml**

600 mM KCl            11.18 g  
100 mM KH<sub>2</sub>PO<sub>4</sub>    3.04 g  
10 mM Imidazole    0.17 g  
pH 8.0

### **BUFFER 2 (Wash Buffer 2, 2x), 250 ml**

600 mM KCl            11.18 g  
100 mM KH<sub>2</sub>PO<sub>4</sub>    3.04 g  
20 mM Imidazole    0.34 g  
pH 8.0

### **BUFFER 3 (Elution Buffer, 2x), 250 ml**

600 mM KCl            11.18 g  
100 mM KH<sub>2</sub>PO<sub>4</sub>    3.04 g  
500 mM Imidazole    8.51 g  
pH 8.0

### **BUFFER 4 (Desalting Buffer, 5x), 250 ml**

685 mM NaCl           10.01 g  
13.5 mM                KCl 0.252 g  
21.5 mM                Na<sub>2</sub>HPO<sub>4</sub>    0.645 g  
40.5 mM                KH<sub>2</sub>PO<sub>4</sub>    1.38 g  
pH 7.0 (pH 7.4 upon dilution)

### **BUFFER 5 (Cleaning Solution 1, 2x), 250 ml**

1 M NaCl                14.61 g  
100 mM Tris            3.03 g  
pH 8.0

### **BUFFER 6 (Cleaning Solution 2, 4x), 250 ml**

2 M NaCl                29.22 g  
400 mM NaOAc        8.20 g  
pH 4.5

### **BUFFER 7 (Storage Buffer, 2x)**

20% EtOH

# References

---

1. Armitage, P., Walden, R. and Draper, J. (1988). Plant genetic transformation and gene expression: Vectors for the transformation of plant cells using *Agrobacterium*. Blackwell Publishing, pp. 3-67.
2. Bergman, J. (1999). ATP: The perfect energy currency for the cell. *Creation Research Society Quarterly Journal*, vol. 36 (1).
3. Boynton, Z.L., Bennet, G.N. and Rudolph, F.B. (1996). Cloning, Sequencing and Expression of genes encoding phosphotransacetylase and acetate kinase from *Clostridium acetobutylicum* ATCC 824. *Applied Environmental Microbiology*, vol. 62 (8), pp. 2758-2766.
4. Brendler, T. and Van Wyk, B.E. (2008). A historical, scientific and commercial perspective on the medicinal use of *Pelargonium sidoides* (Geraniaceae). *Journal Ethnopharmacology*, vol. 119, pp. 420-433.
5. Buss, K.A., Cooper, D.R., Ingram-Smith, C., Ferry, J.G., Sanders, D.A. and Hasson, M.S. (2001). Urkinase: Structure of Acetate kinase, a Member of the ASKHA Superfamily of phosphotransferases. *Journal of Bacteriology*, vol. 183 (2), pp. 680-686.
6. Bystrom, C.E., Pettigrew, D.W., Branchaud, B.P., O'Brien, P. and Remington, S.J. (1999) Crystal structures of *Escherichia coli* glycerol kinase variant S58-->W in complex with nonhydrolyzable ATP analogues reveal a putative active conformation of the enzyme as a result of domain motion. *Biochemistry*, vol. 38, pp. 3508-3518.
7. Cheek, S., Zhang, H. and Grishin, N.V. (2002). Sequence and structure classification of kinases. *Journal Molecular Biology* vol. 320, pp. 855-881.
8. Cheek, S., Ginalski, K., Zhang, H. and Grishin, N.V. (2005). A comprehensive update of the sequence and structure classification of kinases. *BMC Structural Biology* vol. 5 (6), pp. 1-19.
9. Chen, Y., Morera, S., Mocan, J., Lascu, I. and Janin, J. (2002). X-ray structure of *Mycobacterium tuberculosis* nucleoside diphosphate kinase. *Proteins*, vol. 47, pp. 5556-5557.
10. Cirillo, J.D., Weisbrod, T.R., Pascopella, L., Bloom, B.R. and Jacob Jr., W.R. (1994). Isolation and characterization of the aspartokinase and aspartate semialdehyde dehydrogenase operon from mycobacteria. *Molecular Microbiology*, vol. 11 (4), pp. 629-639.
11. Cole, S.T., Brosch, R., Parkhill, J., Garnier, T., Churcher, C., Harris, D., Gordon, S.V., Eiglmeier, K., Gas, S., Barry III, C.E., Tekaiia, F., Badcock, K., Basham, D., Brown, D., Chillingworth, T., Connor, R., Davies, R., Devlin, K., Feltwell, T., Gentles, S., Hamlin, N.,

- Holroyd, S., Hornsby, T., Jagels, K., Krogh, A., McLean, J., Moule, S., Murphy, L., Oliver, K., Osborne, J., Quail, M.A., Rajandream, M.A., Rogers, J., Rutter, S., Seeger, K., Skelton, J., Squares, R., Squares, S., Sulston, J.E., Taylor, K., Whitehead, S. and Barel, B.G. (1998). Deciphering the biology of *Mycobacterium tuberculosis* from the complete genome sequence. *Nature*, vol. 393, pp. 537-544.
12. Darbon, E., Servant, P., Poncet, S. and Deutscher, J. (2002). Antitermination by GlpP, catabolite repression via CcpA and inducer exclusion triggered by P-GlpK dephosphorylation control *Bacillus subtilis* glpFK expression. *Molecular Microbiology*, vol. 43 (4), pp. 1039-1052.
  13. Dartmouth Undergraduate Journal of Science. (2009). Antibiotic resistance of Tuberculosis. Available at: <http://dujs.dartmouth.edu/winter-2009/new-tricks-for-an-old-foe-the-threat-of-antibiotic-resistant-tuberculosis> [Accessed 25 September 2014].
  14. Davis, E. (2007). Gene regulation and DNA repair in the pathogenesis of *Mycobacterium tuberculosis*. MRC National Institute for Medical Research.
  15. Dipple, K., Zhang, Y.H., Huang, B.L., McCabe, L., Dallongeville, J., Inokuchi, T., Kimura, M., Marx, H., Roederer, G., Shih, V., Yamaguchi, S., Yoshida, I. and McCabe, E. (2001). Glycerol kinase deficiency: Evidence for complexity in a single gene disorder. *Human Genetics*, vol. 109 (1), pp. 55-62.
  16. Dower, W.J., Miller, J.F. and Ragsdale, C.W. (1988). High efficiency transformation of *E. coli* by high voltage electroporation. *Nucleic Acids Research*, vol. 16, pp. 6127.
  17. Dreyer, L.L. and Marais, E.M. (2000). Section *Rheniformia*, a new section in the genus *Pelargonium* (Geraniaceae). *South African Journal Botany*, vol. 66, pp. 44-51.
  18. EMD Millipore. (2013). pET *E. coli* T7 expression vectors: Novagen pET vector table. [Online] Available at: <http://www.emdmillipore.com/life-science-research/vector-table-novagen-pet-vector-table> [Accessed 10 June 2014].
  19. Faehnle, C.R., Liu, X., Pavlovsky, A. and Viola, R.E. (2006). The initial step in the archaeal aspartate biosynthetic pathway catalysed by a monofunctional aspartokinase. *Acta Crystallographica*, vol. 62, pp. 962-966.
  20. Fernandez-Patron, C., Calero, M., Collazo, P.R., Garcia, J.R., Madrazo, J., Musacchio, A., Soriano, F., Estrada, R., Frank, R., Castellanos-Serra, L.R. and Mendez, E. (1995). Protein reverse staining: high efficiency microanalysis of unmodified proteins detected on electrophoresis gels. *Analytical Biochemistry*, 224, pp. 203-211.
  21. Flynn, J.L and Chany, J. (2003). Immune evasion by *Mycobacterium tuberculosis*: living with the enemy. *Current Opinion in Immunology*, vol. 15 (4), pp. 450.

22. Gorrell, A., Lawrence, S.H. and Ferry, J.G. (2005). Structure and kinetic analyses of arginine residues in the active site of the acetate kinase from *Methanosarcina thermophila*. *Journal of Biological Chemistry*, vol. 280, pp. 10731-10742.
23. Grundner, C., Gay, L.M. and Alber, T. (2005). *Mycobacterium tuberculosis* serine/threonine kinases PknB, PknD, PknE and PknF phosphorylate multiple FHA domains. *Protein Science*, vol. 14 (7), pp. 1918-1921.
24. Gu, Y., Reshetnikova, L., Li, Y., Wu, Y., Yan, H., Singh, S. and Ji, X. (2002). Crystal structure of shikimate kinase from *Mycobacterium tuberculosis* reveals the dynamic role of the LID domain in catalysis. *Journal of Molecular Biology*, vol. 319 (3), pp. 779-789.
25. Haas, A.L. (2005). *Enzyme Assays and Kinetics*. Department of Biochemistry Med School, pp.1-12.
26. Helmstadter, A. (1996). Umckaloabo- Late vindication of a secret remedy. *Pharmaceutical Historia*, 26, pp.2-4.
27. Horvath, C.G., Preiss, B.A. and Lipsky, S.R. (1967). Fast Liquid Chromatography: An investigation of operating parameters and the separation of nucleotides on pellicular ion exchangers. *Analytical Chemistry*, vol. 39 (12), pp. 1422-1428.
28. Johnson, L.N. and Barford, D. (1993). The effects of phosphorylation on the structure and function of proteins. *Annual review of biophysics and biomolecular structure*, vol. 22 (1), pp. 199-232.
29. KAPA Biosystems. (2014). KAPA PCR kits. [Online] Available at: <http://www.kapabiosystems.com/products> [Accessed 10 March 2014].
30. Kassim, I. and Ray, C.G. (2004). *Sherris Medical Microbiology*. 4<sup>th</sup> ed. McGraw Hill 9, pp. 8385-8529.
31. Kayser, O. and Kolodziej, H. (1995). Highly oxygenated coumarins from *Pelargonium sidoides*. *Phytochemistry*, 39, pp. 1181-1185.
32. Kenyon, C.P., Steyn, A., Roth, R.L., Steenkamp, P.A., Nkosi, T.C. and Oldfield, L.C. (2011). The role of the C8 proton of ATP in the regulation of phosphoryl transfer within kinases and synthetases. *BMC Biochemistry*, vol. 12, pp. 36-53.
33. Kenyon, C.P., Roth, R.L., Van der Westhuyzen, C.W. and Parkinson, C.J. (2012). Conserved phosphoryl transfer mechanisms within kinase families and the role of the C8 proton of ATP in the activation of phosphoryl transfer. *BMC Research Notes*, vol. 5 (131), pp. 1.
34. Kolodziej, H. (2007). Fascinating metabolic pools of *Pelargonium sidoides* and *Pelargonium reniforme*, traditional and phytomedicinal sources of the herbal medicine Umckaloabo. *Phytomedicine*, vol. 6, pp.9-17.



35. Kolodziej, H. (2011). Antimicrobial, antiviral and immunomodulating activity studies of *Pelargonium sidoides* (EPs®7630) in the context of health promotion. *Pharmaceuticals*, vol. 4, pp. 1295-1314.
36. Kotaka, M., Ren, J., Lockye, M., Hawkins, A.R. and Stammers, D.K. (2006). Structures of R- and T-state *Escherichia coli* Aspartokinase III- Mechanisms of the allosteric transition and inhibition by lysine. *The Journal of Biological Chemistry*, vol. 281, pp. 31544-31552.
37. Krishna, S.S., Zhou, T., Daugherty, M., Osterman, A. and Zhang, H. (2001). Structural Basis for the Catalysis and substrate Specificity of Homoserine Kinase. *Biochemistry*, vol. 40, pp. 10810-10818.
38. Kumar, P., Krishna, K., Srinivasan, R., Ajitkumar, P. and Varshney, U. (2004). *Mycobacterium tuberculosis* and *Escherichia coli* nucleoside diphosphate kinase lack multifunctional activities to process uracil containing DNA. *DNA repair*, vol. 3 (11), pp. 1483-1492.
39. Laemmli, U.K. (1970). Cleavage of structural proteins during the assembly of the head of bacteriophage T4. *Nature*, 227, pp. 680-685.
40. Lahlou, M. (2013). The success of Natural Products in Drug Discovery. *Pharmacology and Pharmacy*, vol. 4 (3A), pp. 1-15.
41. Latimer, M.T. and Ferry, J.G. (1993). Cloning, sequence analysis and hyperexpression of the genes encoding phosphotransacetylase and acetate kinase from *Methanosarcina thermophila*. *Journal Bacteriology*, vol. 175 (21), pp.6822-9.
42. Mateos, L.M., Real, G.D., Aguilar, A. and Martin, J.F. (1987). Cloning and Expression in *Escherichia coli* of the Homoserine kinase (thrB) gene from *Brevibacterium lactofermentum*. *Molecular and General Genetics MGG*, vol. 206 (3), pp. 361-367.
43. McCulloch, K.M., Kinsland, C., Begley, T.P. and Ealick, S.E. (2008). Structural studies of Thiamine Monophosphate kinase in complex with structures and products. *Biochemistry*, vol. 47, pp. 3810-3821.
44. Microbiology In Pictures. (2013). *Mycobacterium tuberculosis*. [Online] Available at: <http://www.microbiologyinpictures.com/mycobacterium%20tuberculosis.html> [Accessed 06 May 2014].
45. Muljadi, P. (2011). Enzyme kinetics. [Online] Available at: <http://www.scribd.com/doc/75635532/Enzyme-Kinetics> [Accessed 18 August 2014].
46. Murray, P.R., Rosenthal, K.S. and Pfaller, M.A. (2005). *Medical Microbiology*. Elsevier Mosby.

47. Nelson, S.D. and Trager, W.F. (2003). The use of deuterium isotope effects to probe the active site properties, mechanisms of cytochrome P450-catalyzed reactions, and mechanisms of metabolically dependant toxicity. *Drug metabolism and disposition*, vol. 31 (12), pp. 1481-1497.
48. Nicholl, D.S.T. (2008). *An introduction to Genetic Engineering: Gel electrophoresis*. 3<sup>rd</sup> Ed. Cambridge University Press, pp. 40-41.
49. Patwardhan, B., Vaidya, A.D.B. and Chorghade, M. (2004). Ayurveda and Natural Products Drug Discovery. *Current Science*, vol. 86 (6), pp. 789-799.
50. Pereira, J.H., Oliveira, J.S., Canduri, F., Dias, M.U.B., Palma, M.S., Basso, L.A., Santos, D.S. and Azevedo, W.F. (2004). Structure of Shikimate kinase from *Mycobacterium tuberculosis* reveals the binding of shikimic acid. *Biological Crystallography*, vol. D60, pp. 2310-2319.
51. Promega. (2010). pGem®-T and pGem®-T Easy vector systems. [Online] Available at: <http://www.promega.com/~media/files/resources/protocols> [Accessed 10 June 2014].
52. Qiagen. (2004). Sample and Assay Technologies. [Online] Available at: <http://www.qiagen.com/za/resources/molecular-biology-methods/protein> [Accessed 07 October 2014].
53. Rees, W.D., Hay, S.M. and Flint, H.J. (1992). Expression of *Escherichia coli* homoserine kinase in mouse 3T3 cells. *Biochemistry Journal*, vol. 281, pp. 865-870.
54. Research On Medical. (2013). Natural remedies for 10 common health problems in children. [Online] Available at <http://researchonmedical.com/2013/02/> [Accessed 12 May 2014].
55. Robin, A.Y., Cobessi, D., Curien, G., Robert-Genthon, M., Ferrer, J.L. and Dumas, R. (2010). A new mode of dimerization of allosteric enzymes with ACT domains revealed by the crystal structure of the aspartokinase from Cyanobacteria. *Journal of Molecular Biology*, vol. 399 (2), pp. 283-293.
56. Sambrook, J., Fritsch, E.F. and Maniates, T. (1989). *Molecular cloning: A Laboratory Manual*. Cold Spring Harbor Laboratory Press.
57. Schuldt, L., Suchowersky, R., Veith, K., Mueller-Diekmann, J. and Weiss, M.S. (2011). Cloning, expression, purification, crystallization and preliminary X-ray diffraction analysis of the regulatory domain of aspartokinase (Rv3709c) from *Mycobacterium tuberculosis*. *Acta Crystallographica*, vol. 67 (3), pp. 380-385.
58. Sigrell, J.A., Cameron, A.D., Jones, T.A. and Mowbray, S.L. (1998). Structure of *Escherichia coli* ribokinase in complex with ribose and dinucleotide determined to 1.8 Å resolution: insights into a new family of kinase structures. *Molecular biology*, vol. 6 (2), pp. 183-193.

59. Sikarwar, J., Kaushik, S., Sinha, M., Kaur, P., Sharma, S. and Singh, T.P. (2013). Cloning, Expression and Purification of Nucleoside Diphosphate kinase from *Acinetobacter baumannii*. *Enzyme Research*, Article ID 597028, pp. 1-4.
60. Taylor, P.W. (2004). Antimycobacterial activity of indigenous South African plants. *South African Medical Journal*, vol. 93 (12), pp. 904-907.
61. Tomioka, H., Tatano, Y., Yasumoto, K. and Shimizu, T. (2008). Recent advances in antituberculous drug development and novel drug targets. *Expert Review of Respiratory Medicine*, vol. 2 (4), pp. 455-471.
62. Tripmin, S. and Brizzard, B. (2009). Analysis of insoluble proteins. *Biology Techniques*, 46 (6), pp. 409-419.
63. Tu, Y., Jeffries, C., Ruan, H., Nelson, C., Smithson, D., Shelat, A.A., Brown, K.M., Li, X.C., Hester, J.P., Smillie, T., Khan, I.A., Walker, L., Guy, K. and Yan, B. (2010). An automated high-throughput system to fractionate plant natural products for drug discovery. *Journal of Natural Products*, vol. 73 (4), pp. 751-754.
64. Van der Walt, J.J.A. and Vorster, P. (1988). *Pelargonium* of Southern Africa. Purnell, vol. 1.
65. Walaas, S. and Walaas, O. (1962). The activation of muscle hexokinase by divalent metal ions. *Acta Chemica Scandinavica*, vol. 16 (7), pp. 1682-1694.
66. WORLD HEALTH ORGANISATION. (2008). Stop TB Strategy. Available at: <http://www.who.int/tb/strategy/en/> [Accessed 25 September 2014].
67. WORLD HEALTH ORGANISATION. (2013). Global Tuberculosis Report. [Online] Available at: [http://gamapserver.who.int/mapLibrary/Files/Maps/Global\\_TBincidence](http://gamapserver.who.int/mapLibrary/Files/Maps/Global_TBincidence) [Accessed 8 May 2014].
68. WORLD HEALTH ORGANISATION. (2014). Fact sheet on Tuberculosis. [Online] Available at: <http://www.who.int/mediacentre/factsheets/fs104/en> [Accessed 8 May 2014].
69. WORLD HEALTH ORGANISATION. (2014). World TB Day 2014: Reach the 3 million. [Online] Available at: <http://www.who.int/campaigns/tb-day/2014/en> [Accessed 8 May 2014].
70. Wu, G., Yuan, Y. and Hodge, C.N. (2003). Determining appropriate substrate conversion for enzymatic assays in high-throughput screening. *Journal of Biomolecular Screening*, vol. 8 (6), pp. 694-700.
71. Xu, Y.W., Moréra, S., Janin, J. and Cherfils, J. (1997) AIF3 mimics the transition state of protein phosphorylation in the crystal structure of nucleoside diphosphate kinase and MgADP. *Proceedings of the National Academy of Sciences*, vol. 94 (8), pp. 3579-83.
72. Yang, Q., Liu, Y., Huang, F. and He, Z.G. (2011). Physical and functional interaction between D-Ribokinase and topoisomerase I has opposite effects on their respective activity

in *Mycobacterium smegmatis* and *Mycobacterium tuberculosis*. Archives of Biochemistry and Biophysics, vol. 512, pp. 135-142.

73. Yoshida, A., Tomita, T., Kuzuyama, T. and Nishiyama, M. (2010). Mechanism of concerted inhibition of alpha2beta2-type hetero-oligomeric aspartate kinase from *Corynebacterium glutamicum*. Journal of Biological Chemistry, vol. 285, pp. 27477-27486.
74. Zhang, Y., Zagnitko, O., Rodionova, I., Osterman, A. and Godzik, A. (2011). The FGGY Carbohydrate kinase family: Insights into the evolution of functional specificities. PLOS Computational Biology, vol. 7 (12), pp. 1-9.
75. Zhou, T., Daugherty, M., Grishin, N.V., Osterman, A.L. and Zhang, H. (2000). Structure and Mechanism of homoserine kinase: Prototype for the GHMP Kinase superfamily. Pubmed, vol. 15 (12), pp. 1247-57.